8-1-2006

History and timing of polyphase Proterozoic deformation in the Manzano thrust belt, central New Mexico

Amy Luther

Amy Lynn Luther

Candidate

Earth and Planetary Sciences

Department

This thesis is approved, and it is acceptable in quality and form for publication on microfilm:

Approved by the Thesis Committee:

Karl E Karlstrom, Chairperson

Accepted:

Dean, Graduate School

Date

HISTORY AND TIMING OF POLYPHASE PROTEROZOIC DEFORMATION IN THE MANZANO THRUST BELT, CENTRAL NEW MEXICO

BY

AMY LYNN LUTHER

B.S., GEOLOGY, UNIVERSITY OF ILLINOIS, 2003

THESIS

Submitted in Partial Fulfillment of the
Requirements for the Degree of

Master of Science
Earth and Planetary Science

The University of New Mexico
Albuquerque, New Mexico

August, 2006

ACKNOWLEDGEMENTS

This thesis would not have been possible without support from many different people ranging from professors, students, friends and family. I would first like to thank my advisor Karl Karlstrom for helping me become a more successful field geologist, and having many discussions that helped push forward my research. I would also like to thank the rest of my committee for insight and support throughout the project. I would like to thank Austin Zinsser for always listening and helping me with many aspects of graduate school, and for being a great office mate and friend.

In addition, I would like to thank those for technical support. This research was funded through numerous generous grants from the Geological Society of America and the New Mexico Geological Society. I appreciate help I received from many, many field assistants who were willing to hike through the blazing hot desert with me in the middle of summer. They were Gary Newsom, Kym Samuels, Ryan Crow, Tom Sewar, Eileen Embid, Tony Salem, and Austin Zinsser. I would especially like to thank my field assistants who put in more than their fair share of time—Amber Hawkins and Matt Kirk. Thank you both for the company, assistance, and friendship over the years.

Finally, I would like to thank my friends and family for constant support of the years, especially Matt Kirk and Rosarita Luther. And very special thanks to my parents, Terry and Rick Luther for always being encouraging and also for being great friends.

HISTORY AND TIMING OF POLYPHASE PROTEROZOIC DEFORMATION IN THE MANZANO THRUST BELT, CENTRAL NEW MEXICO

BY

AMY LYNN LUTHER

ABSTRACT OF THESIS

Submitted in Partial Fulfillment of the
Requirements for the Degree of

Master of Science
Earth and Planetary Science

The University of New Mexico
Albuquerque, New Mexico

August, 2006

HISTORY AND TIMING OF POLYPHASE PROTEROZOIC DEFORMATION IN THE MANZANO THRUST BELT, CENTRAL NEW MEXICO

By

Amy Lynn Luther

Bachelor of Science, Geology, University of Illinois, 2003
Master of Science, Earth and Planetary Sciences, University of New Mexico, 2006

ABSTRACT

The Sandia-Manzano-Los Pinos Mountains, on the eastern flank of the Rio Grande rift, provide spectacular exposures of the Proterozoic Manzano thrust belt. This region is an important place to better characterize polyphase deformation and magmatism related to the assembly of Laurentia, particularly the 1.65-1.60 Ga Mazatzal orogeny and the later 1.4 Ga thermo-tectonic event. This study focuses on the Los Pinos Mountains, near the southern end of the Manzano thrust belt, an area that has been only weakly overprinted by a later phase of Mesoproterozoic tectonism and is therefore an ideal place to characterize Paleoproterozoic deformational events. Building on a large amount of prior work to the north, this study allows for a complete cross section to be drawn for the Manzano thrust belt and for the development of a more complete stratigraphic understanding of the Manzano Group.

Paleoproterozoic rocks of the northern Los Pinos Mountains contain three tectonic fabrics that have variable intensities, with the north-northeast-striking S_2 being the dominant foliation. New mapping of the Los Pinos Mountains resulted in the recognition of a new macroscopic D_2 anticline cored by the 1662 ± 1 Ma (Shastri, 1992) Sevilleta metarhyolite. Documentation of the overturned nature of much of the stratigraphy corrects the prior interpretation of Myers et al. (1981). A new U-Pb zircon date of 1601

+4/-3 Ma (Jones, 2005) on the upper Blue Springs rhyolite indicates that the Manzano Group records deposition from 1662-1600 Ma. Additional evidence supports the interpretation of synchronous D_2 deformation and plutonism in the aureole of the 1655 ± 3 Ma Los Pinos pluton (in agreement with Shastri, 1992) indicates that D_2 (attributed to the Mazatzal orogeny) was a protracted event lasting from ~1655 Ma to some time after 1600 Ma. Reverse-sense west-side-up shearing on steeply west-dipping S_2 was a progressive event which resulted in rotation of F_2 folds. This shearing event is interpreted to be broadly synchronous with top-to-the-northwest thrusting elsewhere in the Manzano thrust belt, and hence suggests a bivergent Mazatzal orogeny.

TABLE OF CONTENTS

LIST OF FIGURES AND PLATES

LIST OF TABLES

INTRODUCTION

The Proterozoic tectonic evolution of the southwestern U.S. involved a period of accretion, called the Mazatzal orogeny, in which juvenile arc terranes and diverse tectonostratigraphic blocks accreted to the "southern" margin of Laurentia (Karlstrom and Bowring, 1988; Bowring, 1990; Karlstrom et al., 2001a) between ~1.65 and 1.60 Ga (Figure 1). Following a ~100 Ma period of tectonic quiescence (Karlstrom et al., 2004), the crust was then modified and perforated by 1.45-1.35 Ga granitoids in the Mesoproterozoic (Anderson, 1983; Nyman et al., 1994; Kirby et al., 1995). This was a widespread tectono-thermal event hypothesized to be due to basaltic underplating beneath the stabilizing craton (Karlstrom and Humpreys, 1998; Karlstrom et al., 2004) and resulting in regional metamorphism and plutonism. Variable strain accompanied 1.45-1.35 Ga plutonism, but these rocks are generally less foliated than the country rocks which they intrude (Nyman et al., 1994). Numerous conflicting models surround interpretations of the timing and geometry of deformations and the relative importance of these two main tectonic events in producing the observed features of preserved Proterozoic rocks (Table 1).

A recent seismic experiment (Magnani et al., 2004) was run to delineate the deep structure related to the Proterozoic orogens. A 150-km long line was run across the southern boundary of a wide zone thought to be transitional between the Yavapai and Mazatzal provinces (Karlstrom and Humpreys, 1998) and across the Cenozoic Jemez lineament, a line of NE-trending volcanic centers. This zone appears to coincide with a

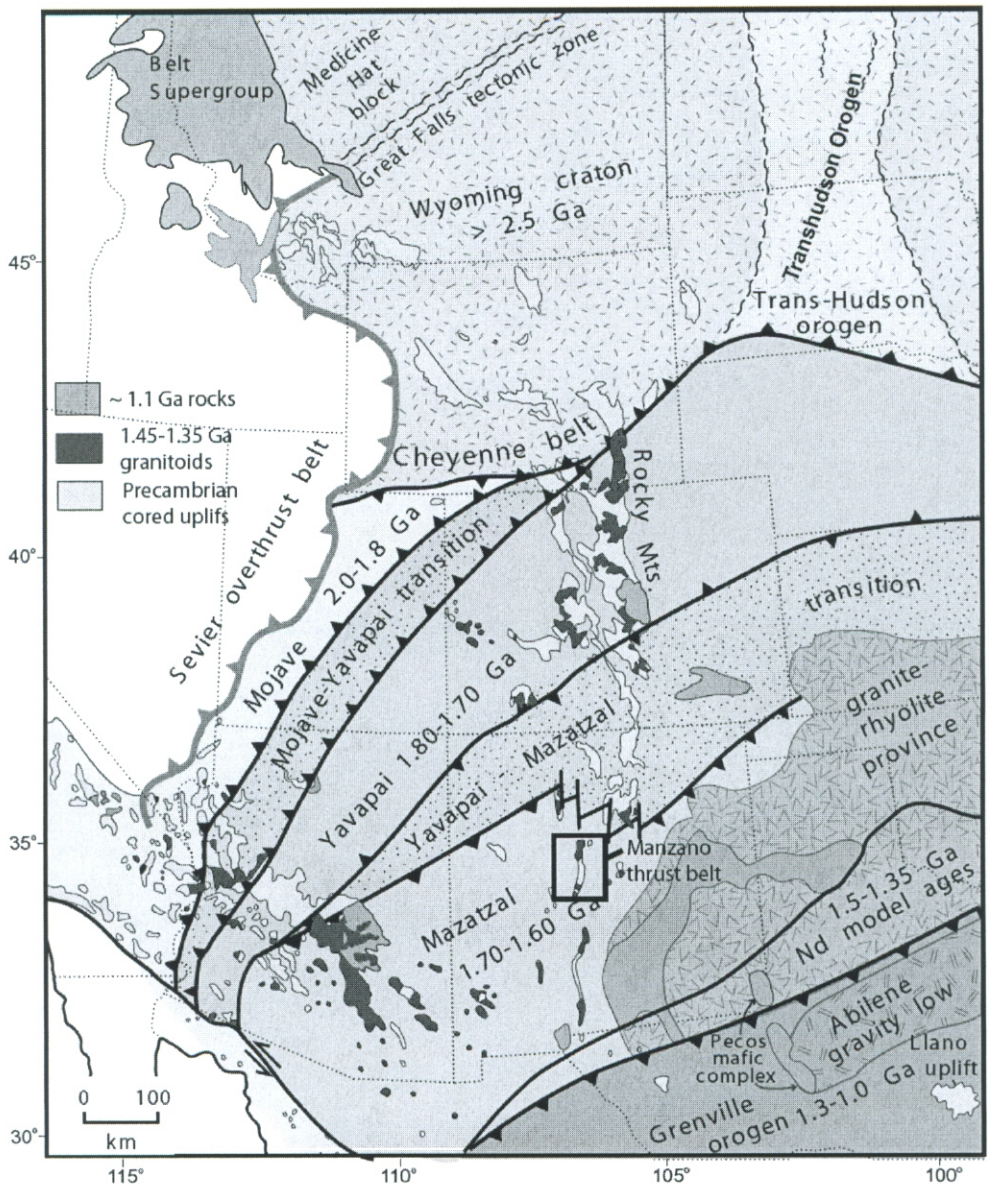

Figure 1. Tectonic province map of the western United States. The box highlights the Manzano thrust belt of central New Mexico. This shows the location of Figure 2 and is the focus of this study (Modified from Karlstrom et al., 2004).

Table 1. Summary of differing hypotheses for timing of Proterozoic orogenesis

	HYPOTHESIS 1 – Paleoproterozoic deformation dominant	HYPOTHESIS 2 Mesoproterozoic deformation dominant	HYPOTHESIS 3- Variable intensity of each event preserved depending on location
1.65-1.60 Ga Tectonism	Dominant regional deformation event during crustal accretion: Synchronous N-vergent thrusting, calc-alkaline magmatism, and bimodal volcanism. Accompanied by greenschist to lower amphibolite facies metamorphism. (Karlstrom and Bowring, 1988; **Bauer et al., 1993)**	Period of magmatism, shallow thrust belt deformation and greenschist or lower grade metamorphism in New Mexico (e.g. Conway and Silver, 1989)	Period of magmatism, shallow thrust belt deformation (Doe et al., 1999) and variable grade metamorphism depending on depth and proximity to plutons.
1.45-1.35 Ga Tectonism	Regional intracratonic plutonism and 300-600° C greenschist to amphibolite grade pluton enhanced metamorphism (**Karlstrom et al., 1997**), reactivation of shear zones and localized strain in pluton aureoles (Nyman et al., 1994; **Kirby et al., 1995**), related to outboard accretion of younger arc terranes (Karlstrom et al., 2001a)	Dominant deformation at this time, regional deformation, metamorphism and plutonism. (**Grambling and Dallmeyer, 1993; Marcoline et al., 1999; Ralser, 2000**; Daniel and Pyle, 2006)	Regional far field stresses (NW contraction) due to southern transpressional plate margin caused strained in regions softened by magmatism and high grade metamorphism (Karlstrom et al., 1994), or in regions at depths below a regional melt-fluid layer (Shaw et al., 2004)
Geochronologic evidence	Deformed 1.65 Ga plutons, truncation of D2 structures by relatively unfoliated 1.43 Ga plutons (**Bauer et al., 1993; Baer, 2004**). Lack of 1.43 Ga overprint outside of this younger suite of pluton aureoles (Conway and Silver, 1989), Ar-Ar ages indicate variable temperatures of 300->500 C at 1.4 Ga (**Thompson et al., 1996; Heizler et al., 1997**)	Monazite geochronology from the Picuris Range of northern New Mexico (Daniel and Pyle, 2006). Interpretation based on lack of older than ~1.43 Ga monazites. All Ar hornblende ages in this region indicate 1.4 Ga metamorphism (**Thompson et al., 1996; Heizler et al., 1997**)	Multiple ages of syndeformational monazite growth (Williams et al, 1999; Kopera), metamorphic sphene (**Shastri, 1992 Bowring, 1983**), and syntectonic plutonism (**Brown et al., 1999; Kirby et al., 1995**). Cold regions (< 350° C and hot regions (> 500° C) at 1.4 Ga indicated by Ar data (Shaw et al., 2005)

Pb-isotopic boundary between Yavapai and Mazatzal crust (Wooden and DeWitt, 1989) and has been interpreted to be a possible Paleoproterozoic suture zone (Karlstrom and Humphreys, 1998). Interpretation of the seismic line involved a bivergent orogen model with south-dipping thrusts and a north-dipping crustal-scale duplex at the boundary between these provinces (Magnani et al., 2004). This implies southward subduction of the Yavapai province beneath the Mazatzal, but also N-directed thrusting, though others have hypothesized southward subduction or tectonic switching (e.g. Cavosie and Selverstone, 2003). The Manzano thrust belt of central New Mexico is a spectacular exposure of imbricating thrusts that represent the style of Mazatzal deformation just south of the inferred suture zone (Karlstrom et al., 2004), and is therefore an important region for studying orogenesis related to continent building processes during the Precambrian.

The Sandia-Manzano-Los Pinos uplift of central New Mexico forms part of the flank uplift of the Rio Grande rift. Proterozoic structures exposed in the range are referred to as the Proterozoic Manzano thrust belt (Karlstrom et al., 2004). This belt records polyphase deformation related to the Mazatzal orogeny and a later ~1.4 Ga thermal event. This study completes a 10-year effort to map the uplift (Karlstrom et al., 1994 ; Read et al., 1995; Chamberlain et al., 1997; Chamberlin et al., 1997; Karlstrom et al., 1999; Karlstrom et al., 2001b; Baer et al., 2004; Luther et al., 2005) by new geologic mapping (~25 km^2) of the Becker Quadrangle, a structural analysis of deformation--including field- and thin section-based studies, and a stratigraphic analysis of the Los Pinos Mountains. Data from this study are then synthesized with this large volume of past work from the rest of the thrust belt in order to discuss the timing and character of Proterozoic orogenesis in the context of the formation of Laurentia. This synthesis

documents syntectonic deposition, magmatism and deformation associated with the Mazatzal orogeny, and strongly hinges on an improved geologic context for the large geochronologic database. Implications of this study include—1) nature of polyphase ductile thrust belts, 2) interaction of deformation and plutonism in convergent settings 3) geochronologic studies leading to evidence for a thrust belt that moved twice 4) shear sense studies indicate the possibility that this is a bivergent thrust belt.

GEOLOGIC BACKGROUND

The north-northeast trending Sandia-Manzano-Los Pinos Proterozoic core exposes a 100 km cross-strike transect of the Mazatzal province (Figure 1). Figure 2 shows the distribution of granitoids, supracrustal rocks, and major shear zones of the Manzano thrust belt as well as all existing U-Pb ages. The oldest deposits in the range are bimodal metavolcanic rocks of the various greenstone belts. These yield ages from ~1680 to ~1660 Ma (Unruh, *unpubl.*). Overlying this are metasedimentary units including quartzite, schist, phyllite and some interbedded metarhyolite. These were tectonized at ductile, middle crustal conditions, in part synchronously with ca. 1650 Ma plutonism (Brown et al., 1999). Based on a lack of U-Pb ages from 1600 to 1460 Ma, these units are interpreted to have remained tectonically buried during a period of quiescence (Karlstrom et al., 2004). At ~1430 Ma, plutons intruded previously deformed rock at depths of about 8-15 km. In the Manzano Mountains, the suite of c. 1430 Ma plutons includes the Sandia granite 1437 ± 47 Ma (recalculated by Kirby et al., 1995 from Ludwig, 1980) and the 1427 ± 10 Ma Priest pluton (Bauer et al., 1993). The approximately 1.65 Ga pluton of the Los Pinos is similar to the rest of the 1.65 Ga suite of plutons exposed throughout the Manzano Mountains. These have been described by previous researchers and are summarized from north to south in Table 2 below. In addition, the two 1.4 Ga plutons are also described in this table.

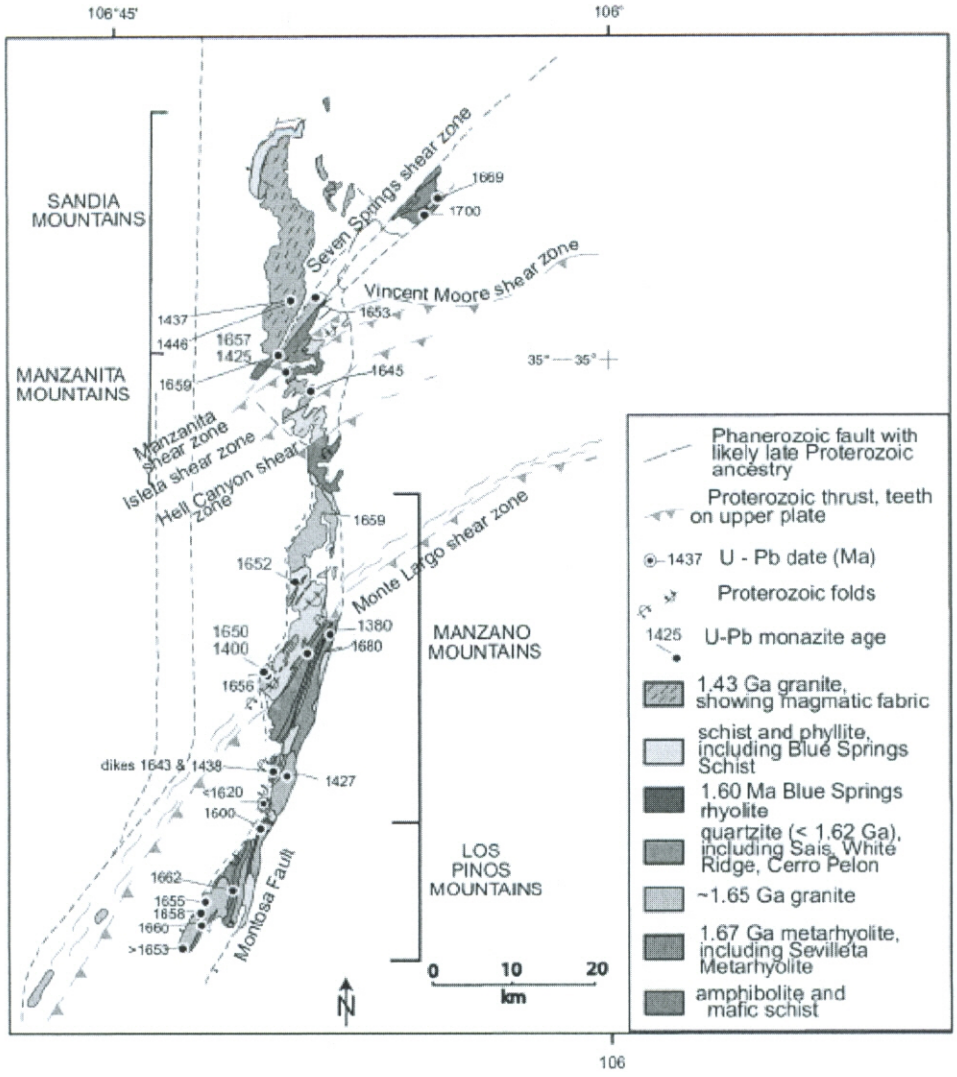

Figure 2. Simplified regional geologic map of the Manzano thrust belt (modified from Karlstrom et al., 2004). Errors on U-Pb ages and references are reported in Table 3. The Los Pinos Mountains at the southern end of the belt are the focus of this study.

Table 2. Description of intrusive units in the Manzano thrust belt

NAME	AGE	CHEMISTRY	DESCRIPTION
Manzanita pluton	1645 ± 16 Ma (Brown et al., 1999)	High-K group with Low REE (Granite)	Homogeneous, pink quartz monzonite with 1-4 cm K-feldspar phenocrysts, with an orange two-mica, medium-grained quartz monzonite on the pluton margins (Chamberlain et al., 1997).
Ojito pluton	1659 ± 5 Ma (Unruh, unpublished data)	High-Ca group (Calc-alkaline)	Medium grained massive quartz monzonite with quartz, sodic andesine, microcline, biotite and accessory hornblende, sphene, epidote, amphibole and tourmaline (Karlstrom et al., 1999)
Monte Largo pluton	1656 ± 10 Ma (Bauer et al., 1993)	High-Ca group (Calc-alkaline)	Medium grained sericitized feldspar, quartz, chloritized biotite, altered hornblende and epidote granodiorite, quartz monzonite, and granite (Bauer et al., 1993)
Sandia pluton	1437 ± 47 Ma (Kirby et al., 1995)	High-Ca group (Calc-alkaline)	Mainly a megacrystic gray to pink monzogranite to granodiorite with 3-5 cm long K-feldspars with a coarse grained matrix of quartz, plagioclase, biotite and ± hornblende (Brookins and Majumdar, 1989)
Priest pluton	1427 ± 10 Ma (Bauer et al., 1993)	High-Ca group (Calc-alkaline)	Megacrystic biotite-quartz-feldspar quartz monzonite with cm-scale microcline phenocrysts (Stark, 1956; Bauer, 1983; Bauer et al., 1993; Baer, 2004)

All ages were obtained using U-Pb zircon dating. Each includes a reference of those who studied the particular pluton, however the geochemical data are all from Condie and Budding (1979).

Geochronologic data

Table 3 summarizes all the U-Pb zircon and sphene ages from the Manzano thrust belt. Sample locations and ages are on the regional geologic map (Figure 2). In addition to the documentation of two phases of plutonism, these ages indicate that in the Los Pinos Mountains the Sevilleta Metarhyolite is 1662 ± 1 Ma and the Los Pinos pluton crystallized at 1655 ± 3 Ma (Shastri, 1992). Three fractions of zircon from the Blue Springs rhyolite at the top of the section yield nearly concordant ages of 1600 +4/-3 Ma for the Blue Springs rhyolite (Jones, 2005). This crystallization age for the rhyolite is the youngest Paleoproterozoic age found in New Mexico thus far. Detrital zircons from the Estadio quartzite (correlative to the White Ridge quartzite in the Los Pinos Mountains) have a maximum age of ~1630 Ma based on the youngest zircon although the error on these analyses is large (~50 Ma; Jones, pers. comm.). A dated dike from Estadio Canyon cross-cuts this unit and is 1643 ± 20 (Unruh, unpubl.). The oldest zircons are Archean. The peak of detrital zircon ages is around 1.7 Ga indicating either a Yavapai source or a local source because the ages of granitoids and rhyolites from nearby are within the error of this age.

Structural geology

Early geologic mapping and discussion of stratigraphy by Stark and Dapples (1946) and Reiche (1949) included descriptions of the intrusive igneous rocks, and divided the metasedimentary rocks into the upper and lower metaclastic series. These units have been further described, mapped, and dated by numerous subsequent workers (e.g. Myers et al., 1981; Shastri, 1992; Bauer et al., 1993; Baer, 2004). Most recent work has shown that three tectonic fabrics developed at variable intensities within the Manzano

Table 3: Compilation of U-Pb ages from the Manzano thrust belt

UNIT	MINERAL	AGE (MA)	UNCERT. (MA)	INTERPRETATION	REFERENCE
Monte Largo Hills metarhyolite	Zircon	1700	20*	Crystallization age	Unruh, *unpubl.*
Sevilleta Metarhyolite	Zircon	1680	20*	Crystallization age	Bowring et al., 1993
Monte Largo Hills granite	Zircon	1669	13	Crystallization age	Unruh, *unpubl.*
Sevilleta Metarhyolite	Zircon	1662	1	Crystallization age	Shastri, 1992
Ojito pluton	Zircon	1659	5	Crystallization age	Unruh, *unpubl.*
Vincent Moore granite	Zircon	1659	13	Crystallization age	Unruh, *unpubl.*
Monte Largo granodiorite	Zircon	1656	20*	Crystallization age	Bauer, 1993
Los Pinos granite, Pb-Pb age	Zircon	1656	3	Crystallization age	Shastri, 1992
Cibola granite	Zircon	1653	21	Crystallization age	Unruh, *unpubl.*
Manzanita granite	Zircon	1645	16	Crystallization age	Unruh, *unpubl.*
Estadio Canyon dikes	Zircon	1643	20*	Crystallization age	Unruh, *unpubl.*
Estadio Canyon dike	Zircon	1438	20*	Crystallization age	Unruh, *unpubl.*
Sandia granite	Zircon	1437	47	Crystallization age	Kirby et al., 1995
Sandia granite	Zircon	1437	47	Crystallization age	Kirby et al., 1995
Priest quartz monzonite	Zircon	1427	10	Crystallization age	Bauer et al., 1993
Sepultura pluton (LP-34)	Zircon	1630-1653		Crystallization age	Shastri, 1992
Aplite dike (LP-86A)	Zircon	1658	12	Crystallization age	Shastri, 1992
Amphibolite (LP-53B)	Zircon	1660	2	Metamorphic age	Shastri, 1992
Amphibolite (LP-53B)	Sphene	1620	slightly discord.	Metamorphic age	Shastri, 1992
Amphibolite (LP-53B)	Apatite	1420 and 1400	slightly discord.	Minimum Metamorphic age	Shastri, 1992
Blue Springs Rhyolite	Zircon	1601	+4/-3	Crystallization age	(Jones, 2005)
Sais /Estadio Quartzite	Detrital Zircon	~1620		Maximum deposition age	(Jones, 2005)

* No error reported

thrust belt. In the Manzano-Los Pinos Mountains, S_1 refers to a bedding-parallel tectonic fabric of aligned mica, quartz, and metamorphic minerals (Doran, 2002) that is axial planar to rare isoclinal folds. This has been refolded and overprinted by a NNE steeply dipping S_2 axial planar cleavage (Bauer, 1983; Thompson et al., 1991; Shastri, 1992; Bauer et al., 1993; Thompson et al., 1996; Brown et al., 1999; Rogers, 2001; Baer, 2004). Studies to date indicate that the Manzano thrust belt consists of northeast-striking, top-to-the northwest, major thrust-related shear zones (shown in blue on Figure 2). These are documented at both margins of the 1.65 Ga Manzanita pluton aureole (Brown et al., 1999) and in the Monte Largo shear zone south of the 1.65 Ga Monte Largo pluton (Thompson et al., 1991; Thompson et al., 1996; Rogers, 2001; Baer, 2004), and are inferred to extend parallel to the Mazatzal-Yavapai suture across New Mexico (Karlstrom et al., 2004). The Monte Largo shear zone juxtaposes amphibolite grade metamorphic rocks on the south with greenschist facies units north of the shear zone (Thompson et al., 1991). Timing of movements on this shear zone is controversial, however preliminary monazite geochronology finds that monazite in the Manzanita shear zone north of this field area with ~1.66 Ga cores and ~1.43 Ga rims that are aligned in the mylonitic fabric of the syntectonic Manzanita pluton aureole. Andalusites within the aureole of 1.69 Ga Ojito pluton contain ~1652 Ma monazite inclusions that are aligned in a strong pre-pluton fabric (Williams et al., 1999). These ages suggest that the area underwent deformation at ~1.65 Ga and ~1.43 Ga, and that at least some of the shear zones may have had more than one period of movement.

The dominant tectonic fabric 'S_2' is preserved in Paleoproterozoic supracrustal sequences and in 1.65 Ga plutons (Figure 3; Bauer, 1983; Shastri, 1992; Bauer et al., 1993; Brown et al., 1999; Rogers, 2001; Baer, 2004). One purpose of this study is to try to correlate this deformation to the fabrics of the Los Pinos Mountains.

The D_3 event, attributed to the 1.43 Ga thermo-tectonic event (Baer, 2004; this thesis), involved extensive plutonism, metamorphism and localized deformation across the Southwest (e.g. Anderson, 1983; Thompson et al., 1991; Kirby et al., 1995; Thompson et al., 1996; Karlstrom et al., 1997; Barnes et al., 2002; Daniel and Pyle, 2006). S_3 development and F_3 folding is variable along the thrust belt. In the 1.4 Ga pluton aureoles, F_3 and S_3 development is intense and refolds F_2 structures, likely due to thermal softening related to emplacement of 1.43 Ga plutons (Nyman et al., 1994). This was also accompanied by reactivation of ductile shear zones initiated at ~1650 Ma (Rogers, 2001; Baer, 2004). The ca. 1430 Priest and Sandia plutons are interpreted to have been emplaced during east-west shortening (Kirby et al., 1995; Baer, 2004). The Sandia pluton was emplaced synchronously with top-to-the NW movement along a normal shear zone (Kirby et al., 1995) and the Priest pluton with top-to-the-northwest thrusting along the Monte Largo shear zone (Rogers, 2001; Baer, 2004).

Metamorphism

Polymetamorphism has been documented in the Manzano thrust belt, particularly in 1430 Ma pluton aureoles (Thompson et al., 1991; Thompson et al., 1996; Larson and Sharp, 2003). Metamorphic minerals from amphibolites in Bootleg Canyon (central Los Pinos Mountains) include sphene, zircon and apatite and yield U-Pb ages of 1620 Ma (slightly discordant), 1660 ± 2 Ma, and minimum ages of 1420 and 1400 (slightly

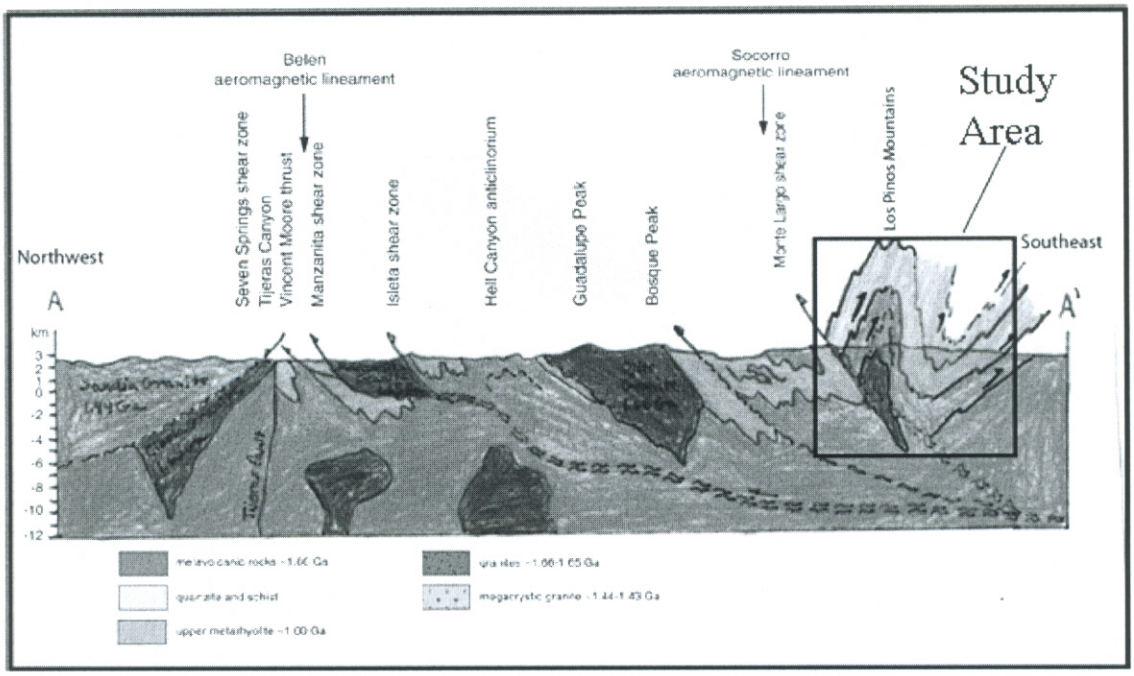

Figure 3. Regional northwest-southeast cross section of the Manzano thrust belt (modified from Cather et al., 2006). This ramp-flat thrust belt has accompanying anticlines and synclines that are shown to fold the supracrustal sequences and 1.65 Ga granitoids, yet are cross-cut by the 1.43 Ga Priest pluton. Northwest-directed thrusts have sheared the Priest pluton. The box highlights the results of this study from the Los Pinos Mountains, and has been projected into the original Cather et al. (2006) cross section. This region has a similar style of deformation to the northern part of the belt, but verges to the southeast.

discordant) (Shastri, 1992). Regional upper greenschist grade to lower amphibolite grade conditions have been documented for the first phase of metamorphism at ~1660 Ma (Bauer, 1983; Shastri, 1992; Larson and Sharp, 2003) and is inferred to be related to the Mazatzal orogeny based on these geochronologic constraints from Shastri (1992). The 1.65 Ga Ojito pluton aureole records andalusite-grade contact metamorphism (Karlstrom et al., 1999) and the Bootleg Canyon peak metamorphism is constrained to be ~5.5 kbars and 480° C, based on garnet compositions, however possible earlier high temperature metamorphism is hypothesized by Shastri (1992) based on brown hornblende cores and actinolite zoning in amphibolites. Synchronous metamorphism and deformation is recorded in the Manzanita pluton aureole based on synchronous-S_2 porphyroblast growth and retrogression in the contact aureole (Brown et al., 1999). The supracrustal package is interpreted to have then resided in the crust at near 300° C-350° C (Larson and Sharp, 2003; Thompson et al., 1996; Karlstrom et al., 1997; Read et al., 1999; Williams et al., 1999) until the emplacement of 1.4 Ga plutons. The last phase of metamorphism began at ~1430 Ma and was amphibolite grade in contact aureoles (Kirby et al., 1995). The Priest pluton contact aureole records metamorphic temperatures of 690° C to 540°C based on oxygen isotope data (Larson and Sharp, 2003) or 650°C to 525°C based on garnet-biotite thermometers and isograds and 4 kbars depth (Thompson et al., 1996). Retrograde metamorphism to greenschist grade overprints this event (Thompson et al., 1996; Larson and Sharp, 2003).

GEOLOGIC MAPPING OF THE LOS PINOS MOUNTAINS

About two months were spent mapping the Becker quadrangle (Plate 1: Luther et al., 2005) in conjunction with the New Mexico STATEMAP program and for the purpose of this project. In addition, about 1 month was spent mapping other regions of the thrust belt including the southern part of the Los Pinos Mountains (1:12,000) in the Cerro Montoso Quadrangle (also in conjuction with NM STATEMAP) and the Abo Pass and Estadio Canyon regions of the Manzano Mountains (1:6,000). Geologic mapping for this project focused on the exposures of Paleoproterozoic supracrustal and intrusive rocks. Major contributions from this project include 1) an open-file report with a detailed stratigraphic section, geologic history, and structural analysis; 2) detailed update of the existing 1: 24,000 map (Myers et al., 1981), including revision of stratigraphic order and structural interpretation; 3) recognition of the Los Pinos anticline cored by Proterozoic metarhyolite units; 4) correlation of this anticlinal structure with units in Bootleg Canyon (Cerro Montoso Quadrangle to the south); 5) documentation of 1655 Ma syntectonic D_2 plutonism; 6) documentation of west-side-up reverse shearing during D_2 deformation; 7) documentation of a weak D_3 overprint in the Los Pinos Mountains.

Stratigraphy of the Manzano Group

Figure 4 shows a generalized stratigraphic section of the Manzano Group, which is a new name used in this paper referring to the 1662 to 1600 Ma rocks found in the Manzano-Los Pinos uplift. Each unit is described below. This work builds on a stratigraphic compilation done by Baer (2004). Map thicknesses were calculated from the Los Pinos Mountains, but are quite variable due to thrusting, isoclinal folding, and

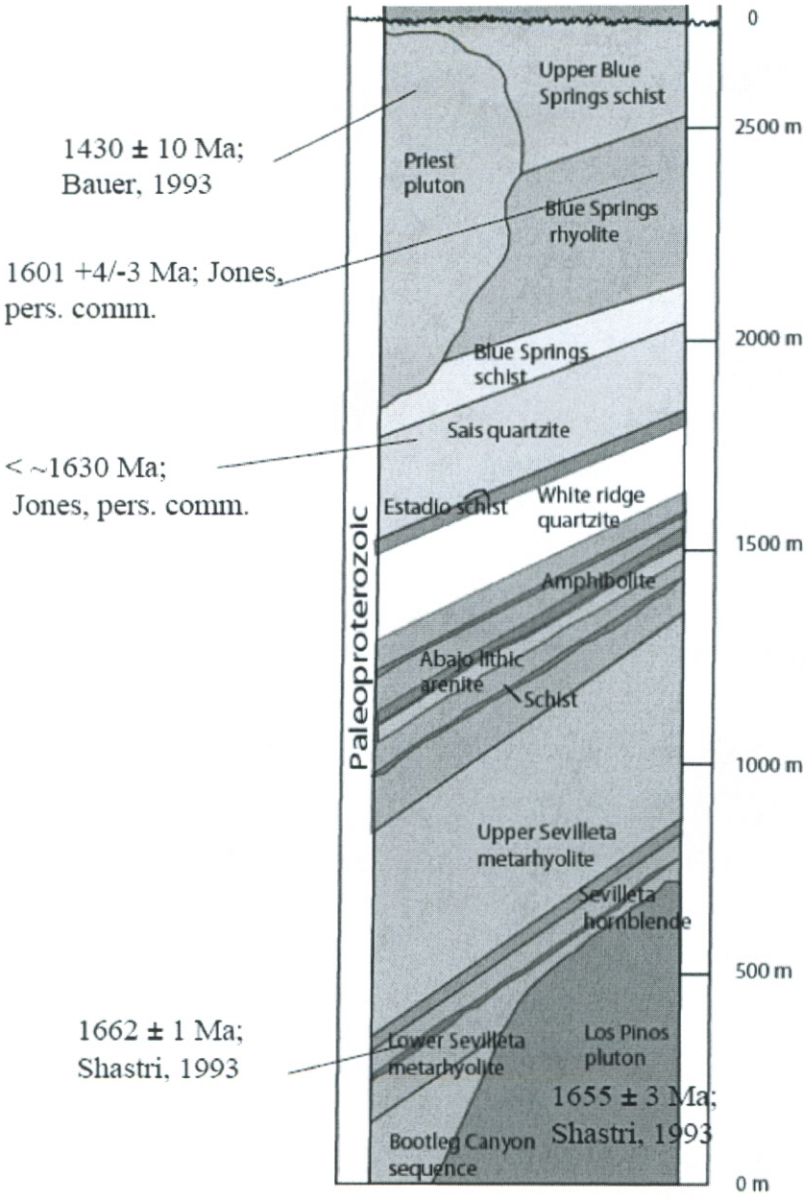

Figure 4. Stratigraphic section of the Manzano Group supracrustal sequence. Thicknesses were calculated from the Becker quadrangle map, but may not be true stratigraphic thicknesses due to ductile deformation and isoclinal folding.

multiple cleavage developments, so, while these are best estimates, these should not be inferred to represent true depositional thicknesses.

The base of the Manzano Group is interpreted to be the Bootleg Canyon sequence based on its location in the core of the newly recognized Los Pinos anticline. The Bootleg Canyon sequence is a ~600-m thick sequence of interbedded amphibolite, pelitic schist, and quartzo-feldspathic schist described previously by Shastri (1992). These rocks are only found locally in Bootleg Canyon of the Los Pinos Mountains exposed between the Los Pinos pluton and the Sepultura pluton—however; these may be correlative with other "greenstone" successions of the Manzano Mountains. The amphibolite layers can be divided into fine-grained and the coarse-grained units. The fine-grained amphibolite consists of dominantly hornblende, epidote, biotite, and quartz with grain sizes of less than 0.25 mm and some plagioclase, magnetite, zircon, sphene and apatite. Coarse-grained amphibolite is black-and-white to greenish-grey to black depending on the mineral content, which is typically hornblende, epidote, biotite, chlorite and actinolite with similar accessory minerals as the finer grained unit. The pelitic schist member is light green to beige and is very fine-grained (< 0.1 mm). Some 1-5 mm garnet porphyroblasts are present locally. The mineral content of this pelitic schist is garnet, biotite, chlorite, muscovite, plagioclase, quartz, Fe-Ti oxides, ± K-feldspar, and ± tourmaline. Some samples contain no chlorite or tourmaline. The quartzo-feldspathic schist of Shastri (1992) is divided into quartz-pod bearing schist and layered schist. Shastri (1992) also includes metarhyolite in this member, but this paper interprets these rocks to be part of the lower Sevilleta metarhyolite unit. Mineral content of the quartz-pod bearing schist consists of a fined grained plagioclase, biotite, and quartz matrix with

8 to 12 cm long ellipsoidal pods of quartz (Shastri, 1992). The layered schist is an interbedded mafic and granitic schist, suggesting that amphibolite supracrustal rocks were complexly intruded by granite (Shastri, 1992).

The Sevilleta metarhyolite ranges from 575-625 m thick in the lower unit to about 1450-1600 m thick in the upper unit and is a sequence of metarhyolite rocks (Figure 6a) interlayered with 100-125 m thick amphibolites. These are divided stratigraphically by the thickest amphibolite unit. These units are interpreted to be metamorphosed rhyolites, basalt to basaltic andesite, and gabbros based on bulk geochemical data from XRF analyses done for this project. Analyses are presented in Table 4, and Figure 5a shows a plot of SiO_2 vs. $Na_2O + K_2O$ on the total alkali silica diagram of Le Bas et al. (1986). Figure 5b shows a plot of FeO (total) vs. MgO on an igneous rock series diagram (Jolly, 1975). These data are all from meta-igneous rocks from the Manzano thrust belt or the Dubois succession, and all represent bimodal successions. One point does plot on the calc-alkaline and andesite field and is from the Manzano rhyodacite, which is likely correlative to the Lacoracah metadacite, a marker bed within the Sevilleta metarhyolite. These are interpreted to have been deposited as volcanic tuffs and flows based on the presence of extrusive primary features such as pumice fragments and pillows. Figure 6b shows an outcrop of the Lacoracah metadacite an interbedded marker layer with up to 3 cm large phenocrysts of K-feldspar, hornblende, and biotite. The metagabbros are coarse grained amphibolite units and weather into rounded outcrops unlike the finer grained metabasalts (Figure 6c). The dominant rhyolite member weathers grey to reddish brown and is generally porphyritic with a fine-grained quartzo-feldspathic matrix and 1-5 mm plagioclase, up to 1 mm quartz grains and up to 1 mm garnet porphyroblasts. Biotite,

Table 4. Results of bulk geochemical analyses (XRF)

Sample ID	SiO_2	TiO_2	Al_2O_3	Fe_2O_3	FeO	MnO	MgO	CaO	Na_2O	K_2O	$H_20(-)$	$H_2O(+)CO_2$	P_2O_5	Total	H2O(+)CO2 /DF (10) & Cover. To %
AL04BQ-2	52.28	1.05	15.38	10.51	0.00	0.17	5.74	6.47	3.23	0.62	0.02	2.28	0.09	97.84	1.0023
BC1-LPG	78.49	0.22	11.49	2.04	0.00	0.03	0.08	0.18	3.06	4.94	-0.11	0.21	0.01	100.67	1.0002
BQAL-38Xa	46.35	1.32	17.20	11.94	0.00	0.18	6.67	8.67	2.79	0.31	0.14	2.07	0.08	97.73	1.0021
BQAL-24Xsrm	77.68	0.28	11.34	2.85	0.00	0.06	0.06	0.43	3.11	4.09	0.02	0.62	0.03	100.58	1.0006
BQAL-21Xsrl	72.33	0.53	11.69	3.52	0.00	0.10	0.20	1.05	3.08	4.19	0.00	0.29	0.08	97.06	1.0003
K05ABO-1	70.71	0.45	15.41	3.64	0.00	0.13	0.89	2.16	5.50	1.86	0.07	0.55	0.11	101.48	1.0005
BQAL-40BC	71.24	0.67	12.95	5.45	0.00	0.09	0.55	1.27	4.25	2.60	-0.10	1.18	0.18	100.33	1.0012

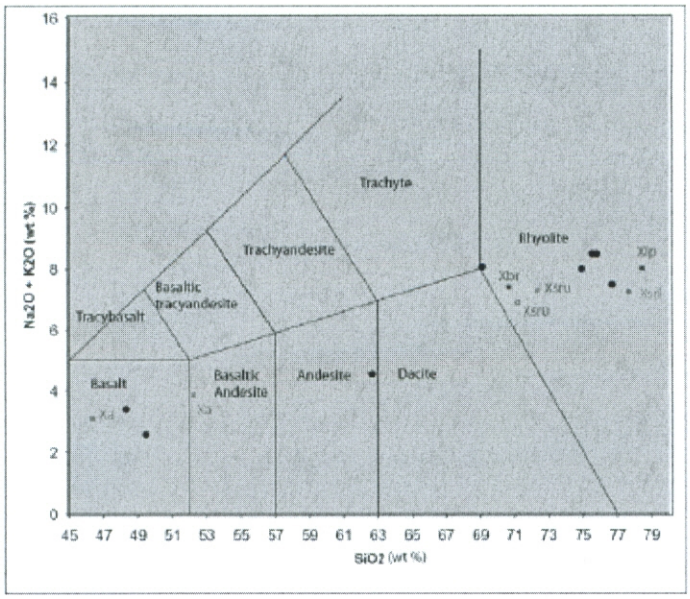

Labeled data from this study
Black dots --Condie and Budding, 1979

after LE BAS et al. [1985]

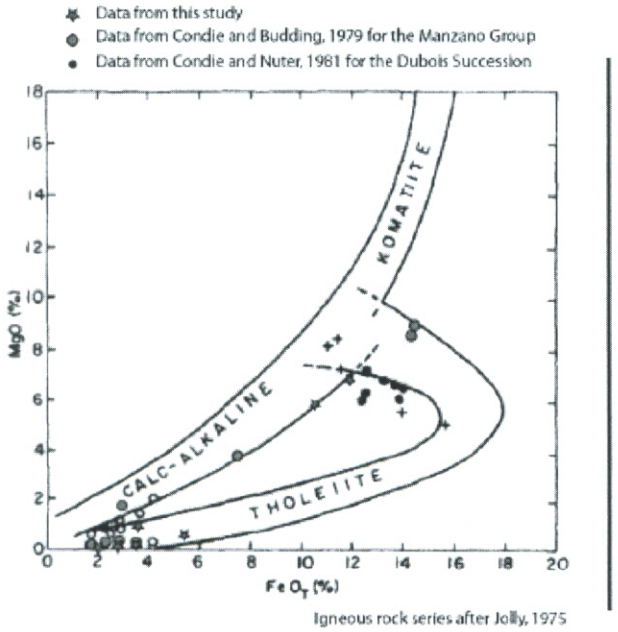

Igneous rock series after Jolly, 1975

Figure 5. Bulk major element geochemical data from the Los Pinos Mountains from this study and compared to geochemical data from Condie and Budding, 1979 and Condie and Nuter, 1981. Data from this study are labeled, and the black dots represent geochemical data from Condie and Budding, 1979. Red stars represent data from this study and are compared to Condie and Budding, 1979 (green dots) and the rest of the data is from another bimodal sequence, the Dubois succession of Colorado (Condie and Nuter, 1981).

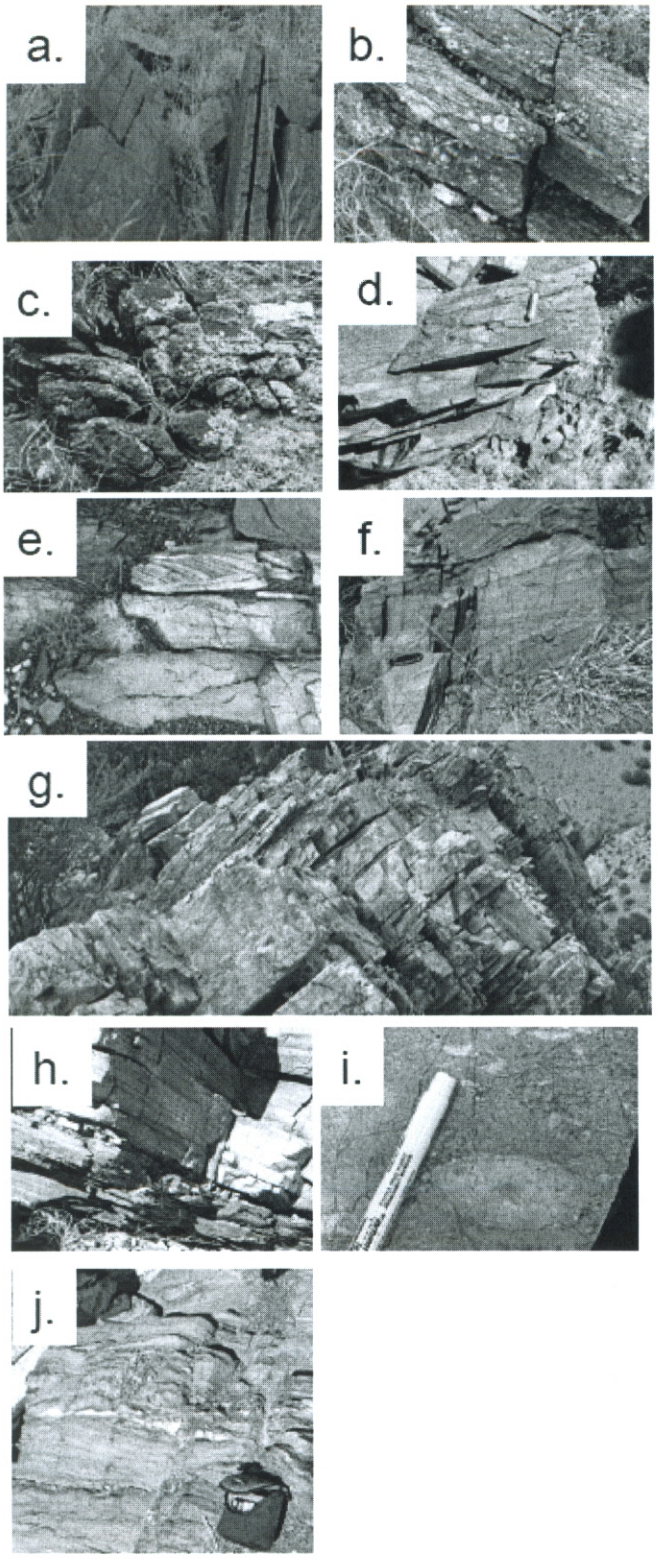

Figure 6. a) Outcrop photograph of the Sevilleta metarhyolite. b) Photograph of the Lacoracah metadacite unit showing cm- scale igneous feldspar grains. c) Outcrop photograph of a gabbroic amphibolite. d) Outcrop photograph of the Abajo lithic arenite. Cross bedding is shown in this photograph. The white mineral is plagioclase feldspar, similar in size and character to those of the Sevilleta metarhyolite from which this sedimentary rock likely was derived. e) Photograph of the White Ridge quartzite unit with overturned cross beds. f) Photograph of the White Ridge quartzite with a series of cross bedded layers. g) Photograph of the Sais quartzite illustrating the massive ridge forming characteristic of this unit. h) Photograph of the Blue Springs schist in contact with the overlying Sais quartzite. These units are strongly overturned and have a gradational contact. i) Photograph of the Blue Spring Rhyolite with cm-scale lapilli indicative of the extrusive nature of this unit. This is also the sample used for Jones' zircon geochronology (Jones et al., 2005). j) Photograph of the Blue Springs upper schist which it's characteristic blue color.

muscovite, and some feldspar are also present in this unit. Stretching lineations of the Sevilleta metarhyolite are well developed and are defined by stretched plagioclase and garnet. The contact between the Sevilleta metarhyolite unit and the Los Pinos pluton seems to be gradational, and is indistinguishable in this region. This relationship suggests a possible shallow level plutonic-caldera succession.

The 1000-1200 m thick Abajo lithic arenite (the Mixed Flow unit of Myers et al. (1981)) in the Los Pinos Mountains is composed of lithic arenite, and intercalated amphibolites, metarhyolites and quartzo-feldspathic schists. This unit is designated the Abajo lithic arenite in the Becker quadrangle map (plate 1). This sequence is the transition between bimodal volcanic rocks and sedimentary rocks in the Los Pinos Mountains, and these quartzo-feldspathic sedimentary rocks are interpreted to be genetically related to the underlying Sevilleta metarhyolite. Quartz grains are well rounded, and can be up to 2 mm in diameter. The lithic arenite also contains layers with millimeter-scale compositional bands of hematite, oxides and quartz. The lithic arenite is a massive, resistant quartz- and feldspar-rich sedimentary unit with preserved cross-beds (Figure 6d). Interbedded amphibolites are fine-grained and rich in hornblende, with some plagioclase and in some places quartz. These amphibolite layers are thin, usually only about a meter thick. The amphibolites include fine-grained rocks that contain amygdules and are interpreted to be metabasalt flows that are interlayered with coarse-grained gabbros that are interpreted to be sills and dikes. Major element chemistry (see Table 4) from typical amphibolite samples from this layer indicates that these are metabasalts and meta-basaltic andesites. Thin, 50-250-m thick quartz-muscovite-biotite-garnet-chlorite ± staurolite schists are found locally. All contacts between layers are transposed into

parallelism with S_2. The lithic arenite has a gradational contact with the overlying White Ridge quartzite.

The White Ridge quartzite (600-700-m thick) is a sequence of metamorphosed quartz arenites containing > 95-99% quartz and small amounts of oxides and chlorite or muscovite. Accessory minerals include zircon, epidote, and monazite. These crop out as thick, resistant units with preserved cross-bedding (Figure 6e,f) and weather to grey, red, and purple. Most quartz grains recrystallized and are difficult to recognize in hand sample, but some 2-4 mm rounded and flattened quartz grains are discernable. The basal layer is coarse-grained, and this unit is more oxide-rich than the Sais quartzite. Interbedded schists are also quartz rich, weather brown and contain chlorite and muscovite. 125-175-m thick Estadio schist marker bed is a quartz-chlorite schist, and marks the division between the White Ridge quartzite and the Sais quartzite.

The 650-750-m thick Sais quartzite is also a metamorphosed quartz arenite. The base of this unit is massive and defines the ridge in the Los Pinos Mountains (Figure 6g). This unit weathers grey at the base and weathers more pink to white higher up the section. Some regions contain 6-8 cm beds defined by cross-beds and hematite-rich layers. Relict quartz grains can be seen in some hand samples and are well rounded, and are only 1-2 mm. This quartzite contains large regions fractured and filled by quartz veins (Figure 6h).

The upper Manzano Group unit is the ~1500-1800-m thick Blue Springs Formation consisting of 3 informal members: 1) schist/quartzite, 2) rhyolite, and 3) phyllite. The lower schist member (Figure 6i) is a green to brown chlorite-muscovite schist with a fine-grained matrix of quartz and feldspar. Garnet porphyroblasts as large as

2 mm in diameter are common. Some millimeter-sized plagioclase grains are also found in hand sample and has millimeter-scale compositional bands. The lower schist is interbedded with thinly bedded medium grained quartzite and a discontinuous hematite-rich quartzite near the Priest pluton (Baer, 2004). Above this schist is the 1600 +4/-3 Ma Blue Springs rhyolite member, which is brown to orange in outcrop and has pink streaky quartzo-feldspathic compositional bands in some cases (Figure 6j). The rhyolite is composed of a quartzo-feldspathic matrix, with biotite, epidote, and oxides. Primary features such as lapilli (Figure 6k) indicate the extrusive nature of this unit. The upper phyllitic member, which cores the Manzano Peak synclinorium (mapped as Upper Blue Springs schist), contains quartz and feldspar with chlorite, biotite, clinozoisite, hematite, carbonate, and tourmaline. This schist weathers to green, blue-green, and brown, and is generally very fine-grained with garnet porphyroblasts up to 1 m in diameter.

Intrusive units

Los Pinos pluton

The Los Pinos pluton crystallized at 1655 ± 3 Ma (Shastri, 1992) and intrudes the Sevilleta metarhyolite on the western edge of the Los Pinos Mountains (plate 1). Prior descriptions and modal abundance calculations from Beers (1976) indicate that this pluton has a granitic composition. The pluton is dominantly K-feldspar, quartz, and plagioclase, with some biotite, Fe-oxides, zircon, and garnet in pluton margins in agreement with Shastri (1992). This study focused primarily on the northern end of the pluton, and Figure 7 shows outcrop photographs with typical textures found in this region. The Los Pinos pluton weathers to pink, red and brown, and contains quartz grains that are generally 2-4 mm. K-feldspar is the dominant mineral. Miarolitic cavities (Figure

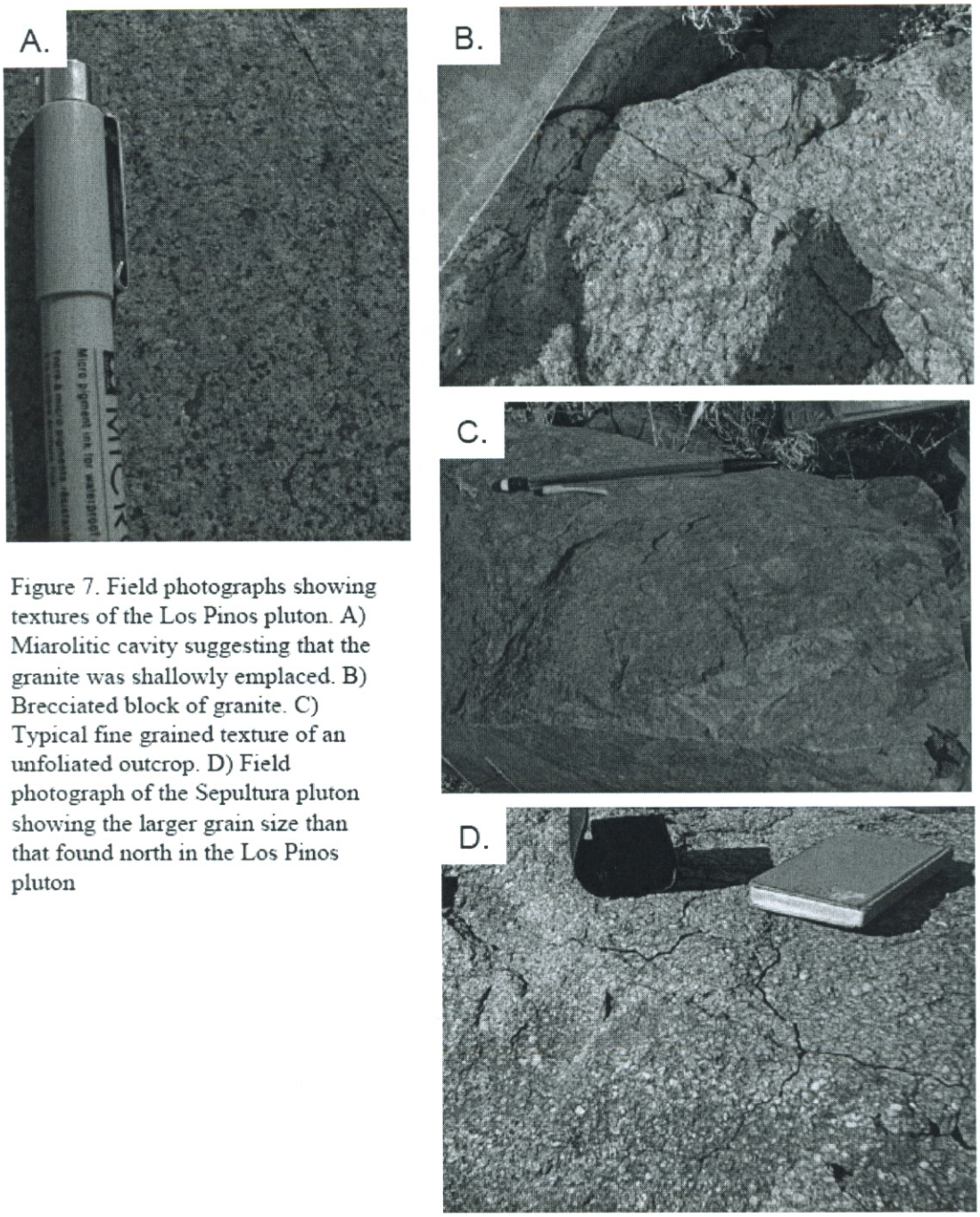

Figure 7. Field photographs showing textures of the Los Pinos pluton. A) Miarolitic cavity suggesting that the granite was shallowly emplaced. B) Brecciated block of granite. C) Typical fine grained texture of an unfoliated outcrop. D) Field photograph of the Sepultura pluton showing the larger grain size than that found north in the Los Pinos pluton

7a) found in the northern part of the pluton indicate that this area was possibly a hypabyssal intrusion, which is also supported by the fine-grained nature of the pluton. The southern end of the pluton is equigranular to massive (Shastri, 1992). Variable textures are found in samples from different regions of the pluton. Relatively undeformed regions of the fine-grained plutonic samples have K-feldspar with a myrmekitic texture. The outer edge of the pluton has local breccia zones that may be related to emplacement of the granite (Figure 7b, d). Pegmatite and aplite dikes intrude the Sevilleta metarhyolite and are common in the units exposed in Bootleg Canyon. Quartz veins are also found in these regions and generally trend parallel to the S_2 fabric. This pluton falls into the high-silica group from bulk geochemical data from Condie and Budding (1979), that is characterized by high SiO_2 (73-78%), unusually low Mg contents ($\leq$ 0.2%) and has moderate K_2O (3.5-5%) and low CaO (0.5-1.0 %). These data agree with one new analysis of major element geochemical data from this study (Table 4). The Sevilleta metarhyolite has very similar chemistry (as also shown by Condie and Budding, 1979). These geochemical similarities and the overlap of ages may indicate a possible genetic relationship between this plutonic body and the extrusive rocks it intrudes, and therefore I interpret the pluton to be the subvolcanic equivalent to the Sevilleta metarhyolite.

Sepultura pluton

The exposure of granite south of Bootleg Canyon is mapped as the Sepultura pluton (Myers et al., 1986), however, Shastri (1992) and Myers et al.(1986) found no discernable difference between this intrusive body and the Los Pinos pluton. Prior distinction of these two granites was based on Rb-Sr ages of 1601 ± 239 Ma for the Los Pinos pluton and 1350 ± 150 Ma for the Sepultura granite (Brookins et al., 1980).

However, new and more precise U-Pb zircon ages were obtained for both of these plutons of 1655 ± 3 Ma for the Los Pinos pluton and between 1630 Ma and 1653 Ma for the Sepultura pluton (Shastri, 1992). Therefore, this study refers to them as one intrusive body. This unit is more coarse-grained than the northern part of the Los Pinos pluton and contains 1 cm K-feldspar phenocrysts sometimes with rapikivi texture, and some schlieren (Figure 7d).

STRUCTURAL GEOLOGY OF THE LOS PINOS MOUNTAINS

The goal of this section is to describe overprinting relationships of tectonic fabrics and document the relative timing of plutonism and fabric formation in order to understand the deformational history of Proterozoic rocks of the Los Pinos Mountains.

D_1

The first phase of deformation (D_1) involved layer-parallel thrusting and isoclinal folding of S_0. S_0 (primary layering) is recognized by relict primary features such as compositional banding in schist and rhyolite units (Figure 8a, b) and cross-beds in quartzite. S_0 has been transposed sub-parallel to S_1 except in the hinges of F_1 folds (Figure 8c, d). These are tight to isoclinal, upright folds, and can be found throughout the Manzano Group strata. The average S_1 orientation is north-northeast striking and fans from moderately west dipping to steeply west dipping downsection. Figure 12 shows a stereonet of poles to S_1.

Microstructurally, the S_1 fabric is defined by quartz-mica domains and an alignment of mica, oxides, quartz, and feldspar. Figures 9a and 9b show photomicrographs with overprinting relationships from the upper Blue Springs schist near the syncline axis and from the Abajo lithic arenite. In the schist sample, the compositional band S_0 is at a low angle to S_2, but a high angle to S_1 inclusions in biotite porphyroclasts. S_1 and S_2 are not well developed as separate fabrics in the more quartz-rich resistant layer, suggesting there is a rheologic control on fabric development. Figure 9d shows a rootless fold in the Blue Springs schist defined by compositional banding (S_0). The axial plane of this fold is subparallel to the limbs illustrating the isoclinal nature

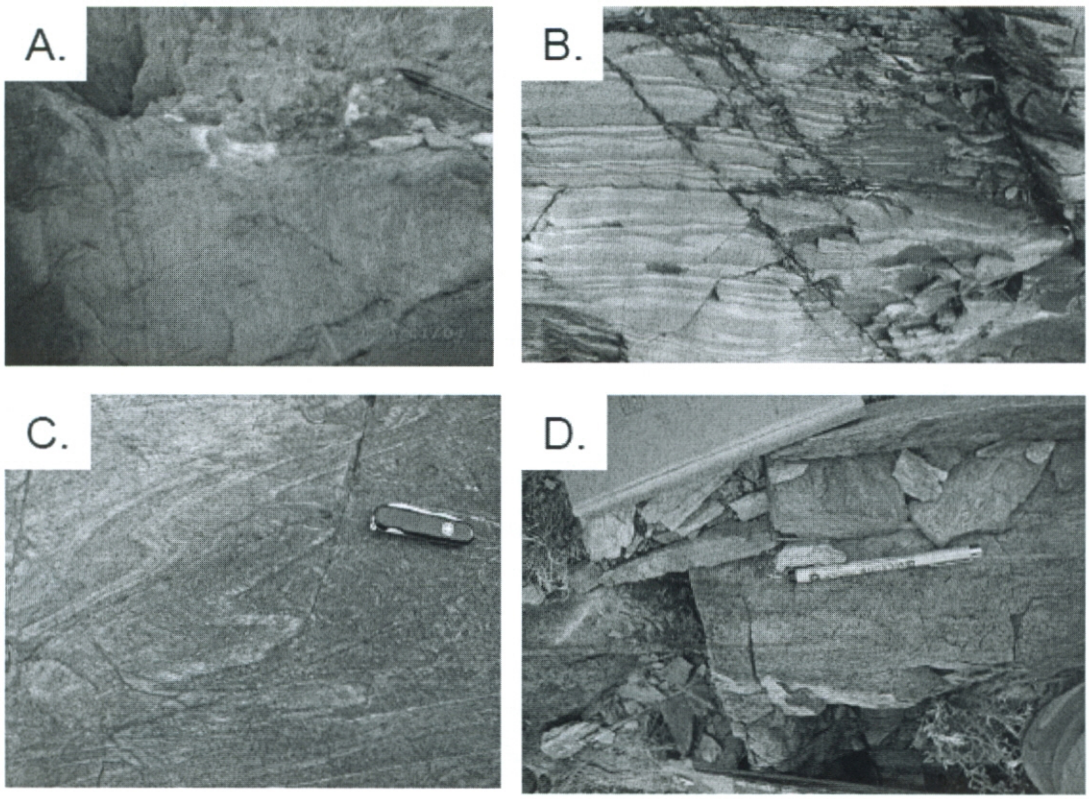

Figure 8. Field photographs of S_0 (primary compositional banding). A) Vertical compositional bands in schist of the Bootleg Canyon sequence perpendicular to S_2 foliation. B) Compositional bands in the upper Blue Springs schist showing chlorite-rich and quartz- rich layers. C) F_1 folding primary banding in the Sevilleta metarhyolite, with S_0 sub-parallel to S_1. D) An F_1 fold in the Sevilleta metarhyolite unit.

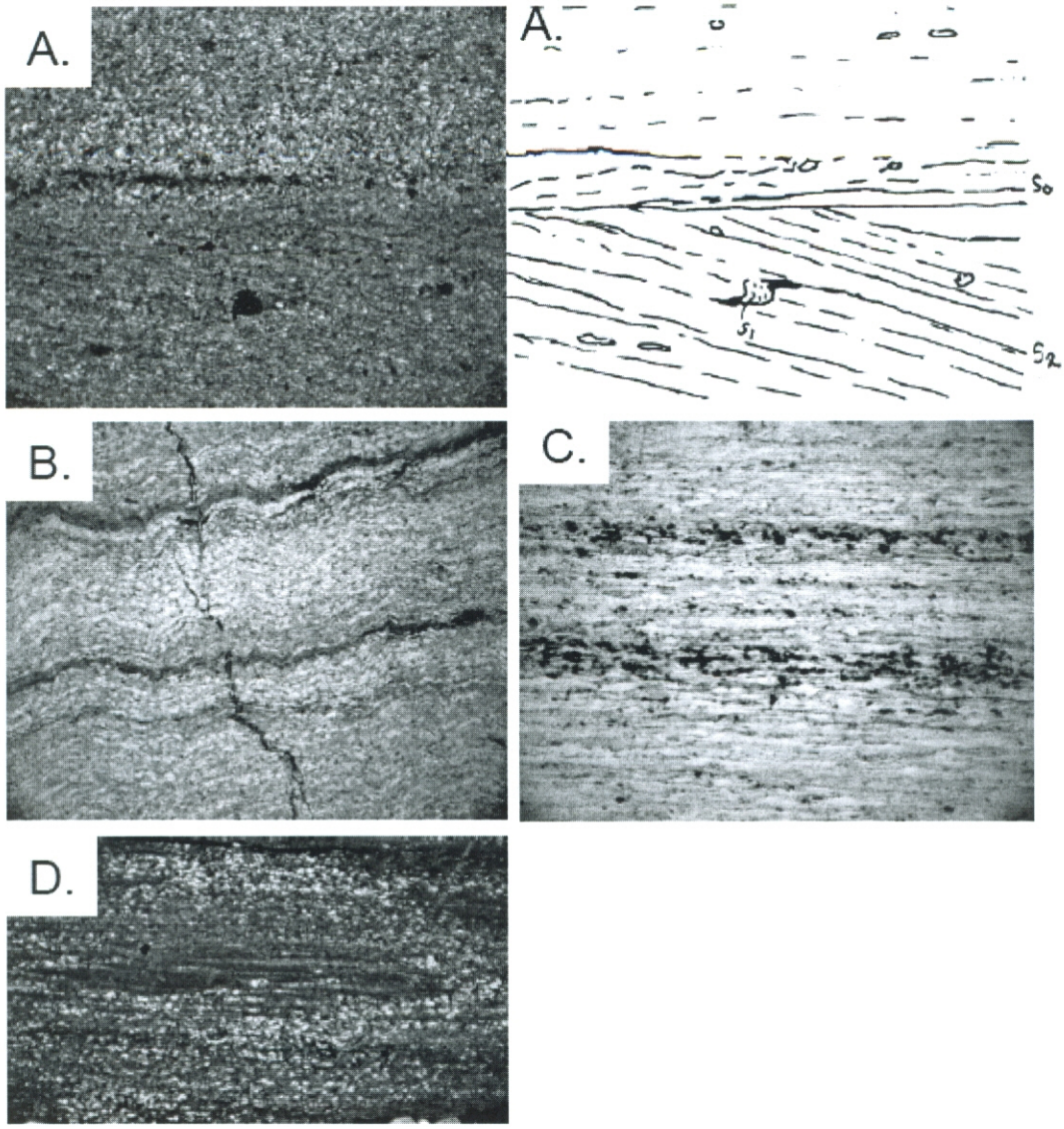

Figure 9. Photomicrographs showing S_0 and F_1 from the Los Pinos Mountains. (For further descriptions and oriented photomicrographs of each sample see appendix and sample locations are on plate 2.) A) Photomicrograph on the left and sketch of fabric relationships shown in this thin section of the Upper Blue Springs schist. S_0 and S_2 are at a low angle to one another and S_1 inside the biotite porphyroblast is at a high angle to S_0. B) Crenulation cleavage from a schist in the Abajo lithic arenite unit. Compositional bands are defined by quartz and mica layers. C) Compositional bands from the Abajo lithic arenite, and which are folded by F_1 in the hand sample, illustrating the difficulty of finding F_1 folds away from hinges. D) Rootless F_1 fold from the Blue Springs schist.

of many folds. In addition, in map scale, contacts between compositional units are subparallel to the S_2 axial planar cleavage of the dominant folds.

I infer D_1 to be progressive with D_2 deformation, as suggested by Bauer et al., (1993). The younger and older sequence of rocks in the Los Pinos Mountains both have S_1 and S_2 developed, but based on syntectonic 1655 Ma plutonism with D_2, this fabric developed in the older units before the upper part of the section was deposited. Therefore, S_1 and S_2 are interpreted to have formed progressively from before 1655 Ma and through 1600 Ma.

D_2

D_2 refers to the dominant deformational event in the Los Pinos Mountains that resulted in large macroscopic folds, transposition of earlier fabrics sub-parallel to S_2, and east-verging shear (west-side-up) on the steeply west dipping S_2 foliation. The Manzano Group in the Los Pinos Mountains is folded into a north-striking overturned syncline-anticline pair (F_2) (see plate 1, plate 2 and figure 10 for map and cross-section showing these structures). At the surface, the syncline folds the upper Manzano Group and is cored by the Upper Blue Springs Schist. This correlates to the Manzano Peak synclinorium of Baer (2004) and can be traced north along the thrust belt. This structure is truncated by the northern contact with the 1.43 Ga Priest pluton (Bauer et al., 1993). In the Los Pinos Mountains, cross-beds in quartzite units generally show younging towards the center of the syncline, with west-dipping layers on the west limb, indicating the overturned nature of the syncline. Repetition of the Blue Springs rhyolite and the Sais quartzite on the east side of the Los Pinos Mountains defines the hinge region of this macroscopic fold. S_1 and S_2 are at a high angle in the hinge, and in hinges of mesoscopic

Figure 10 **GEOLOGIC CROSS-SECTION FROM A TO A'**
Becker 7.5 minute quadrangle
Modified from Luther et al., 2005

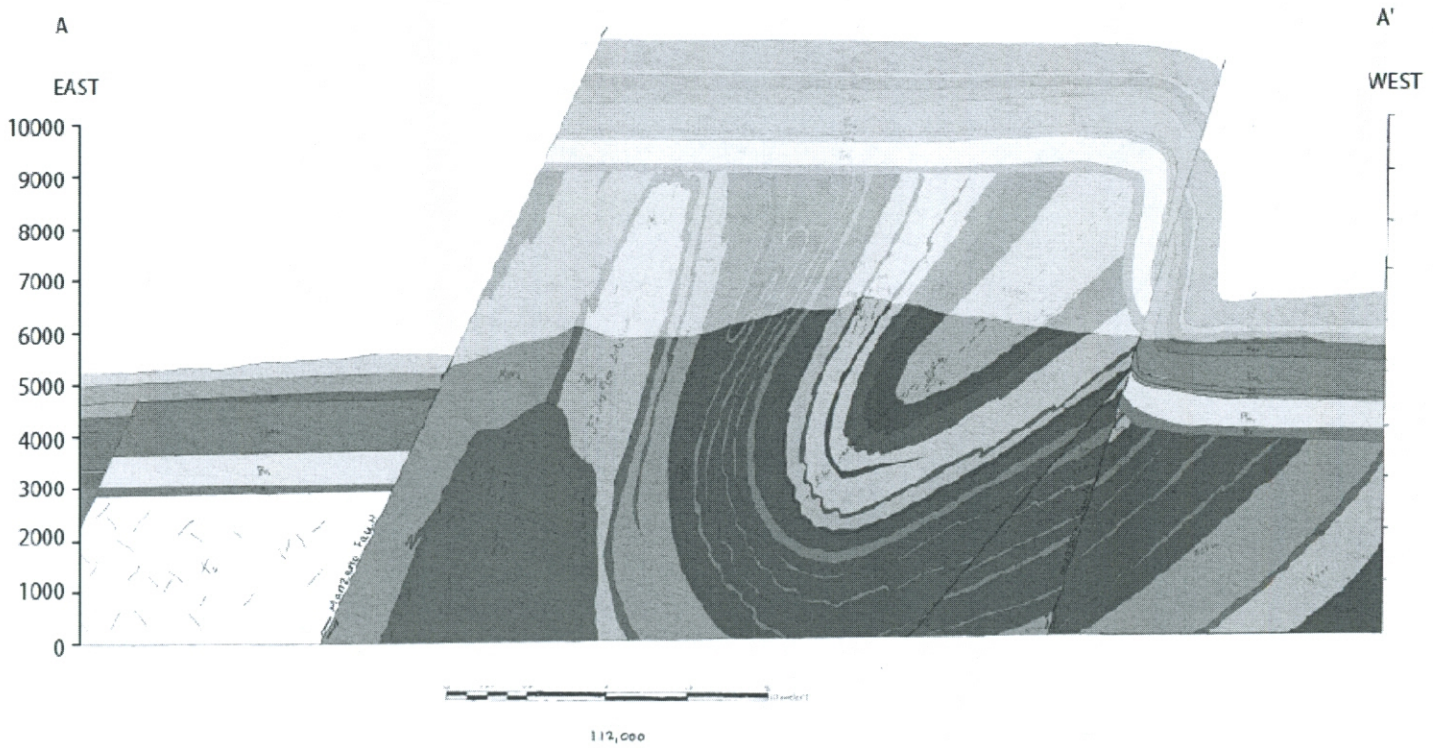

F_2 folds, but are subparallel everywhere else. The Los Pinos anticline, exposed in the older units of the Manzano Group, is cored by the lower Sevilleta metarhyolite, with an F_2 axial plane north of the Los Pinos pluton. Bootleg Canyon, in the middle of the pluton has metarhyolite and schist units exposed, which are interpreted to be older and core the Los Pinos anticline in this region. Evidence for the presence of the anticline is as follows: the exposed upper Sevilleta metarhyolite unit repeats itself, and repeating amphibolite layers provide good marker beds for recognition of this structure. The relationship between axial planar cleavage S_2, and S_0/S_1 changes from roughly perpendicular in the hinges to parallel in the limbs.

In the Sevilleta metarhyolite, S_2 is defined by a fine-grained quartz rich matrix, with biotite (and/or muscovite), plagioclase and quartz strongly aligned in S_2 in a slaty cleavage or a quartz-feldspar mylonitic fabric (Figure 11a and b). In more schistose units, quartz and mica domains define S_1 and have stage 2 to 3 differentiated crenulation cleavages with S_2 axial planes (Figure 11c). Some samples contain spaced anastomosing cleavages. Metasedimentary units contain aligned muscovite, oxide and quartz grains in S_2. Figure 11d shows quartzite with an F_2 fold in a schist interbed and an alignment of micas that wrap around the fold (S_1) and an S_2 axial planar cleavage. The amphibolite units have garbensheifer texture (Figure 11e) that seems to be oriented in two foliations at a high angle to one another based on the optical orientation biotite. Figure 11f shows S_1 and S_2 at an angle to one another, with S_2 axial planar to crenulations of S_1. Oxide porphyroclasts have quartz strain shadows only developed on one side parallel to S_2.

Figure 12b shows a stereonet projection of poles to S_2 with a mean axial plane of 208, 49 west, and the dip of this axial plane fans from steep to shallow up-section. The

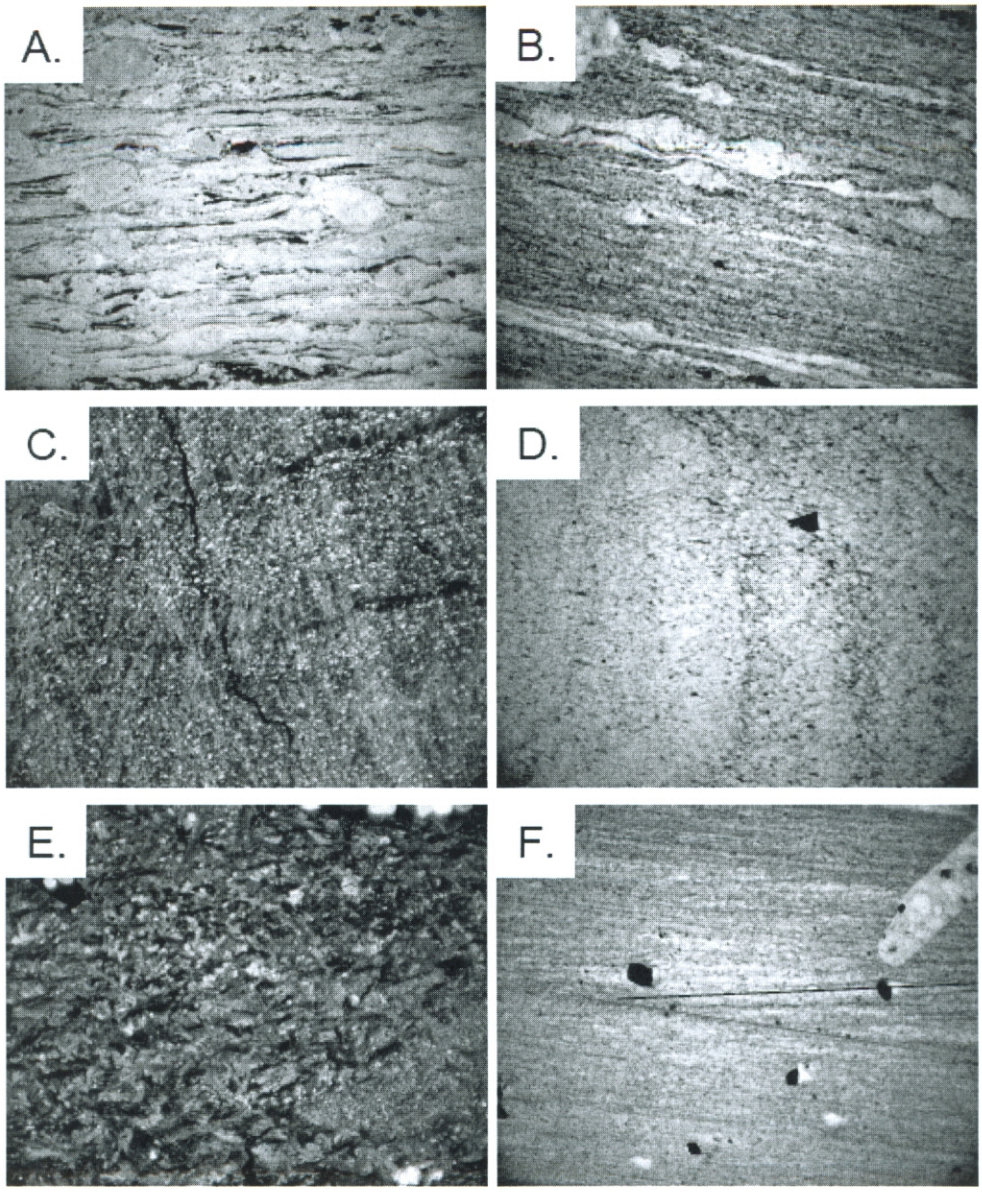

Figure 11. Photomicrographs of S_2 foliation and D_2 folds. A) Mylonitic fabric from the Sevilleta metarhyolite. B) Strong alignment of quartzo-feldspathic matrix with aligned plagioclase porphyroclasts in the Sevilleta metarhyolie. C) Crenulation cleavage of S_1 with S_2 axial planar cleavage. D) F_2 fold in a schistose unit in quartzite, folding quartz-mica domains (S_1). E) Garbenschiefer texture in amphibolite. F) S_1 shown in orange and S_2 in black. S_2 is the axial plane of crenulations in schist unit. Tails on oxide porphyroclasts aligned in S_2 foliation.

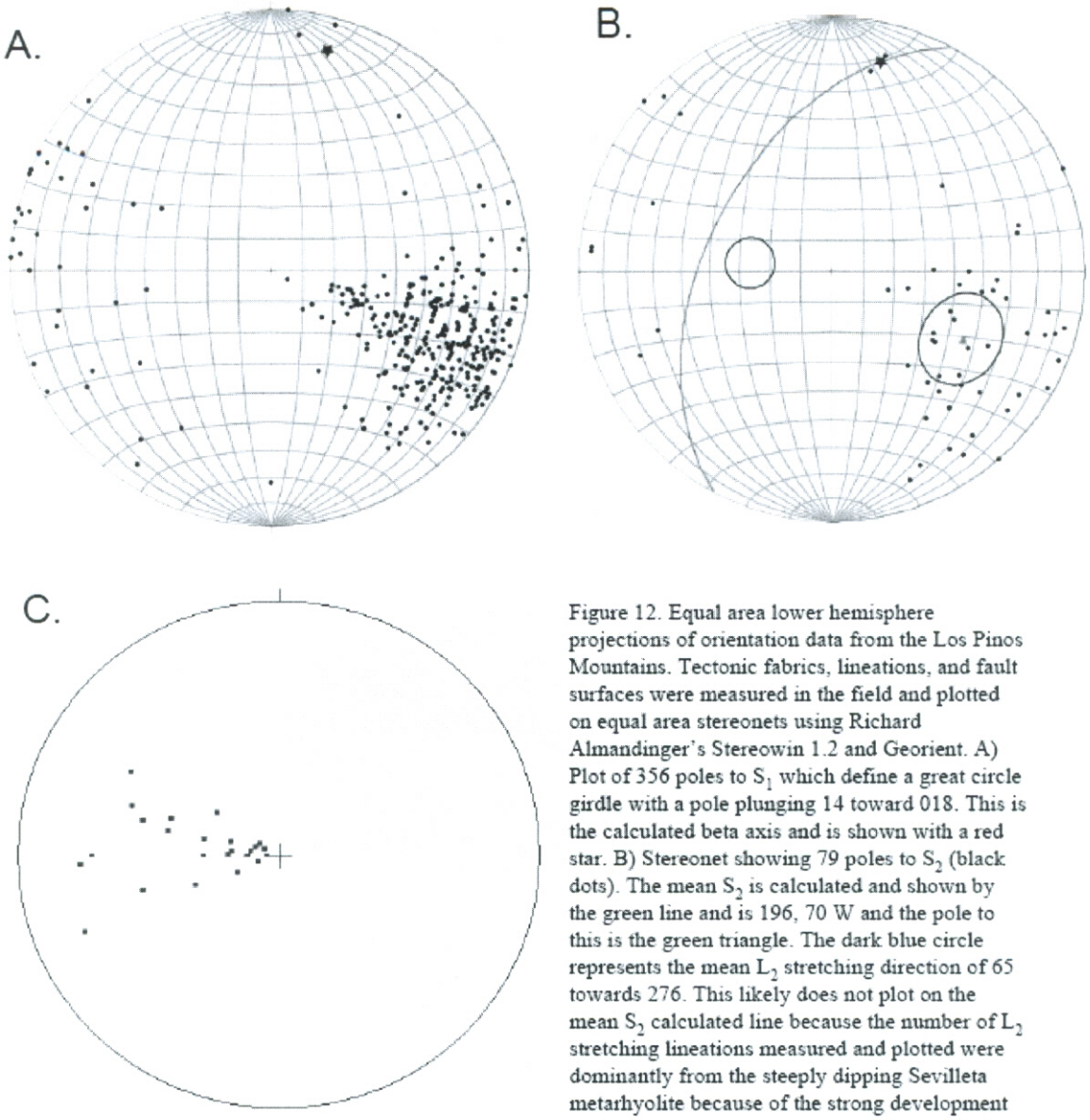

Figure 12. Equal area lower hemisphere projections of orientation data from the Los Pinos Mountains. Tectonic fabrics, lineations, and fault surfaces were measured in the field and plotted on equal area stereonets using Richard Almandinger's Stereowin 1.2 and Georient. A) Plot of 356 poles to S_1 which define a great circle girdle with a pole plunging 14 toward 018. This is the calculated beta axis and is shown with a red star. B) Stereonet showing 79 poles to S_2 (black dots). The mean S_2 is calculated and shown by the green line and is 196, 70 W and the pole to this is the green triangle. The dark blue circle represents the mean L_2 stretching direction of 65 towards 276. This likely does not plot on the mean S_2 calculated line because the number of L_2 stretching lineations measured and plotted were dominantly from the steeply dipping Sevilleta metarhyolite because of the strong development in this unit. Therefore the sampling density of the two plots were not consistent (plot of the distribution of L_2 strech lineations is shown in stereonet C). The beta axis calculated from the first plot and represents the macroscopic fold axis of the large scale folds in the Los Pinos Mountains, and does plot on the calculated S_2 axial plane of these folds.

macroscopic fold axis calculated from S_1 foliation measurements plunges 16 towards 014 (shallowly to the north). Figure 12c is a stereonet projection of stretching lineations on S_2 which all point in the down-dip direction ranging from ~265-285° and from shallowly plunging to subvertical, indicating D_2 east-west shortening. The mean S_2 lineation is 65 toward 275 (west), indicating an approximately dip parallel elongation direction.

D_{2b}

D_{2b} structures are defined as those that folded or reactivated D_2 fabric elements, but have the same orientation of axial planes and fold axes as D_{2a} folds. Examples of F_2 folds are shown in Figure 13, ranging from large, tight folds in quartzite units (13a), folded crenulation cleavages (13b) and tight chevron folds (13c) in schistose units. Fold axes from the western limb of the syncline are plotted on Figure 14, as well as their vergence. This plot shows that these folds have been rotated during progressive thrusting, based on a Hansen analysis (Hansen, 1971). These folds have been rotated clockwise in the north and counterclockwise in the south along a great circle girdle that is sub-parallel to S_2. Figure 15 shows a photograph and sketch of an outcrop with rotated folds to illustrate this relationship. These folds are interpreted to be related to thrusting along S_2 as a part of D_{2b}. The east-vergencing folds are inconsistent with the top-to-the-east interpretation for F_1 (Doran, 2002). Similarly, these are not considered to be parasitic to the macroscopic F_2 folds because their vergence is not consistent with that of the large scale fold. Thus, these folds are consistent with west-side up shearing which is also seen in microscopic evidence.

Shear sense microstructures indicate west-side-up (top-to-the-east) shearing on steeply west-dipping S_2 throughout the supracrustal sequence in the Los Pinos

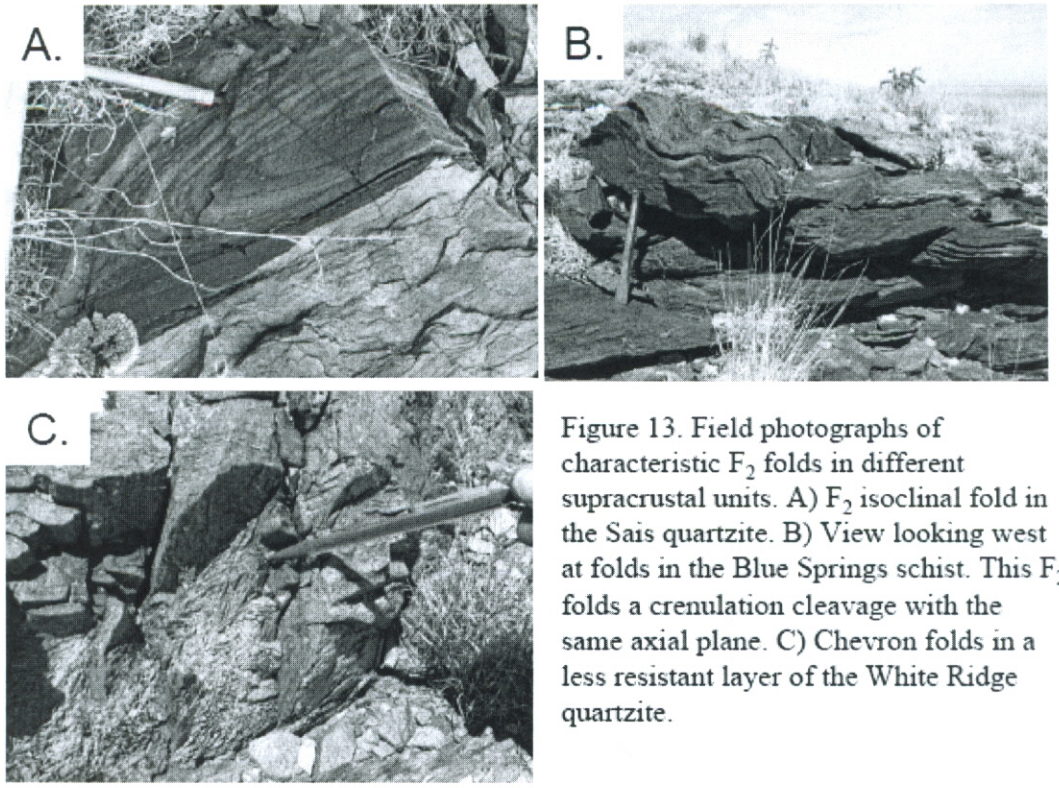

Figure 13. Field photographs of characteristic F_2 folds in different supracrustal units. A) F_2 isoclinal fold in the Sais quartzite. B) View looking west at folds in the Blue Springs schist. This F_2 folds a crenulation cleavage with the same axial plane. C) Chevron folds in a less resistant layer of the White Ridge quartzite.

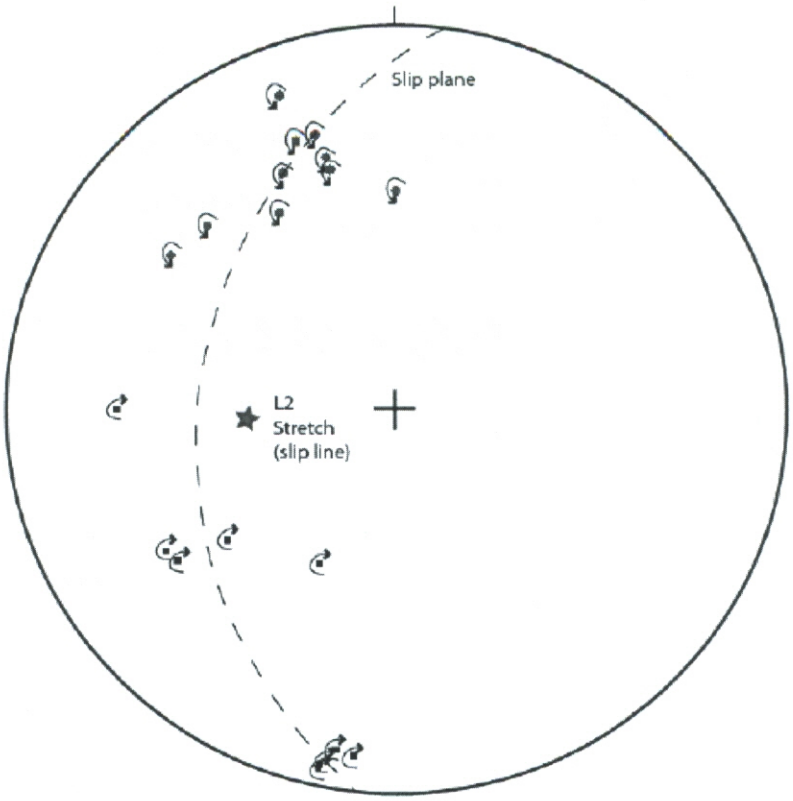

Figure 14. Hansen analysis (Hansen, 1971).
Equal area projection of F_2 fold axes. Z-folds shown in purple have a counterclockwise vergence. S-folds shown in black and have a clockwise vergence. Both sets of folds have a west-side up vergence, and the mean L_2 stretching lineation is the slip line. These folds have been rotated during progressive shear.

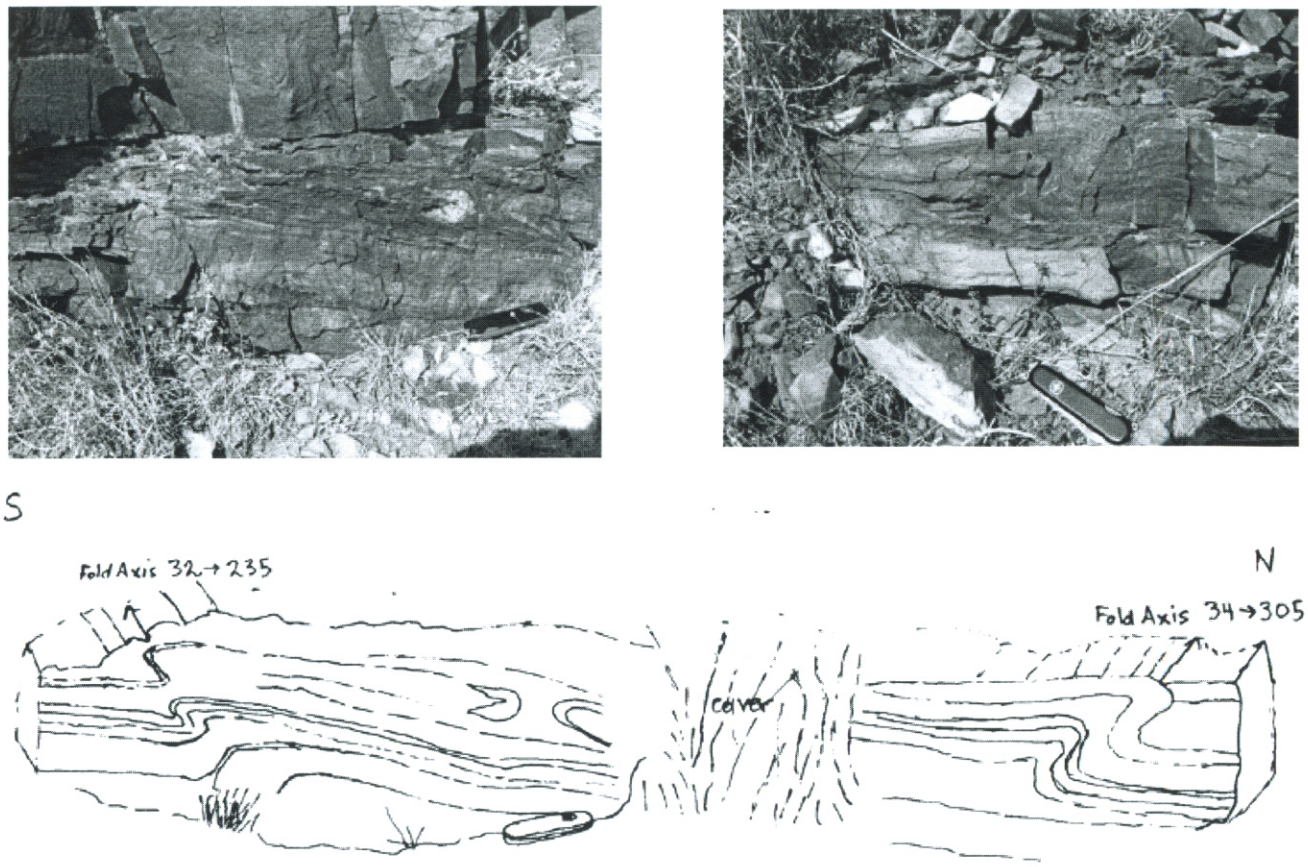

Figure 15. Field photo and sketch of an outcrop in the Blue Springs schist showing progressively rotated folds

Mountains. Plate 1 contains sample locations and Figure 16 depicts samples in their correct orientation and showing the shear sense indicator (see Appendix 2 for detailed descriptions of each sample studied for this project). A few kilometers north of the Los Pinos pluton a delta garnet clast shows top-to-the-east shear in the upper Sevilleta metarhyolite. This unit also contains numerous porphyroclasts with tails that are generally ambiguous or symmetric, indicative of either intense shear or a compenent of pure shear. Moving up section, the Abajo schist (sample BQAL-10) has a synthetic offset in plagioclase in addition to being a sigma clast, and both kinematic indicators show west-side-up shear. The next sample shows an S-C fabric from the White Ridge quartzite, showing S_1 at an angle to S_2 and a relict grain with a west-side-up sigma clast. In the youngest exposed unit, the upper Blue Springs schist is a sample with west-side-up shearing on a biotite porphyroblast indicated by the strain shadows. These samples indicate that thrust-sense shearing occurred during D_{2b} because the shearing takes place on already formed S_2.

Metamorphic porphyroblasts from samples in the Los Pinos Mountains include garnet and biotite. Garnet growth is common in metarhyolite and schist, and these are generally less than 1 mm. Garnet inclusion trails vary from those that include internal S_1 inclusion trails perpendicular to the S_2 matrix fabric to fabrics that are only slightly deflected from that of the matrix. Garnet overgrows S_1 and S_2 in a schist from within a km of the pluton (Figure 17a), and is interpreted to be syn-tectonic based on the inclusion of both S_1 (quartz and mica domains) and S_2 (axial plane of crenulation cleavage), yet, S_2 is more strongly developed in the matrix. In one sample from the Abajo lithic arenite (Figure 17b), garnet growth is interpreted to be syntectonic with D_2 based on the

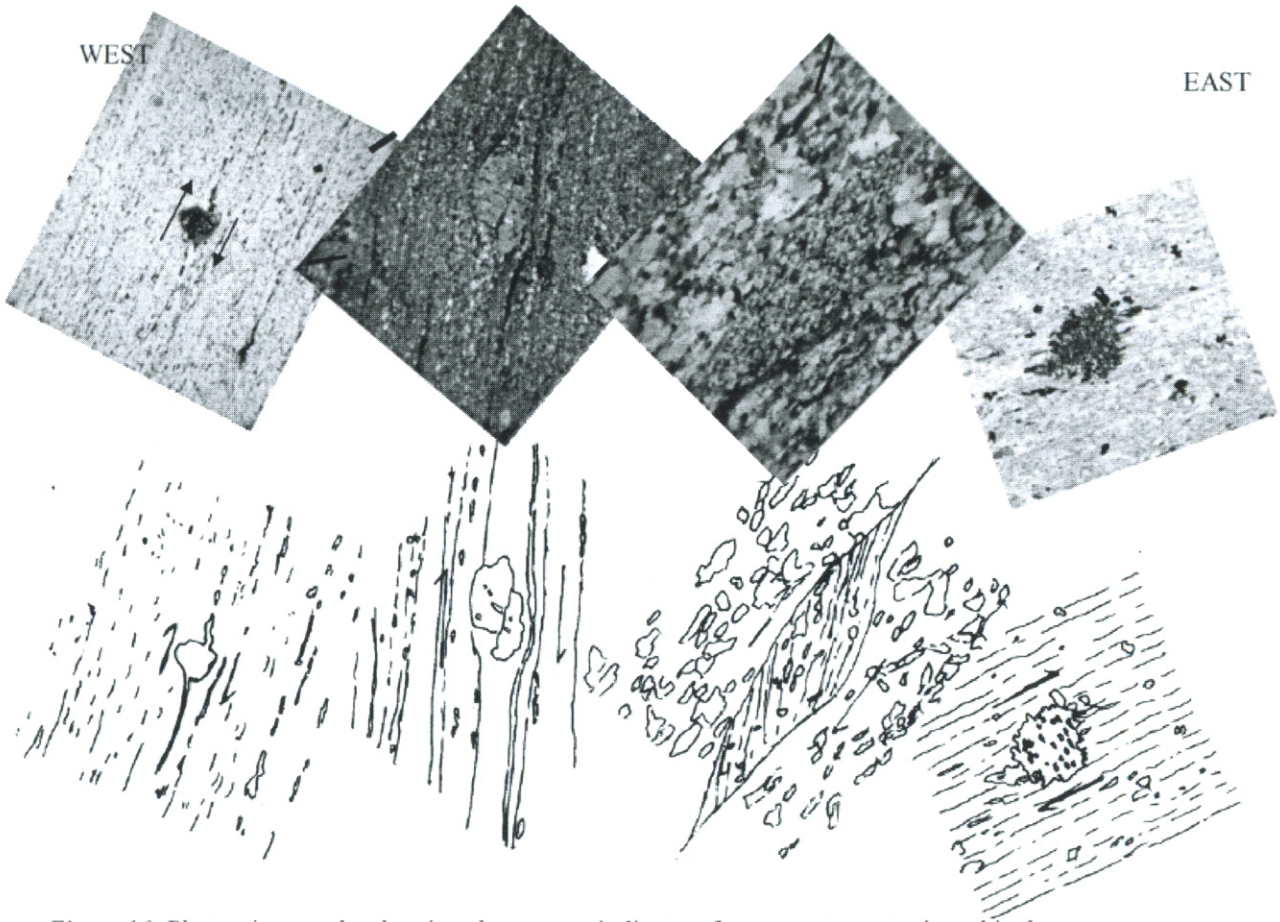

Figure 16. Photomicrographs showing shear sense indicators from west to east oriented in the cross sectional view at the correct dip. Each shows west-side up shear related to D_{2b}.

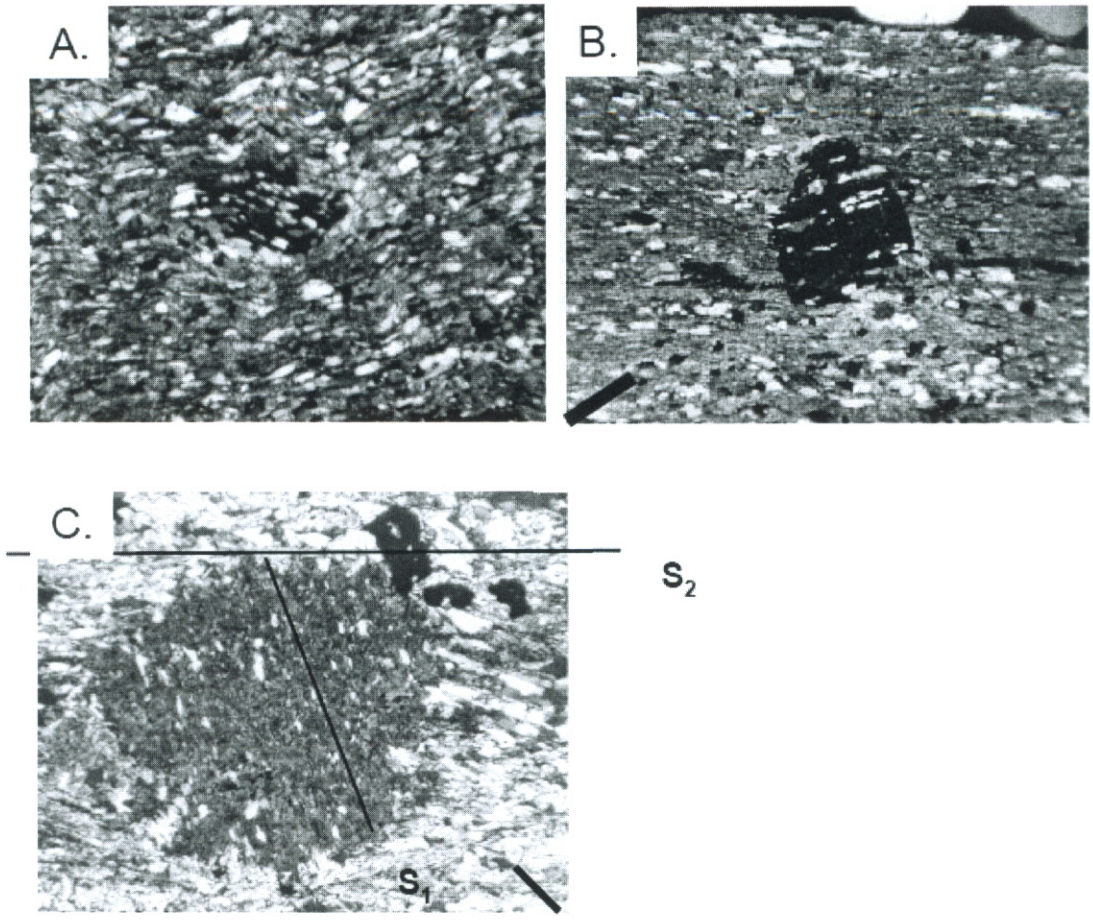

Figure 17. A) Post-S_1 and post-S_2 garnet porphyroclast. B) Rotated syntectonic D_2 garnet porphyroclast with internal inclusion of S_2. C) Syntectonic biotite porphyroclast which includes S_1 at a high angle to S_2.

inclusion of S_2 and with continuous strain has been rotated. Garnets within 50 m of the pluton contact overgrow S_2 with no deflection of the fabric, indicative of post-S_2 growth. In this same sample brittle offset of plagioclase indicates deformation at a low temperature, indicating that deformation occurred at high and low temperatures. In the upper Blue Springs schist, biotite is aligned in S_2, but also includes a fabric perpendicular to the matrix fabric, interpreted to represent S_1 (Figure 17c). This biotite also has strain shadows indicating continued deformation after metamorphism.

Evidence for plutonism syntectonic with D_2

Timing of plutonism relative to deformation is an important constraint for assigning timing of orogenesis. Fabrics parallel to S_1 and S_2 are variably developed in the 1655 ± 3 Ma (Shastri, 1992) Los Pinos pluton. Stereonet data of S_2 measurements from the Sevilleta metarhyolite (~1662 Ma), the Blue Springs rhyolite (~1600 Ma) and the Los Pinos pluton illustrate the subparallel nature of the fabric in these units (Figure 18). In addition, shear zones in the pluton generally strike north with steeply dipping stretching lineations to the west, consistent with stretching lineations from the supracrustal sequence. The margins of the pluton are locally strongly sheared, whereas the interior of the pluton contains fewer shear zones. Petrographic data also show variable deformation across the pluton. A sample from the interior of the pluton contains feldspar with a myrmekitic texture (Figure 19a). Mylonitic fabrics in Figure 19b, c are from the margins of the pluton. Figure 19c shows a contact between the country rock and the granite with west-side-up shearing in both units. A sample along strike with the anticlinorium axis shows two fabrics at a high angle to one another (Figure 19d).

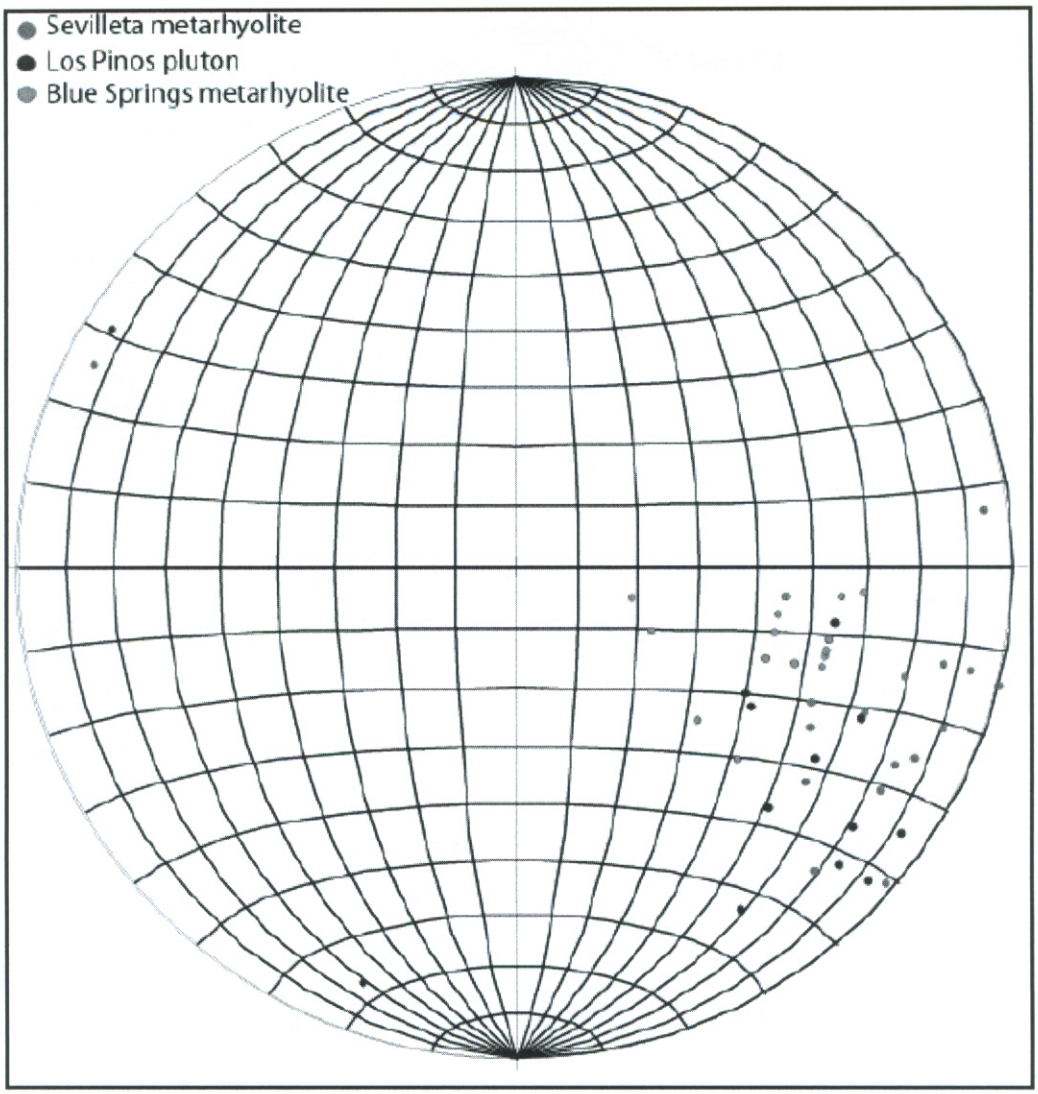

Figure 18. Lower hemisphere projection of poles to S_2 in the ~1662 Ma Sevilleta metarhyolite, ~1655 Ma Los Pinos pluton and the ~1600 Ma Blue Springs metarhyolite. These foliation measurements are subparallel indicating that S_2 is developed in the pluton and that this fabric is pervasive throughout the Manzano Group.

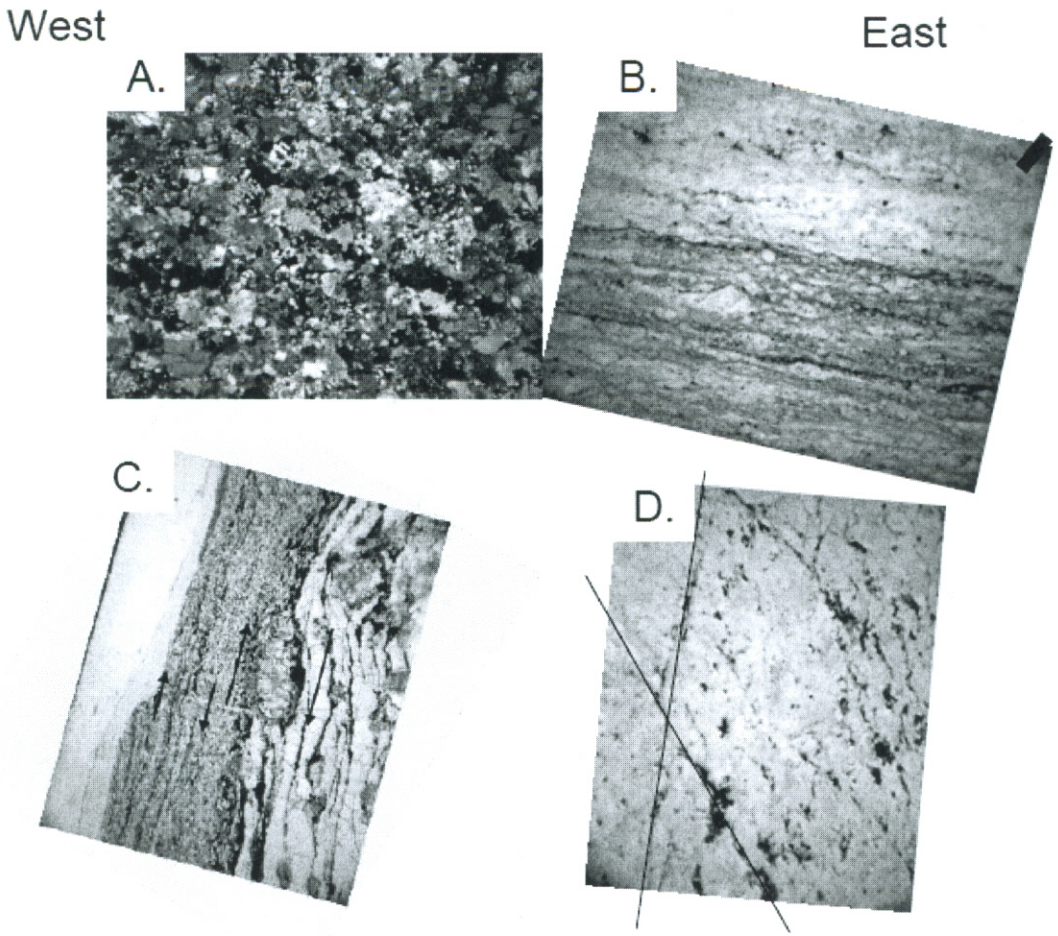

Figure 19. Photomicrographs of the Los Pinos pluton showing variably developed deformational fabrics. These thin sections are oriented in cross-sectional view. A) Unfoliated granite sample with myrmekite texture. B) Mylonitic foliation in the Los Pinos pluton. C) Mylonite fabric showing the contact between the Sepultura pluton and country rock. Both samples show west- side- up shear sense. D) Two fabrics developed in the Los Pinos pluton.

Syntectonic plutonism has previously been documented in the Manzano thrust belt for the 1646 ± 16 Ma Manzanita pluton (Brown et al., 1999). Bauer et al. (1993) and Shastri (1992) both conclude that the Monte Largo and Los Pinos plutons are either syn- or post-tectonic. Figure 20 illustrates a key area mapped for the purpose of this project that shows cross-cutting relationships from a small region southwest of Bootleg Canyon, which provides evidence that the Los Pinos pluton was emplaced syntectonically. The schematic map drawn for this figure illustrates the intrusive contact between the Sevilleta metarhyolite and the Sepultura pluton. As discussed earlier, contacts between the pluton and supracrustal sequence are commonly difficult to differentiate, however, in the region of this map, the granite is coarser-grained, and the presence of a volcanic conglomerate bed provides evidence that the pegmatites are intruding a supracrustal sequence. Figure 20a shows a folded aplite dike cross-cutting the S_2 foliation that is also folded and 20b is a field photograph of a folded aplite dike in a granite shear zone. Large pegmatite dike intrusions are parallel to the S_2 foliation. Xenoliths of foliated metavolcanic rocks are also found throughout Bootleg Canyon (Figure 20c). Some contain foliations parallel to magmatic fabrics or shear zones in the pluton, whereas some foliated xenoliths are contained in unfoliated regions of the pluton. Figure 20d is a photomicrograph of the foliation of a xenolith being deflected by the igneous growth of an undeformed K-feldspar grain, indicating that this foliation had formed prior to crystallization of this portion of the pluton.

Feldspar solid-state fabrics indicate variable temperatures of deformation even in the same thin section. Two photomicrographs from a sample taken from the same area as

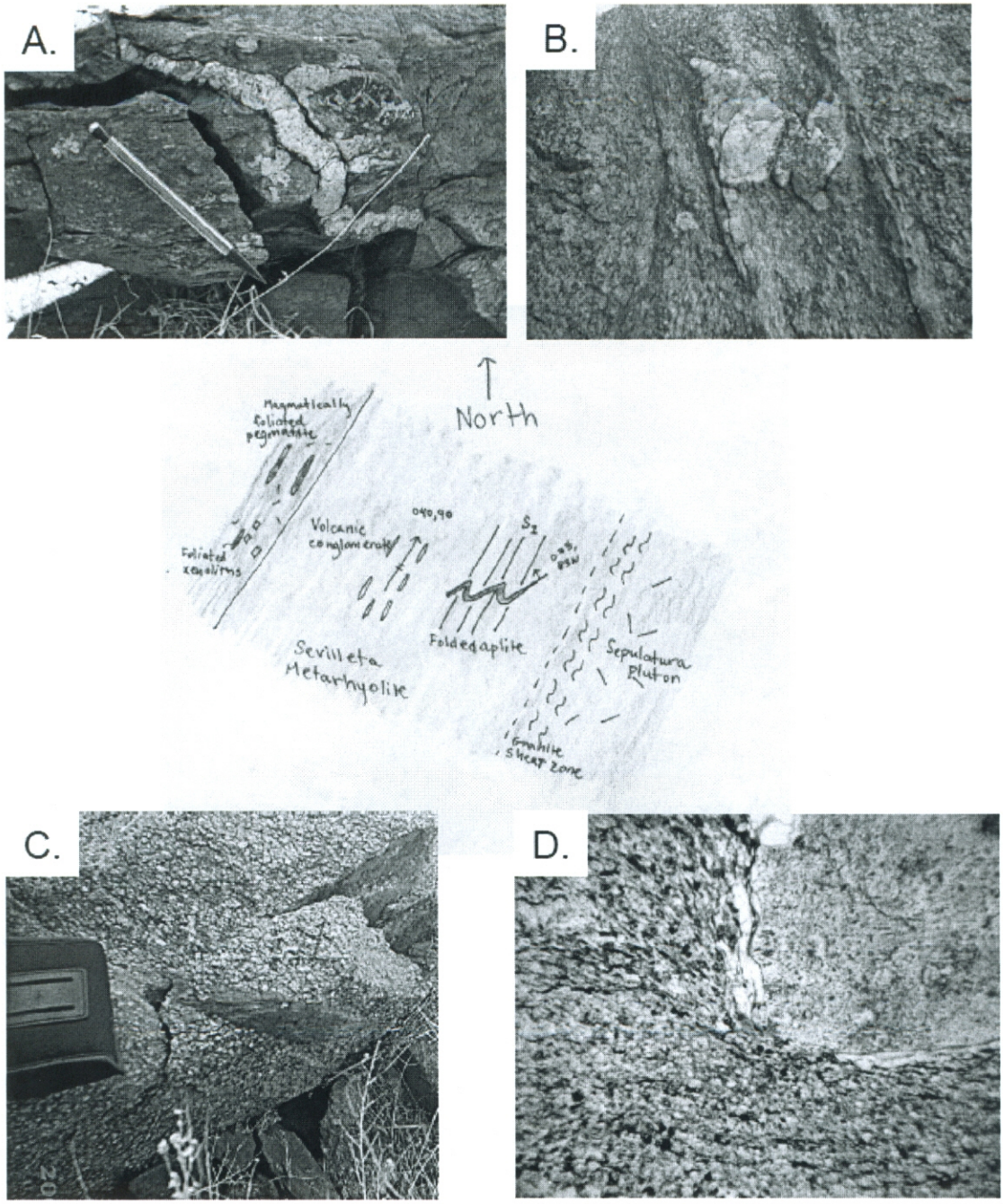

Figure 20. Schematic map illustrating syntectonic nature of 1.65 Ga magmatism in the Los Pinos Mountains (center). Photomicrographs document what is illustrated in the map. A) Folded aplite dike cross-cutting the S2 foliation. B). Folded quartz vein in granite shear zone. C) Foliated xenolith in magmatically foliated pluton. D) Deflection of S_2 foliation by igneous growth of feldspar.

the schematic map of Figure 20 and one from the center of the northern part of the Los Pinos pluton illustrate these variable temperature conditions. Figure 21a shows the brittle deformation of feldspar in a relatively undeformed matrix of myrmekite.

Photomicrographs b and c are from the same thin section, one with dynamic recrystallization of feldspar (shown by subgrain development) indicative of temperatures greater than 500° C (Hirth and Tullis, 1992); thin section c shows brittle deformation of feldspar that is indicative of temperatures less than 500° C (Hirth and Tullis, 1992). These four field and microstructural observations of cross-cutting relations and solid state deformation are interpreted to indicate that 1.65 Ga plutonism in the Los Pinos Mountains cooled through 500° C during D_2 deformation.

D_3

Overprinting of D_3 deformation in the Los Pinos Mountains is very weak, and very few outcrops contain three deformational fabrics. Therefore this section provides data only for deformational temperatures in the region, and then a discussion of Estadio Canyon and Abo Pass, two regions more strongly overprinted by D_3. Quartz and feldspar fabrics can provide insight into the relative temperature of deformation depending on strain rate. Two quartzite samples shown in Figure 22 have similar quartz deformation textures, and were analyzed using the regimes of Hirth and Tullis (1992). A sample from the White Ridge quartzite (Figure 22a) shows quartz grains that exhibit sweeping undulose extinction, a weak shape preferred orientation, and slight recrystallization of quartz grains around relict grain boundaries, indicative of temperatures of about 250° C. The sample from the Sais quartzite (Figure 22b) contains deformation lamellae, moderate grain shape preferred orientation with high axial ratios and some recrystallization around

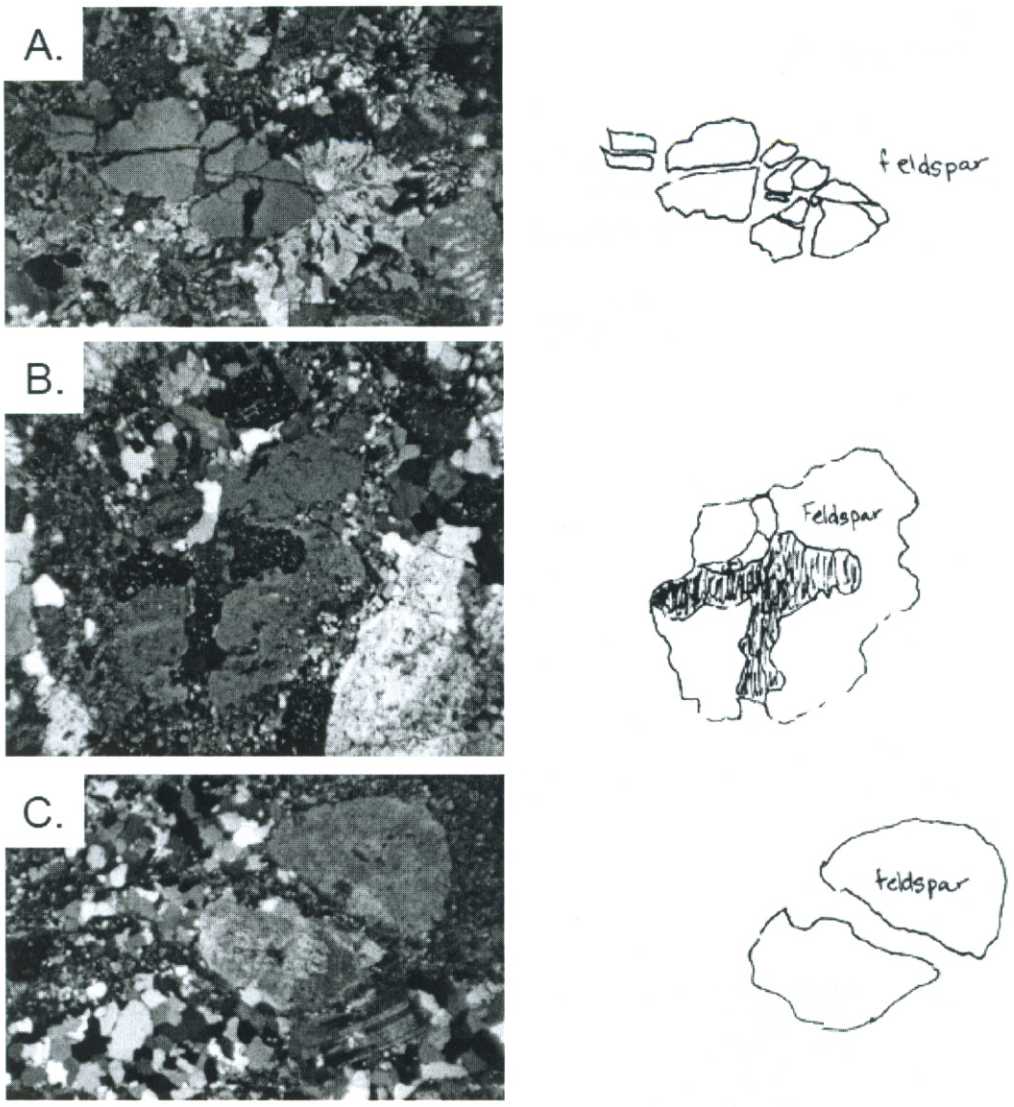

Figure 21. Photomicrographs and accompanying sketch of solid state deformation in feldspar grains from the Los Pinos pluton. Approximate deformation temperatures were obtained using quartz and feldspar dynamic recrystallization regimes of Hirth and Tullis (1992) and Smith and DePaor (1991). A) Brittle shattering of a feldspar grain. B) Subgrain development in feldspar grain from sample ALO6 CM-6. C) Brittle crack in plagioclase grain also from sample AL06 CM-6.

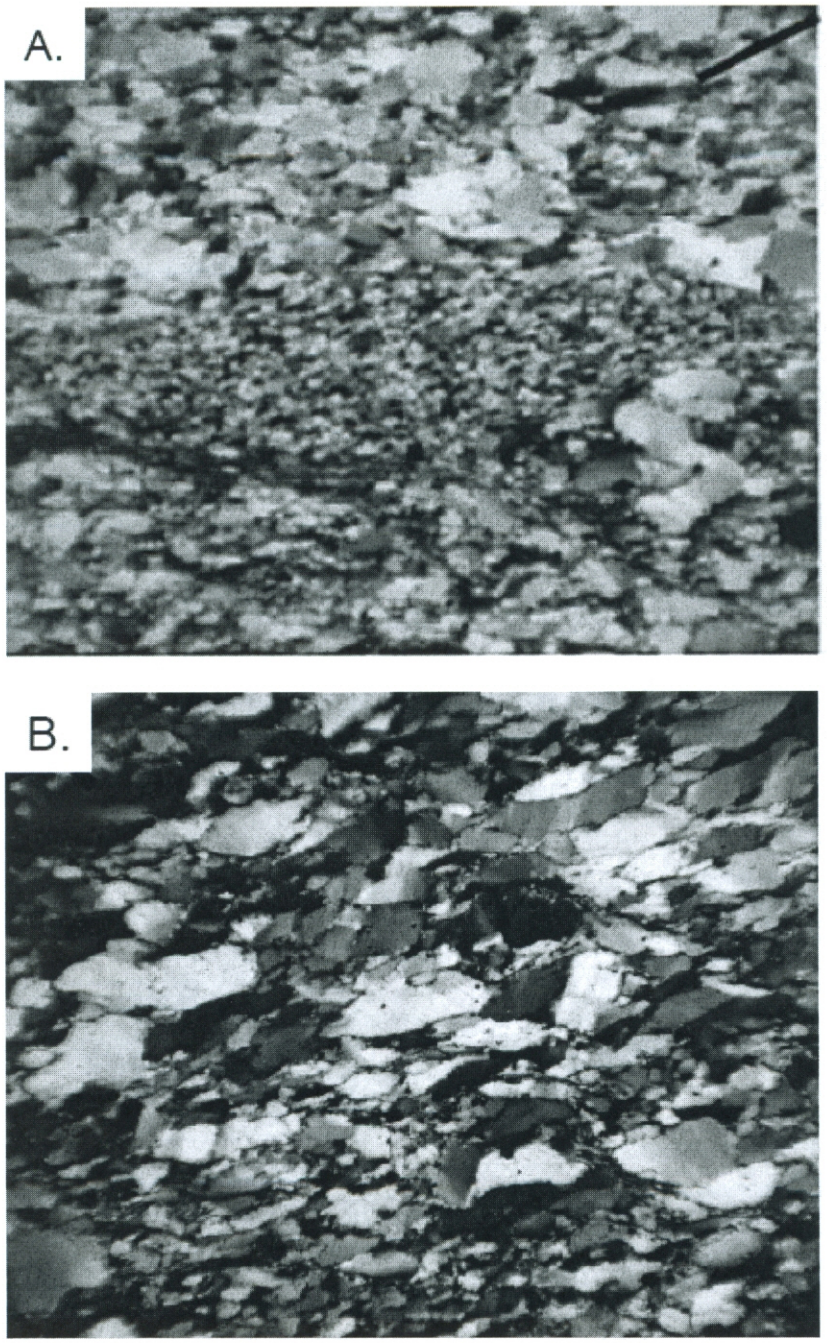

Figure 22. Quartz solid state deformation fabrics from quartz arenite units.

the rims of grains due to grain boundary accommodated dislocation creep. The lamellae indicates that deformation was slightly higher in temperature at about 300-350° C according to Hirth and Tullis (1992). The solid state deformation is relatively low temperature, and is likely related to D_3 because it was the last documented heating event in the region (Shastri, 1992).

Due to this weak development of S_3 in the Los Pinos Mountains and thus the lack of detailed structural data, a discussion of two key regions in the Priest pluton aureole is necessary to fully describe this deformational event. This region includes Abo Pass and Estadio Canyon, both within a kilometer of the Priest pluton. The purpose of this section is to describe data from this study that characterize the refolding of the Manzano Peak synclinorium by F_3, and illustrate the relative lack of D_3 deformation away from 1.4 Ga pluton aureoles.

The Estadio Canyon region exposes the upper part of the Manzano Group folded into the Manzano Peak synclinorium whose axial plane can be traced down the exposure of this structure in the Los Pinos Mountains. Two structural domains in this canyon have shallowly northwest dipping S_2 axial planes with S_1/S_2 intersection lineations and F_2 fold axes which plunge shallowly to the northeast and southwest on the northern half of the canyon, but plunge sub-vertically in the southern half due to refolding of this structure by F_3. Figure 23 shows the great circle distribution of these fold axes and the resultant F_3 fold axis with a sub-horizontal northeast trending fold axis. The trend of S_2 is north-northeast striking (subparallel to the Priest pluton contact) dipping moderately to steeply to the west. Intersection lineations (S_2/S_3) plunge shallowly north-northeast. Macroscopic folding in Estadio Canyon (the Estadio Canyon antiform of Baer (2004) is a synclinal

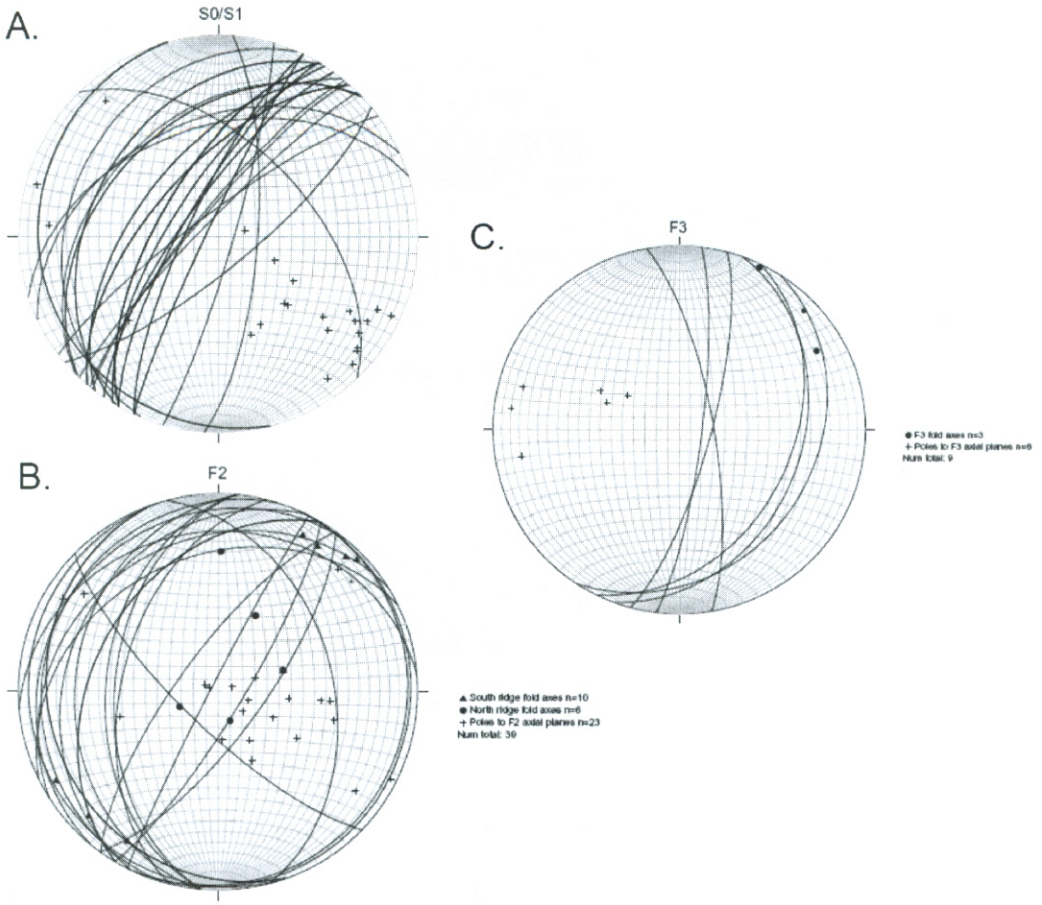

Figure 23. Lower hemisphere equal area projection of structural data from Estadio Canyon. A) S_0/S_1 strike northeast and dip shallowly to steeply to the northwest. B) F_2 strikes north and northeast and dips shallowly to moderately to the west. Fold axes generally fall along a northeast-southwest trending great circle. Axes on the north ridge are sub-vertical, whereas axes on the south ridge are sub-horizontal. C) S_3 strikes north to north-northeast and dips moderately to steeply to the east-southeast. Fold axes plunge shallowly to the northeast.

antiform recognized by southeast-verging folds that are inconsistent with the vergence of the Manzano Peak synclinorium. This antiform refolds the western limb of this syncline. The Abo Pass region is similarly deformed and plate 3 shows a cross-section drawn from the Scholle quadrangle map (Scott et al., 2005) and the Becker Quadrangle map (Luther et al., 2005) that depicts the refolding of the Manzano Peak synclinorium. Thus, deformation related to D_3 involved the refolding of macroscopic F_2 folds, broad folds in quartz rich units and crenulation cleavage development in the Blue Springs schist all within a few km of the 1.43 Ga Priest pluton aureole.

SYNTHESIS OF THE MANZANO THRUST BELT

Sedimentation and volcanism in the Manzano thrust belt began before 1662 ± 2 Ma (Shastri, 1992) and continued through 1601 +4/-3 Ma (Jones, 2005) based on U-Pb ages of the metarhyolite units. Deposition of bimodal volcanic rocks, quartz-rich sediments, and mudstone is interpreted to be syntectonic with the Mazatzal orogeny. Bimodal volcanism included intrusive and extrusive units, and the 1655 ± 3 Ma Los Pinos pluton is interpreted to be genetically related to the Sevilleta metarhyolite along the belt. This is the only intrusive body in the region with a documented lack of a metamorphic aureole suggesting a gradational contact between the units. In addition, geochemical data from this study, in agreement with Condie and Budding (1979), indicates that these two units differ from the other felsic igneous rocks in the belt. This volcanism was followed by deposition of sediments that become more mature up-section, grading from lithic arenite to quartz arenite. This succession is gradational in nature, but the ceasing of basaltic volcanism occurred before quartz arenite deposition. Following this deposition was another period of silicic volcanism at 1600 Ma and deposition of mudstones. The syntectonic nature of this Paleoproterozoic sequence and the lack of recognized unconformities in the belt indicate that the Mazatzal orogeny was protracted and involved a complex temporal interplay between sedimentation, magmatism and deformation from ~1655 through 1600 Ma.

D_1 and D_2 deformation is pervasive in the Manzano thrust belt. The first involved layer parallel east-verging thrusts (Doran, 2002). F_1 folds and S_1 foliations were then transposed parallel to S_2 during the D_2 event. D_2 first resulted in macroscopic folding was followed by thrusting on S_2. The regional cross section of (Cather et al., 2006, *in press*)

depicts these structures as being related to a ramp-flat thrust belt geometry. This geometry is consistent with the model of Kalakey et al. (2001) for a fold-and-thrust belt in Montana related to Sevier orogenesis. In this model, frontal ramps are zones of thrusting that displace the hanging wall up and over the footwall block, which may create space at the ramp-flat interface for magma emplacement. In addition this model also accounts for flat-related synclines and ramp-related anticlines which correspond to the region of pluton emplacement. Figure 3 shows the regional cross-section of Cather et al. (2006) modified by the projection of the result of this study into the southern end of the figure. The Los Pinos Mountains exposes similar folds to the rest of the belt, however, D_2 shearing and folding have the opposite vergence (toward the southeast). I have attributed this shearing to be part of D_{2b}, and the model for magma emplacement synchronous with thrusting is inconsistent with this interpretation. Several possible explanations for this exist—1) east-verging shear in the Los Pinos Mountains was synchronous with top-to-the-northwest thrusting and thus is part of a bivergent structure 2) east-verging shear related to D_{2b} occurred after initiation of thrusting in the north-west direction and after the ramp-flat thrust belt had formed 3) east-verging shear could have been the dominant shearing direction during the Mazatzal orogeny, and the northwest verging shear sense represents 1.43 Ga reactivation of shear zones initiated during the Mazatzal orogeny.

The bivergent orogen model is preferred based on a seismic interpretation of the CD-ROM line (Magnani et al., 2004). Preliminary monazite geochronology from Williams (1999) suggests that these northwest-vergent thrusts moved at two times in the history of the belt. In addition, while D_{2b} could have been later in the history of the belt, I interpret deformation related to the Mazatzal orogeny to be a progressive event, and

therefore later west-side up shear would still be part of a bivergent orogen, as opposed to a discrete later event. The particular region of the seismic line of interest images the crust 60 km northeast of the Pedernal Hills and 120 km northeast of the Manzano-Los Pinos Mountains, and interprets the structure to have north directed shear above a south directed duplex which projects to the southern end of the belt (Magnani et al., 2004). This geometry is consistent with the surface geology of the Manzano-Los Pinos Mountains, and is a possibility for interpretation of opposing vergence shear sense data.

A new crystallization age of 1600 Ma from the Blue Springs rhyolite from this study indicates that the Mazatzal orogeny lasted through this time period, yet the duration of time from 1.6 to 1.43 Ga is difficult to characterize based on a lack of U-Pb ages from New Mexico (Figure 24). This period has been previously interpreted to be a tectonic lull (Karlstrom et al., 2004). Only one recent study documents deformation within this gap and is from the Cheyenne Belt of Wyoming. This study by Duebendorfer et al. (2006) documents reactivation of the Cheyenne belt at 1.60 Ga based on Ar/Ar ages, although the authors do not necessarily attribute this reactivation to the Mazatzal orogeny. In the Los Pinos Mountains, the nature of deformation is such that deformation at 1600 is correlative with the rest of the D_2 deformation along the belt, and thus I relate the young deformation to later parts of a long-lasting Mazatzal orogeny. Two possible interpretations of these new data exist and cannot be fully sorted out with the existing data set. The first interpretation is that Mazatzal deformation was protracted or episodic lasting from ~1660 through 1600 and waned soon after the final phases of magmatism (for example through ~1.59 Ga). Thus, this tectonic gap still exists in the region and then D_3 deformation was a separate, later event related to differential uplift in the stabilizing

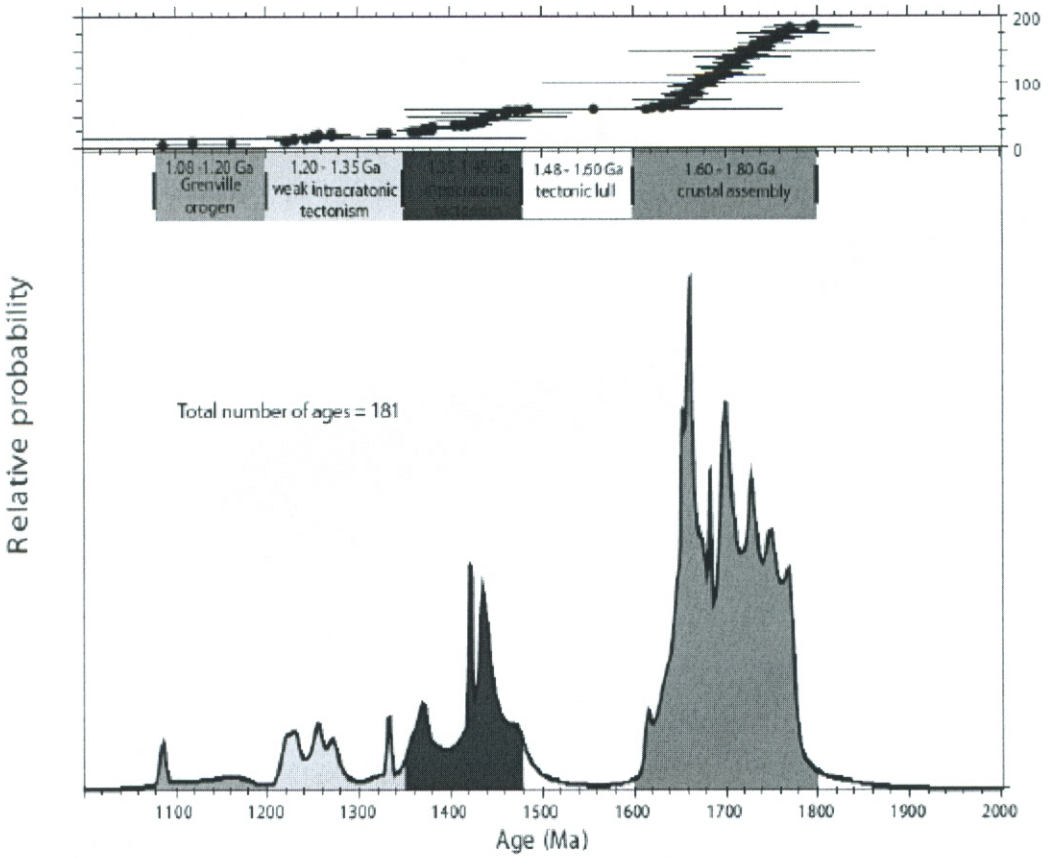

Figure 24. Histogram of U-Pb zircon ages from New Mexico from Karlstrom et al. (2004) illustrating the tectonic gap from 1.6 Ga to 1.48 Ga. This gap is being narrowed based on new data from this study and from Jones (2005).

craton. The second possible interpretation is that shearing and folding in the Manzano thrust belt is a result of more continuous deformation and an even shorter or possibly no discernable tectonic gap exists. Though the D_2 structure is truncated by the 1.43 Ga Priest pluton, no definitive evidence exists that this structure was not still forming just prior to emplacement of the pluton. Thus D_2 and related east-west shortening could have begun prior to ~1660 Ma this style of deformation continued long after until 1.4 Ga or so.

In the Manzano thrust belt, D_3 deformation is localized in 1.43 Ga pluton aureoles. Deformation involved ductile thrust-sense shearing along east-west trending shear zones, initiation of new shear zones in 1.4 Ga plutons and also refolding of macroscopic folds in these aureoles (Baer, 2004). Metamorphism was regional in nature. This interpretation is based on ~1.4 Ga apatite metamorphic ages in the Los Pinos Mountains (Shastri, 1992) and 1425 to 1380 Ma monazite metamorphic rim ages from other regions of the belt (Williams et al., 1999).

REGIONAL IMPLICATIONS

The paleogeographic setting of the Mazatzal tectonic block is an important factor for fully understanding the formation of North America. As discussed earlier, a commonly hypothesized tectonic setting involves collision of diverse juvenile terranes with southern Laurentia during subduction at the margin (e.g. Karlstrom and Bowring, 1988; Bowring, 1990; Karlstrom et al., 2001a). In the Yavapai province to the north, these juvenile arcs were built upon preexisting continental crust in some places (Hawkins et al., 1978; Hill and Bickford, 2001). This study allows for reexamination of this issue, based on geochemical and sedimentological analyses. Structural analyses, in conjunction with geochronologic data, are interpreted to indicate a long-lived compressional regime. Therefore, a closer look at the change from bimodal volcanism to quartz-rich deposition may provide more insight into the tectonic setting.

In order evaluate the tectonic environment wherein these bimodal volcanic rocks of the Manzano thrust belt were deposited, a more detailed geochemical and petrographic study is necessary. These metavolcanics units are well-exposed and highly variable across strike. A comprehensive analysis of trace elements as well as major elements may provide more insight into the source from which these rocks were derived. In addition more geochemical data and correlation of rock types of units along strike with the Manzano thrust belt are important.

Another important rock type deposited in the Manzano thrust belt that may provide interesting insight into the paleogeographic setting of the Mazatzal block is quartz arenite. Ultramature quartzites that range in thickness from 10's to several hundred meters thick are found throughout the southwestern United States Proterozoic tectonic

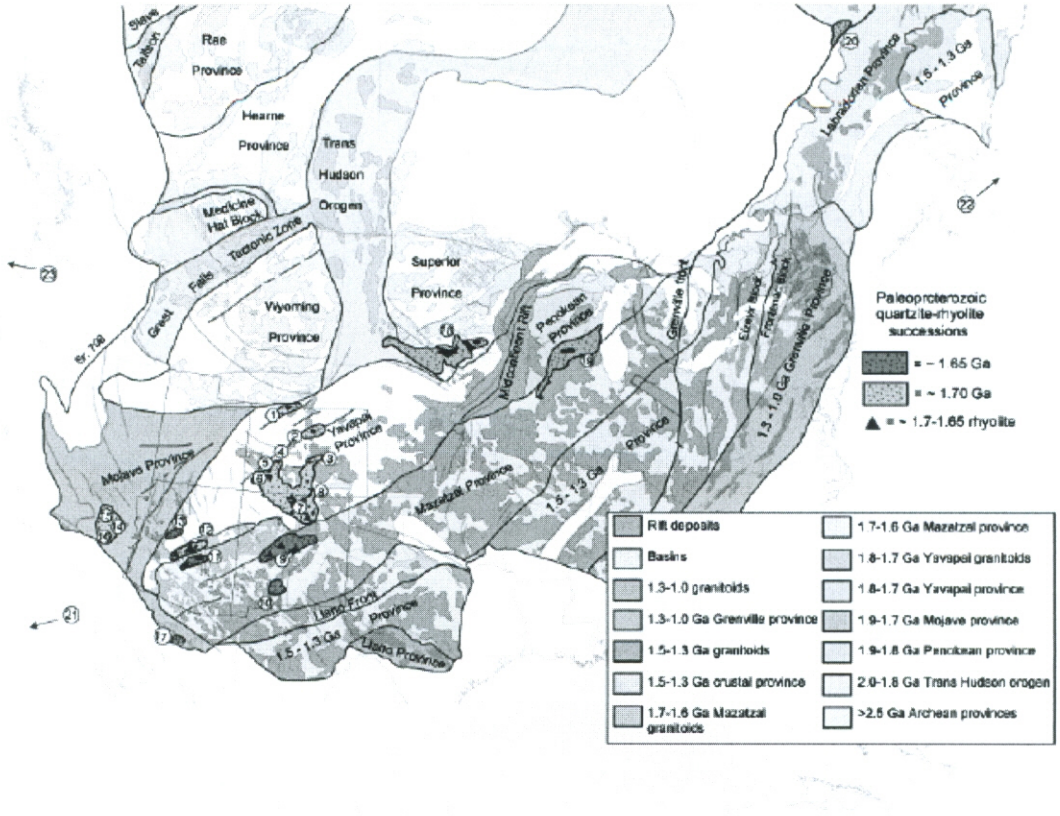

Figure 25. Proterozoic quartzite map from Karlstrom (unpublished compilation for the IGCP 440 Rodinia map). The distribution of these quartzites are not meant to represent specific basins, just the regions which these are exposed. Those shown in yellow represent 1.70 Ga quartzites and those in yellow represent the ~1.65 Ga quartzites. The red triangles represent exposures of associated caldera related rhyolites. The Manzano thrust belt is represented by number 9.

provinces (Figure 25). These quartz arenites are often in contact with caldera-related rhyolite units. Quartz arenites are interpreted to be shallow marine to fluvial sequences and some are located on the Yavapai and Mazatzal Provinces. The Ortega (Northern New Mexico, Soegaard and Eriksson, 1985, 1989), Uncompahgre (Colorado, Harris et al., 1987; Harris and Eriksson, 1989), and the White Ridge/Sais Quartzites (central New Mexico, Myers et al., 1981; Myers et al., 1986; Karlstrom et al., 2004) have been dated at either ~1.70 Ga or ~1650 Ma, marking two temporally separate but similar tectonic events related to Paleoproterozoic orogenesis. These two ages for quartzite successions have been hypothesized before, however, this study confirms this. Geologic and geochronologic data from the nearby regions suggest, however, that they were deposited at nearly the same time as deformation, metamorphism, and granitoid plutonism in the region (Karlstrom and Bowring, 1988; Karlstrom et al., 2004), leading to the hypothesis that the quartzites represent syntectonic basins (Jessup et al., 2005) directly related to the tectonic setting of the formation of North America. The origin of the silica-rich nature of these sequences is not yet well understood, but may have important implications for processes unique to the Paleoproterozoic (Karlstrom et al., 2004).

Future work is necessary to address these issues, Collins (2002) discusses a model in which the upper plate of a subduction system extends during slab-rollback and allow for arc splitting, microcontinental slivers and back-arcs basins. The regime switches when the subducting slab becomes flat, and compression causes deformation and crustal thickening. This process may account for both the bimodality of metaigneous rocks and the seemingly long-lived compressional regime. Quartzite basins may also be explained

in terms of slab roll-back forming short-lived extensional basins that subsequently close during continued compression.

CONCLUSIONS

The Manzano Group stratigraphy is now well defined based on new field observations, structural interpretations and an improved geologic context for U-Pb age data. This study documents the overturned nature of quartzite beds based on preserved cross-bedding which is in conflict with the prior stratigraphy of Myers et al. (Myers et al., 1981). This interpretation is greatly reinforced by U-Pb zircon ages of the older Sevilleta metarhyolite (1662 ± 1 Ma; Shastri, 1992) and the younger Blue Springs rhyolite (1601 +4/-3 Ma). A final improvement to the stratigraphic section of the Manzano Group is the correlation between a newly recognized anticline north of the Los Pinos pluton and the anticlinorium in Bootleg Canyon of Shastri (1992). Therefore, the exposed units in Bootleg Canyon are interpreted to core this anticlinorium and are thus the oldest exposed Manzano Group sequence recognized in the Los Pinos Mountains (possibly correlative to greenstone belts exposed in Tijeras Canyon). These data allow for a new, improved compilation of the stratigraphic section of Baer (2004).

New geologic mapping at 1:12,000 of the Los Pinos Mountains resulted in several new observations and interpretations. The recognition of the Los Pinos anticline has important implications for the stratigraphy of the region as discussed above, and also the tectonic framework of the southern of the Manzano thrust belt. In addition, documentation and chronology of overprinting relationships between three tectonic fabrics in this region has not yet been done, and this study attributes S_1 and S_2 to the Mazatzal orogeny and documents the lack of strong D_3 deformation in the southern end of the thrust belt. This study also interprets plutonism to be synchronous with deformation. Characterization of the nature of D_2 includes the documentation of northerly

trending macroscopic isoclinal folds followed by east-vergent thrusting. This layer parallel thrusting was progressive and involved rotation of these folds from north to south.

This study also contributes to prior work in the Manzano thrust belt by a compilation of the extensive unpublished geochronologic data. These ages are invaluable to the reconciliation of the complex temporal interplay between Mazatzal deformation and sedimentation, and the intense reactivation at 1.4 Ga. In addition, the new age of 1600 +4/-3 Ma is the youngest reported crystallization age in the southwestern United States, which has important implications for Mazatzal accretion and the tectonic gap following this orogeny. Preliminary U-Pb monazite data documenting two phases of movement on the thrust belt and the 1.4 Ga overprint has also not been published and is an important addition to the nearly mature dataset in the Manzano thrust belt.

APPENDIX I. PETROGRAPHY APPENDIX

Explanation: This section contains the mineralogy of each unit found in thin section. In addition, this appendix contains at least one photomicrograph of each thin section with a brief description of important features. Many of these photomicrographs are shown in the correct orientation in order to analyze the structures. The black tick marks on each photomicrograph allow for an oriented reference back to the original rock sample. Sample locations are shown on the map below. Petrographic studies involved characterization of microstructures including a description of each fabric generation, porphyroblast-fabric relative timing relationships and determination of shear sense direction using the methods described by Simpson and Schmid (1983), Passchier and Trouw (1996), and Johnson (1999).

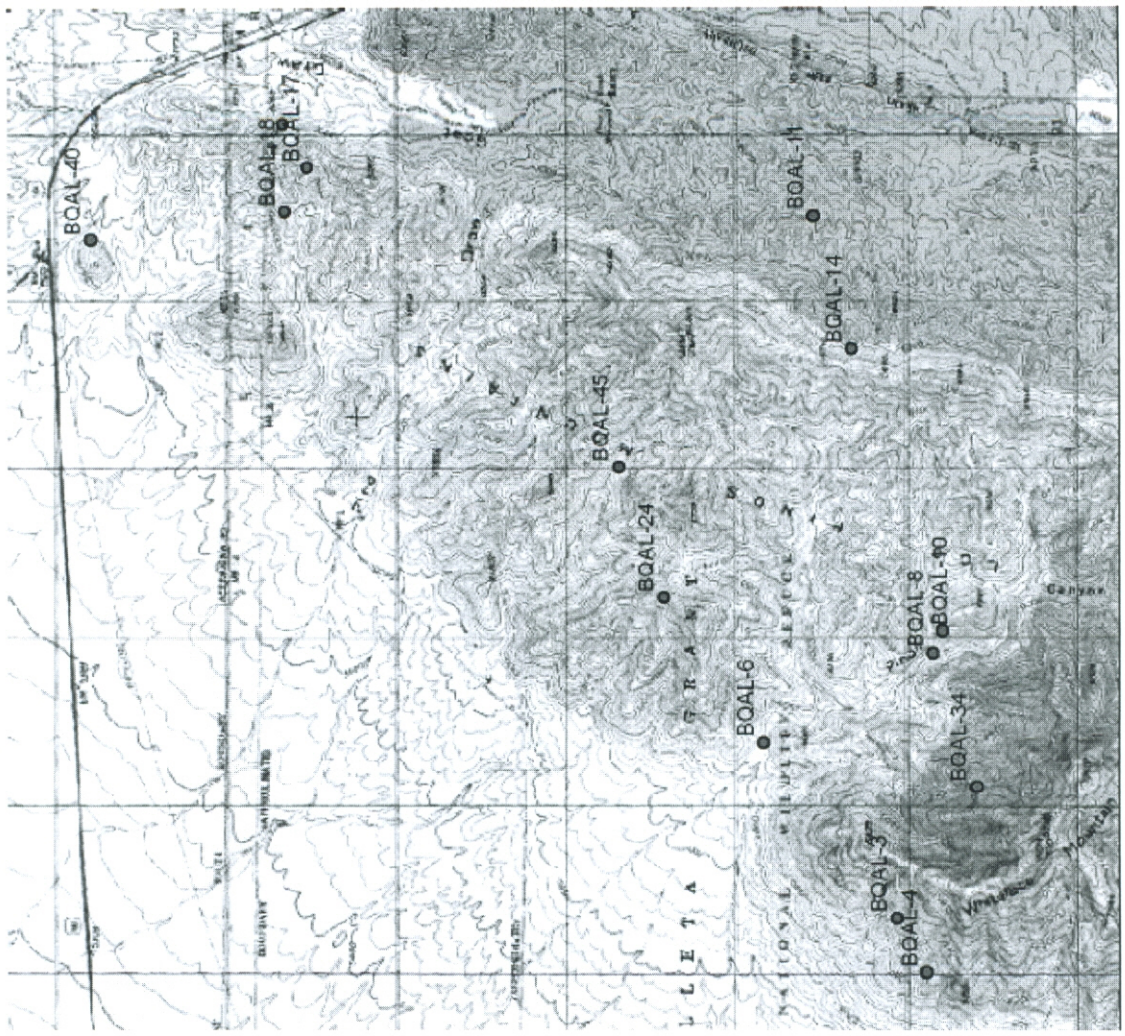
BQAL-40
BQAL-18
BQAL-17
BQAL-11
BQAL-14
BQAL-45
BQAL-24
BQAL-6
BQAL-8
BQAL-10
BQAL-34
BQAL-3
BQAL-4
GRANT
LLETA

SEVILLETA METARHYOLITE – UPPER UNIT

Quartzo-felspathic fine-grained matrix with aligned biotite, oxide and small amounts of carbonate. Garnet, plagioclase and quartz porphyroclasts. Some samples have white mica, sphene, and epidote within plagioclase. K-feldspar is found in tails of porphyroclasts.

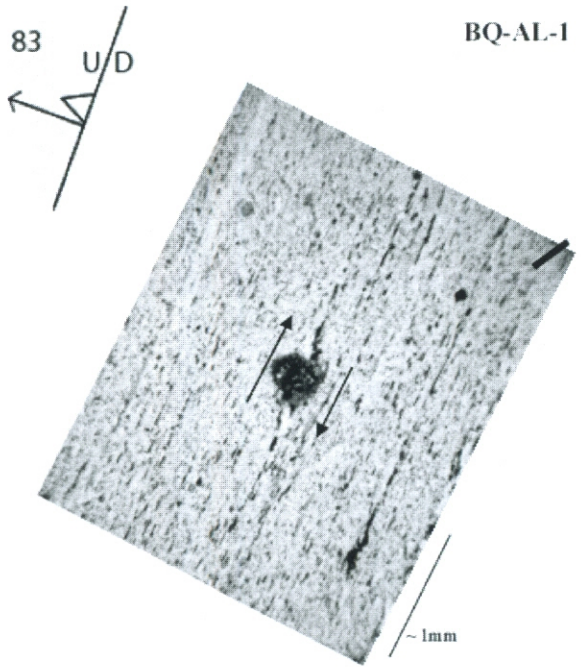

Garnet delta clast showing top-to-the-east shear on S_2.

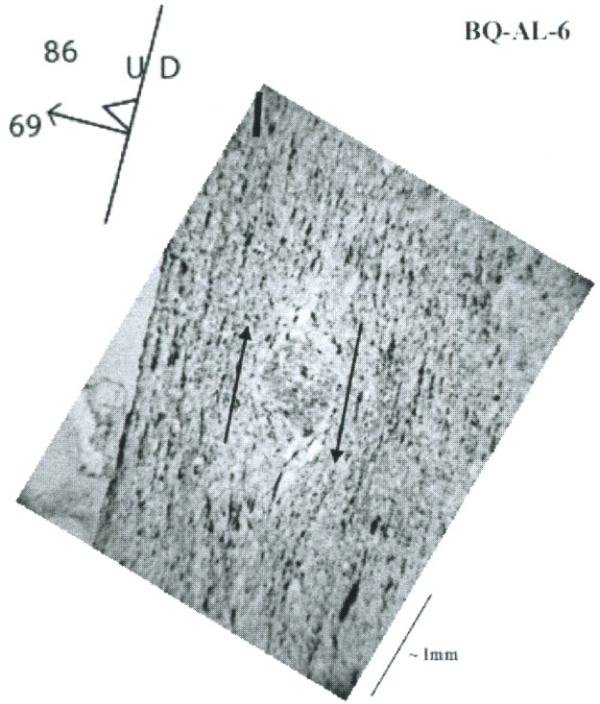

Plagioclase sigma clast showing top-to-the-east shear on S_2.

78

BQ-AL-24

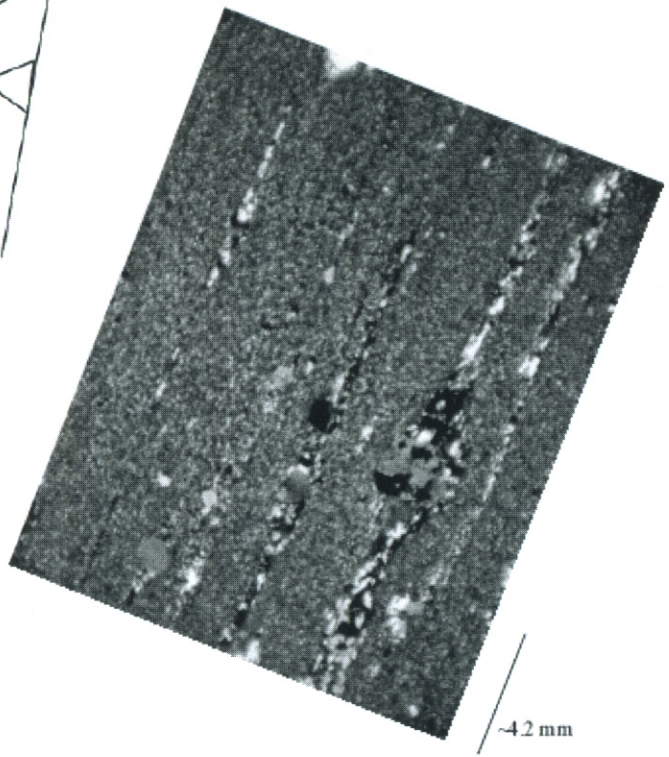

Photo showing typical fabric in Sevilleta metarhyolite of strong alignment of fine grained quartz, feldspar, and mica. Quartz and feldspar porphyroclasts have symmetric tails.

78

BQ-AL-24

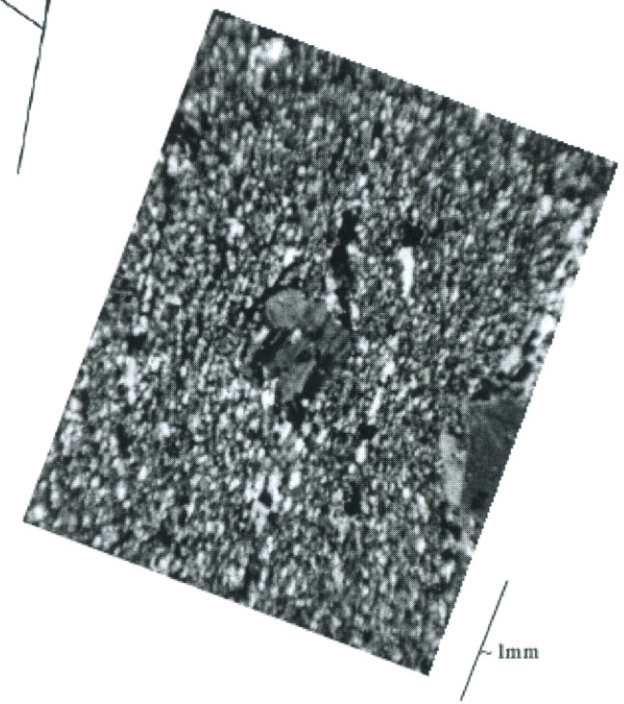

Plagioclase porphryoclast showing deformation twins.

SEVILLETA METARHYOLITE – LOWER UNIT

Fine grained quartzo-feldspathic matrix with white mica, oxides, and some epidote and biotite. Dominantly plagioclase phenocrysts that are sericitzed. Garnet and quartz porphyroclasts as well.

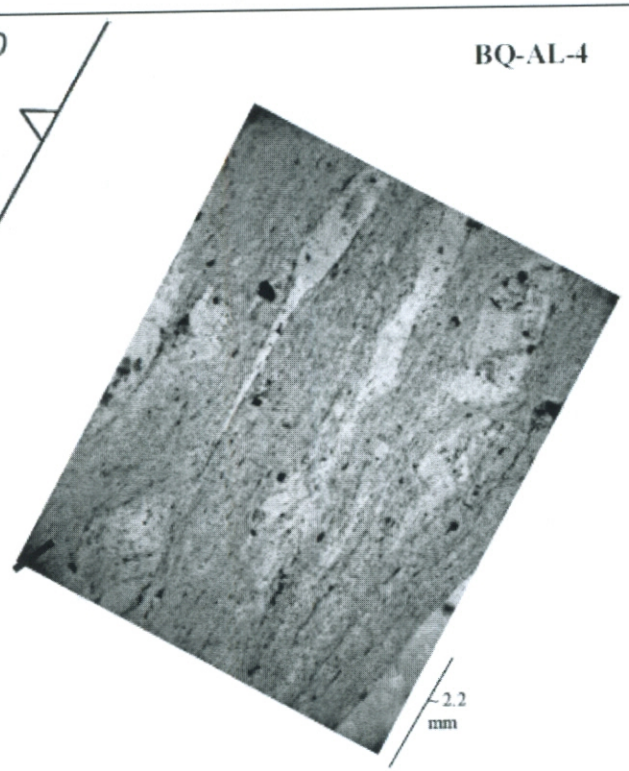

Typical metarhyolite texture showing aligned matrix and boudinaged quartz and feldspar grains.

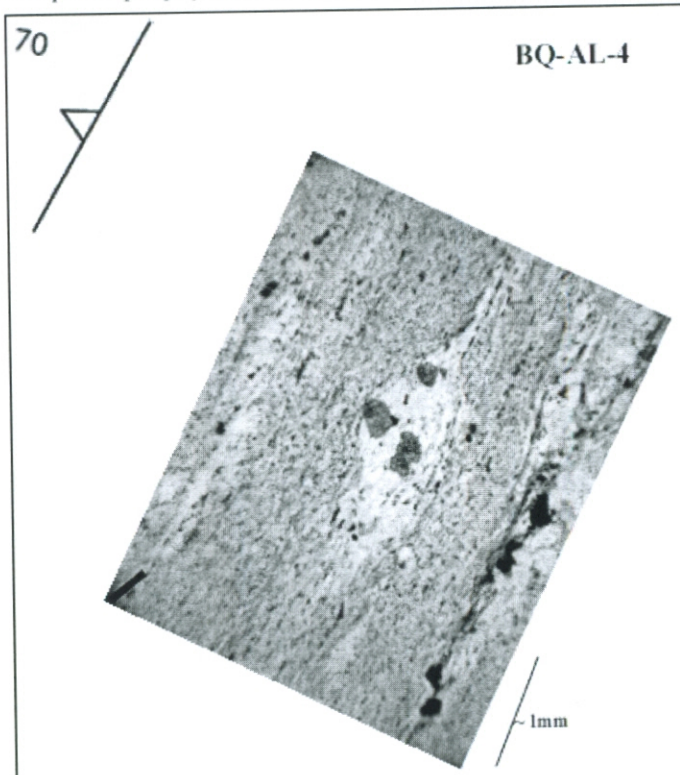

Garnet inside a plagioclase porphyroclast

BQ-AL-40

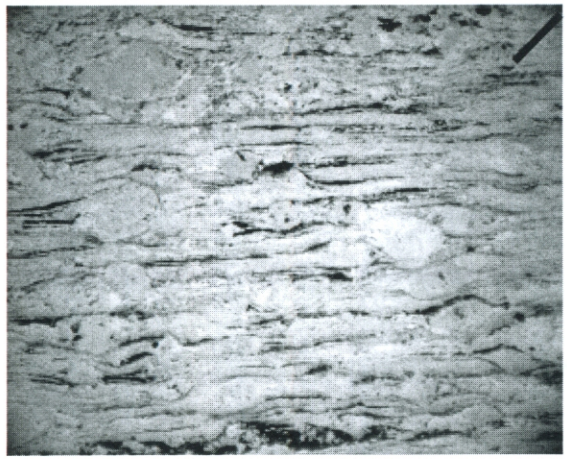

Mylonite fabric in metarhyolite.

BQ-AL-40

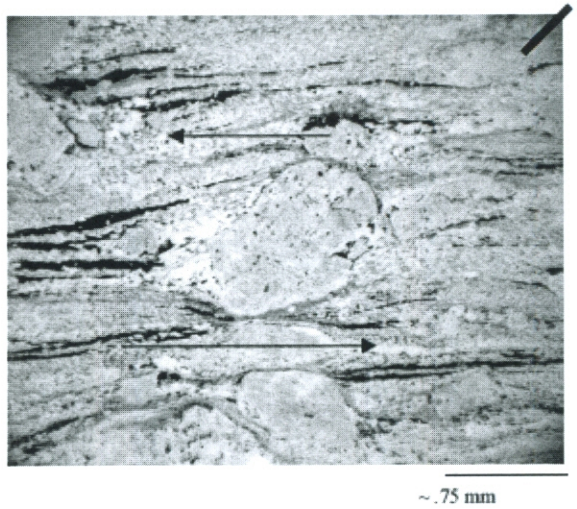

Plagioclase sigma clast showing sinistral shear.

70

BQ-AL-8

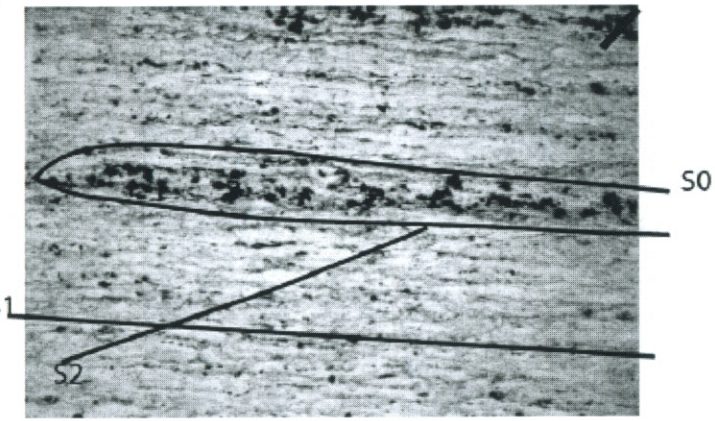

~4.2 mm

Folded compositional bands in lithic arenite sample with an S1 axial plane. Axis of crenulations is S2.

70

BQ-AL-8

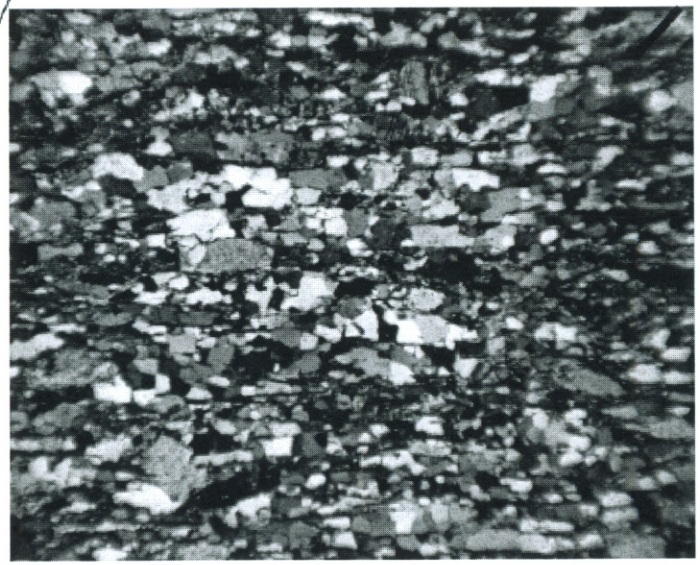

~4.2 mm

Texture of lithic arenite.

LITHIC ARENITE—SCHIST MEMBER

Quartz, muscovite, Mg-chlorite, garnet and oxides.

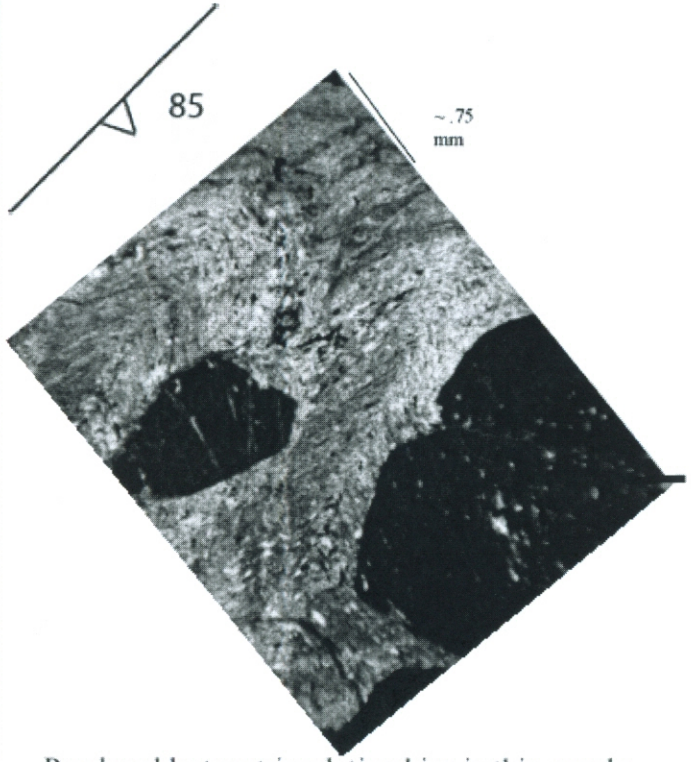

Porphyroblast-matrix relationships in this sample show syn-S2 garnet growth based on deflection of crenulation cleavage and the inclusion of S2 in the garnet.

BQ-AL-45

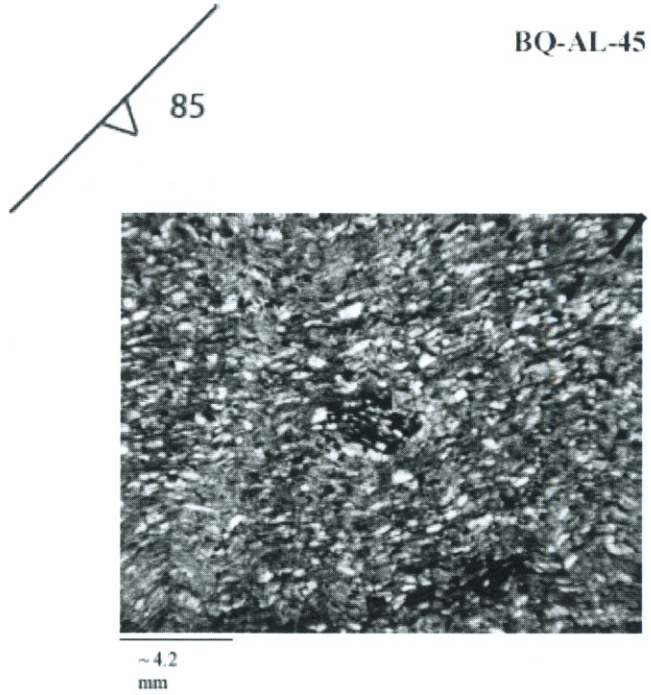

Porphyroblast-matrix relationships in this sample show syn-S2 garnet growth based on inclusion of crenulation cleavage, and a stronger crenulation cleavage developed in the matrix.

BQ-AL-45

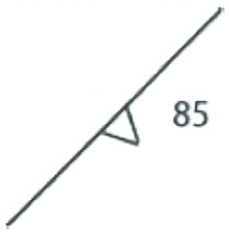

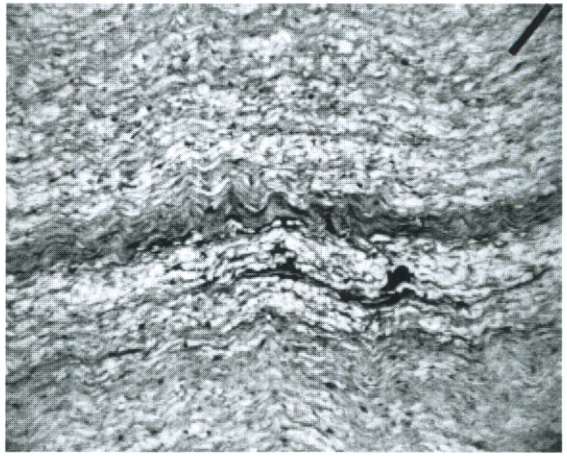

~4.2 mm

Crenulation cleavage.

LITHIC ARENITE—ANOTHER SCHIST MEMBER

Quartz, muscovite, plagioclase, biotite, Fe-chlorite, oxides, and garnet

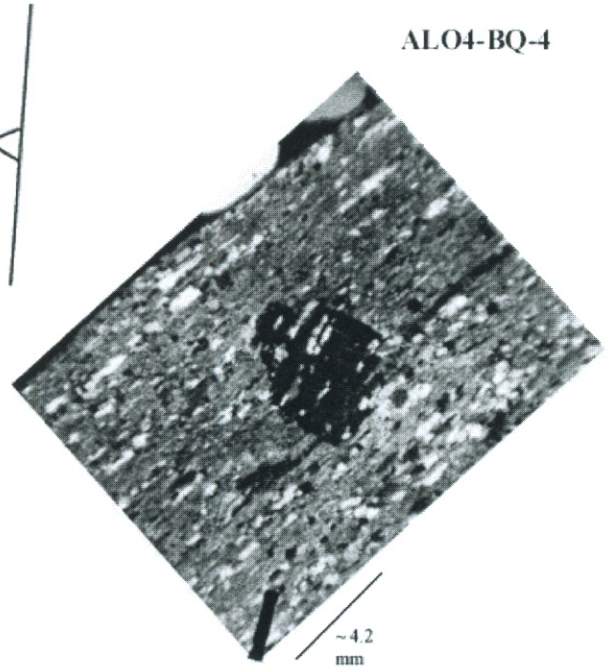

Synkinematic garnet porphyroblast.

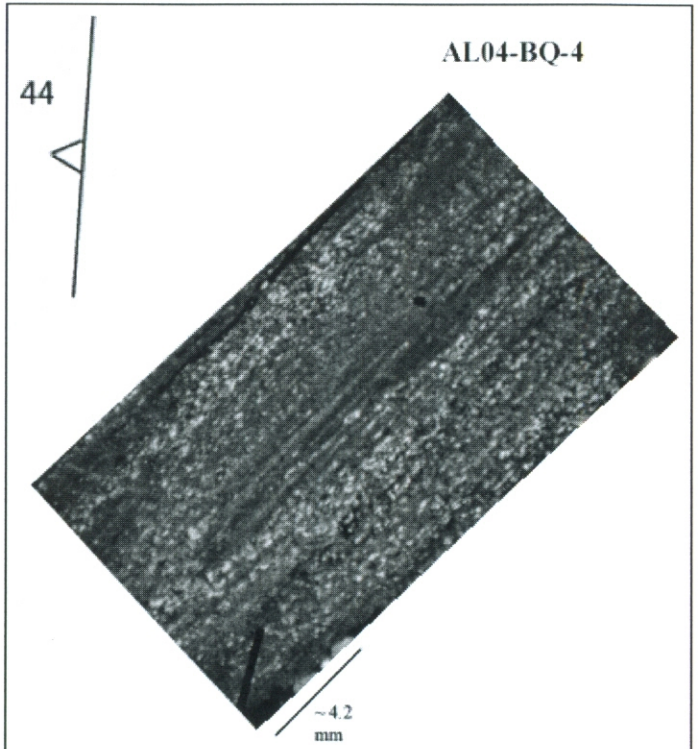

Isoclinal rootless fold of compositional banding.

LITHIC ARENITE—METARHYOLITE?

Fine grained quartzo-feldspathic matrix with plagioclase and quartz porphyroclasts, with muscovite and biotite. Sample AL04-BQ-5 contains chlorite, muscovite, biotite, oxides, and a lot of carbonate.

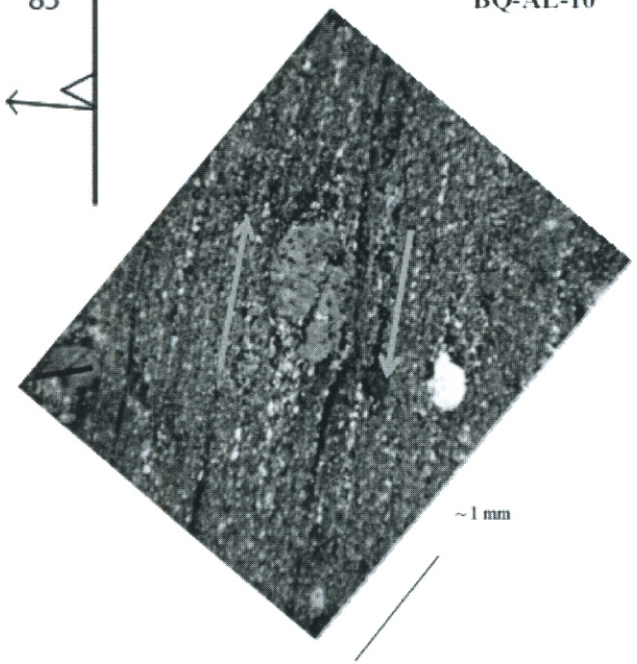

Synthetic offset on brittle plagioclase grain showing top-to-the-east thrust movement.

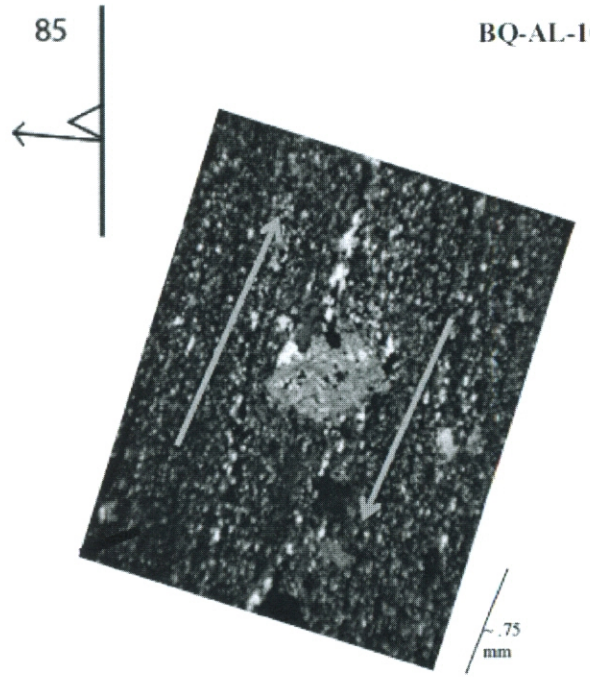

Plagioclase sigma clast showing top-to-the-east shear on S2.

62

ALO4-BQ-5

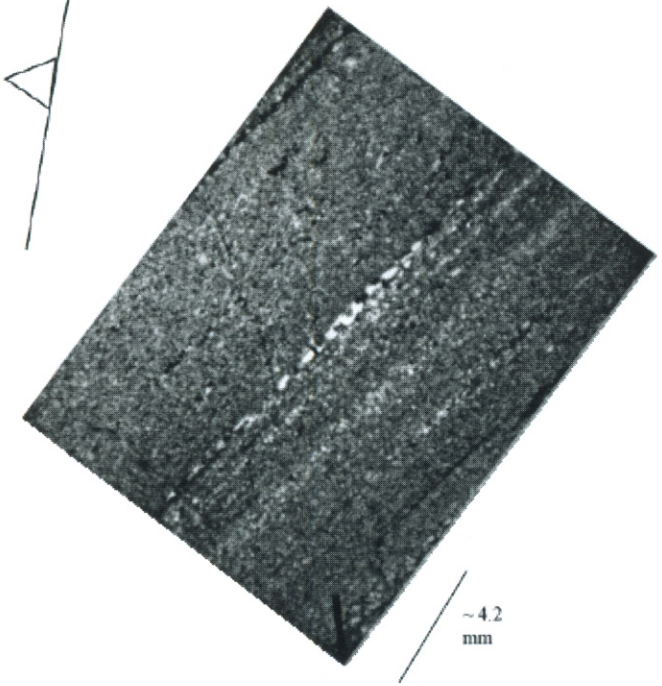

Typical amphibolite foliation.

59

ALO4-BQ-7

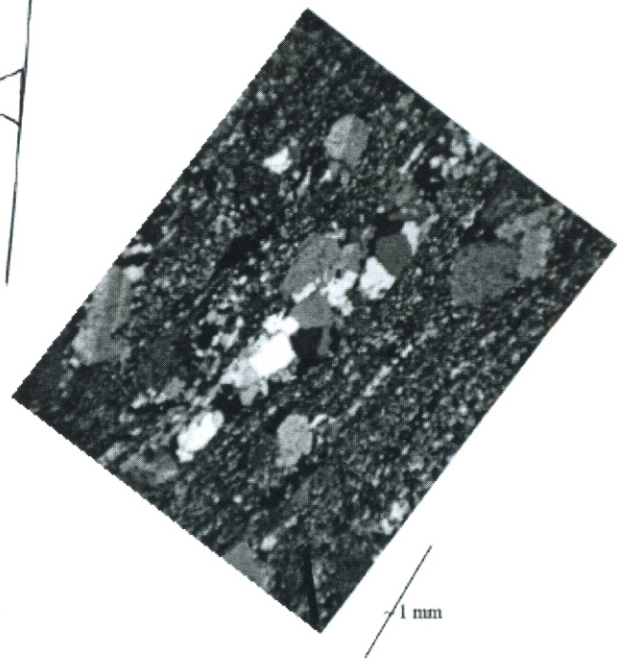

Recrystallized quartz.

LITHIC ARENITE—AMPHIBOLITE

Mostly hornblende, some plagioclase and a little quartz

AL04-BQ-2

Garbensheifer texture in amphibolite. Possibly defines two foliations.

AL04-BQ-3

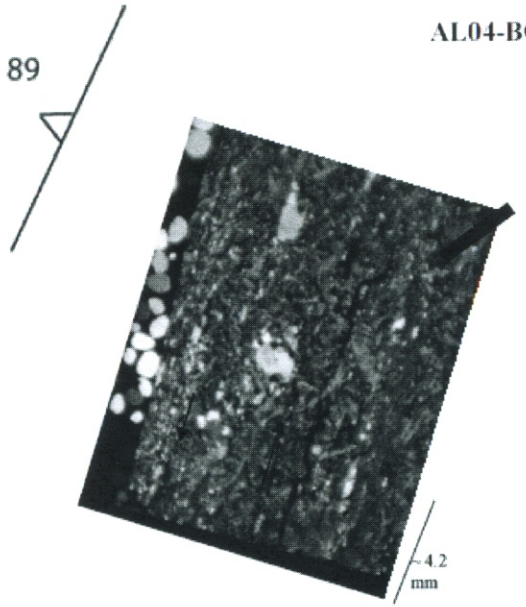

Plagioclase sigma clast showing down-to-the-east shear on S2. Garbensheifer texture.

WHITE RIDGE QUARTZITE

Quartz rich quartzite with very small amounts of muscovite and some high relief accessory minerals (zircon, monazite, etc.)

AL04-BQ-1

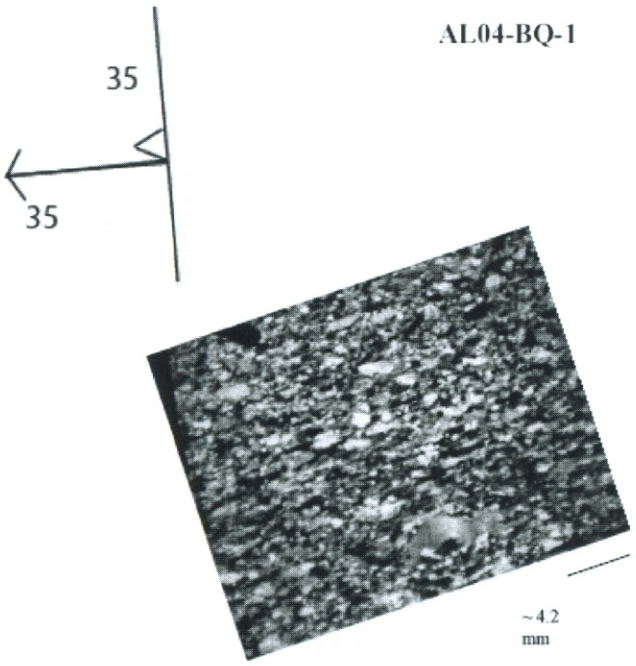

Sweeping undulose extinction, weak SPO. Foliation develops as alignment of quartz and mica.

BQ-AL-18

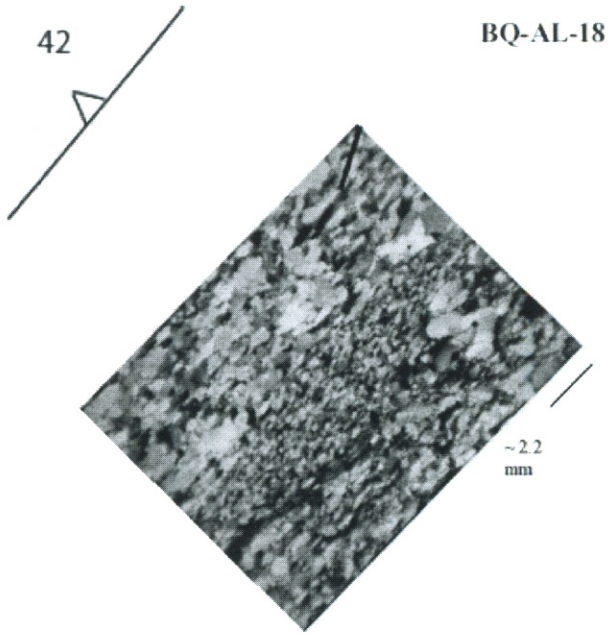

Relict? sigma clast showing top-to-the-east shear on S2. S-C fabric in matrix shows same sense of shear.

SAIS QUARTZITE

Quartz arenite with less than 1% white mica.

46

BQ-AL-27

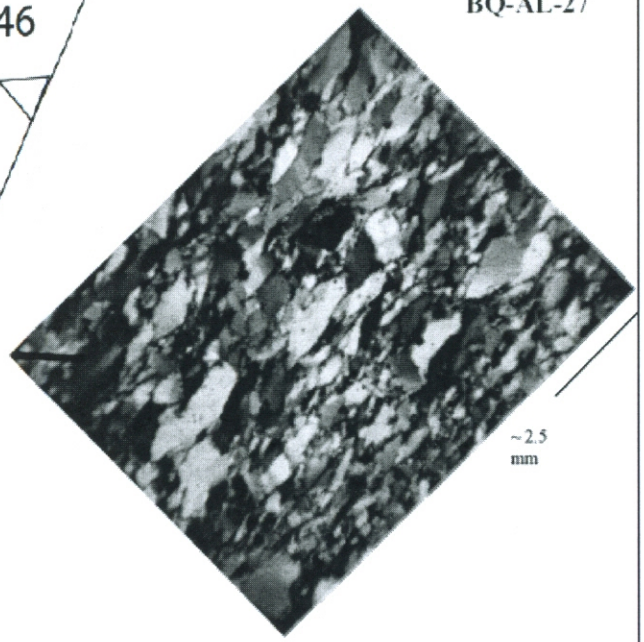

Sweeping undulatory extinction, weak SPO, deformation lamellae.

SAIS QUARTZITE—SCHIST

~90 % quartz, Fe-chlorite, and plagioclase.

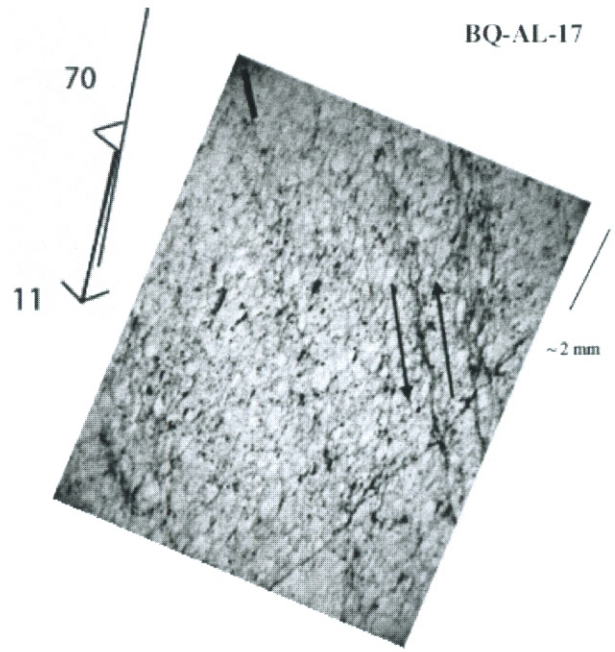

Sinistral shear bands in schist. Related to shearing between folded layers.

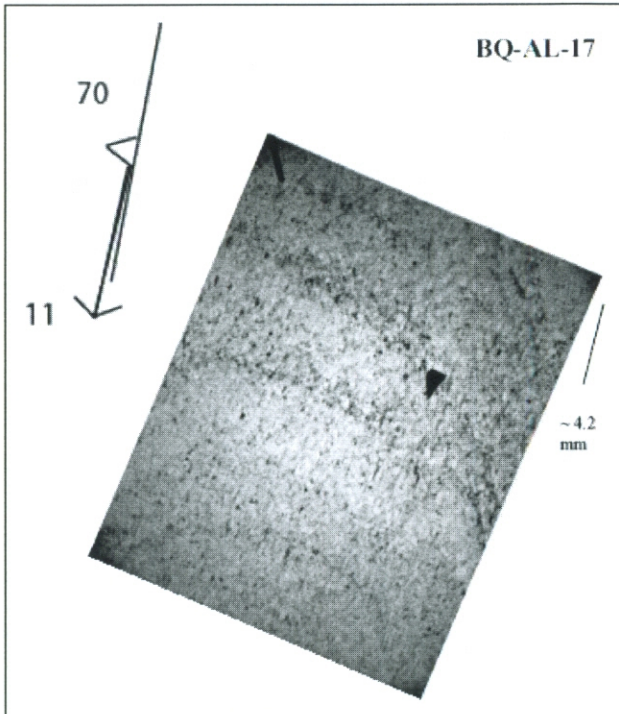

F2 fold in schist.

BLUE SPRINGS SCHSIT

Fine grained quartzo-feldspathic schist with muscovite, Mg-chlorite, garnet, and tourmaline.

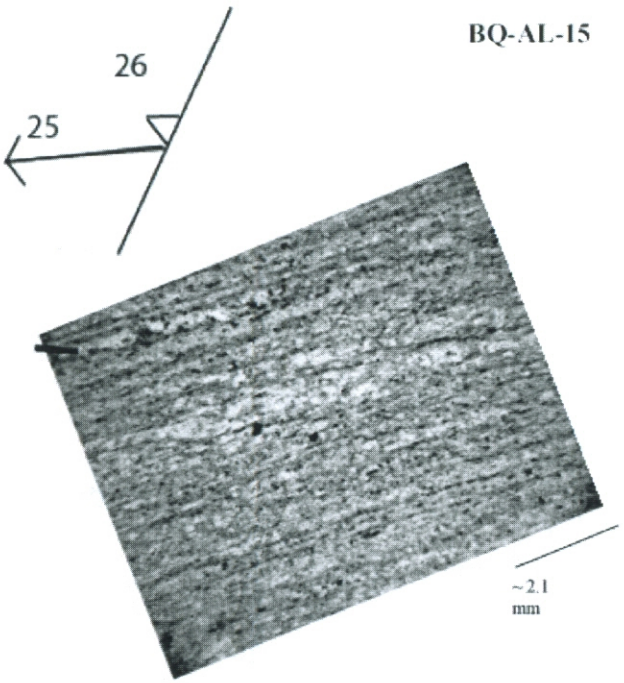

Crenulation cleavage.

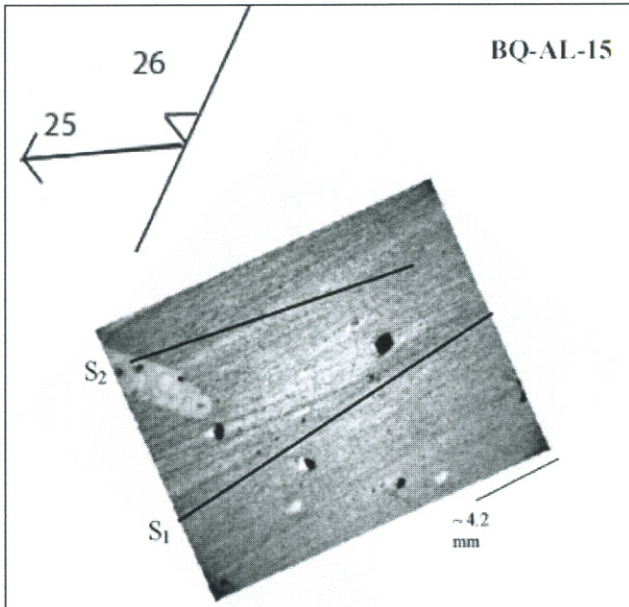

Photo showing two tectonic fabrics, S_1 and S_2.

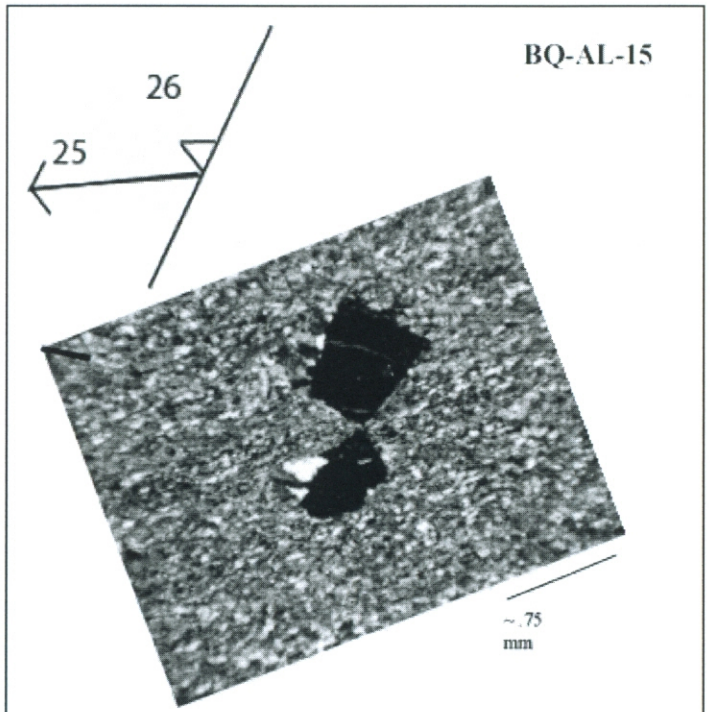

Strain shadows on oxide porphyroclasts.

BLUE SPRINGS RHYOLITE

Fine grained quartzo-feldspathic schist with biotite, epidote and oxides.

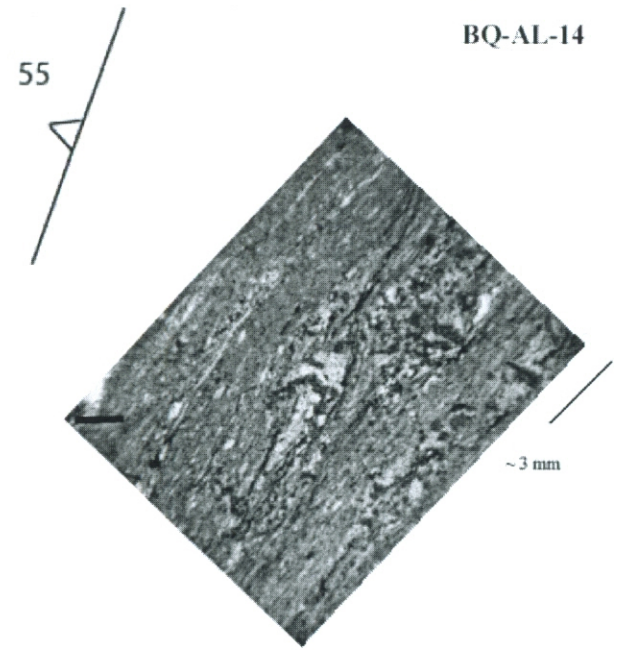

Abundant epidote, stage 1 crenulation cleavage.

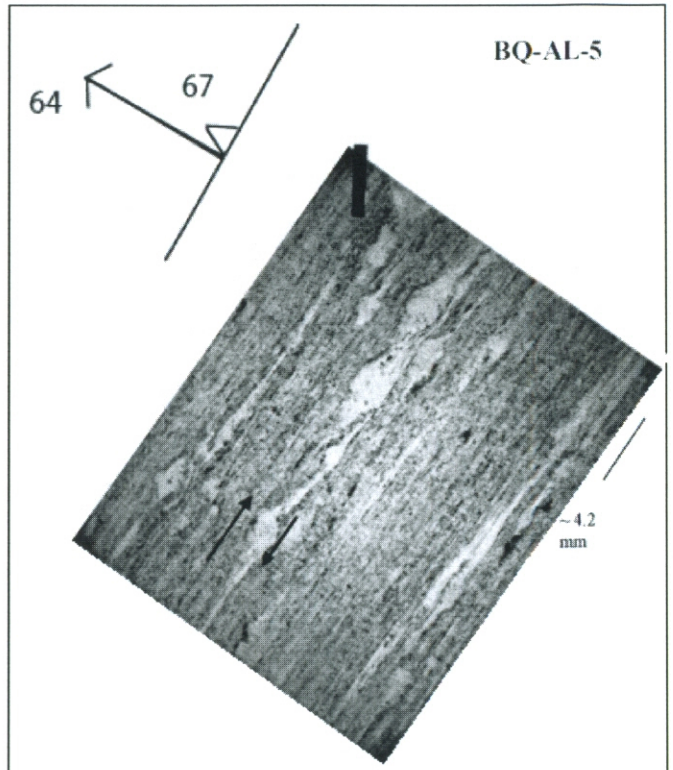

Plagioclase delta clast showing top-to-the-east shear on S2.

UPPER BLUE SPRINGS SCHIST

Fine grained quartzo-feldspathic schist with biotite, carbonate, Fe-chlorite, clinozoisite, epidote hematite, and some tourmaline.

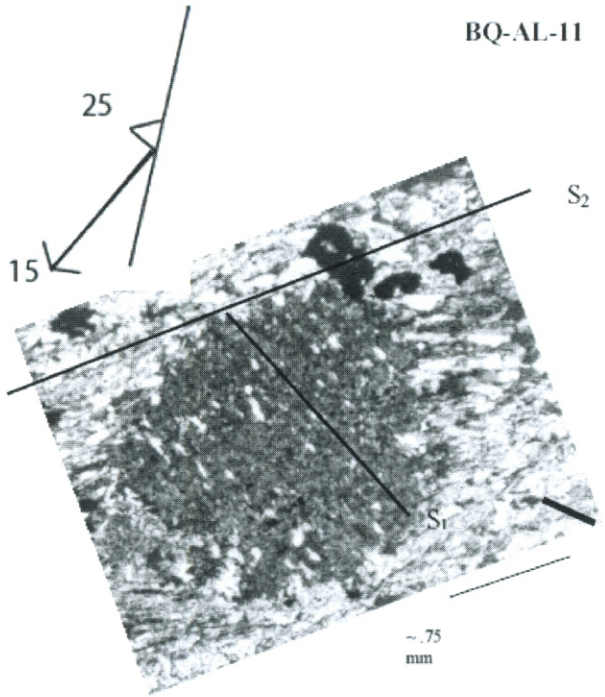

Biotite porphyroclast with strain shadows aligned in S_2 and S_1 included within the grain (typical of all grains in this slide)

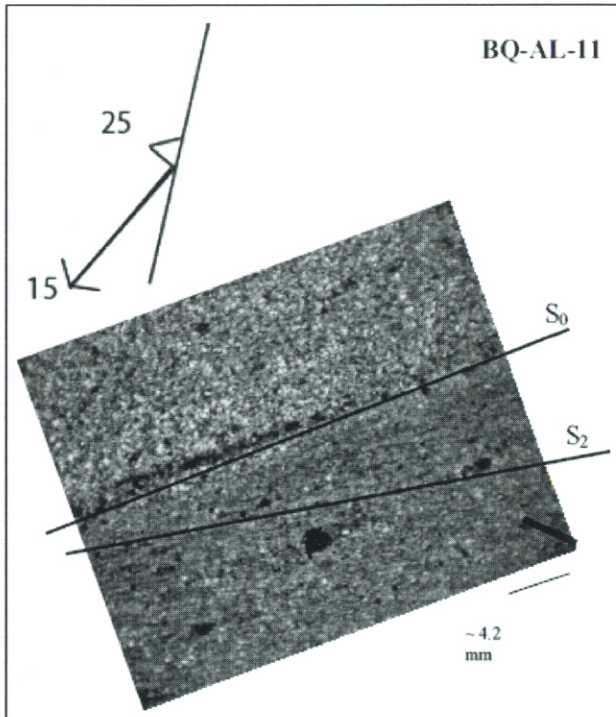

Photo showing compositional bands with S_2 at an angle to it.

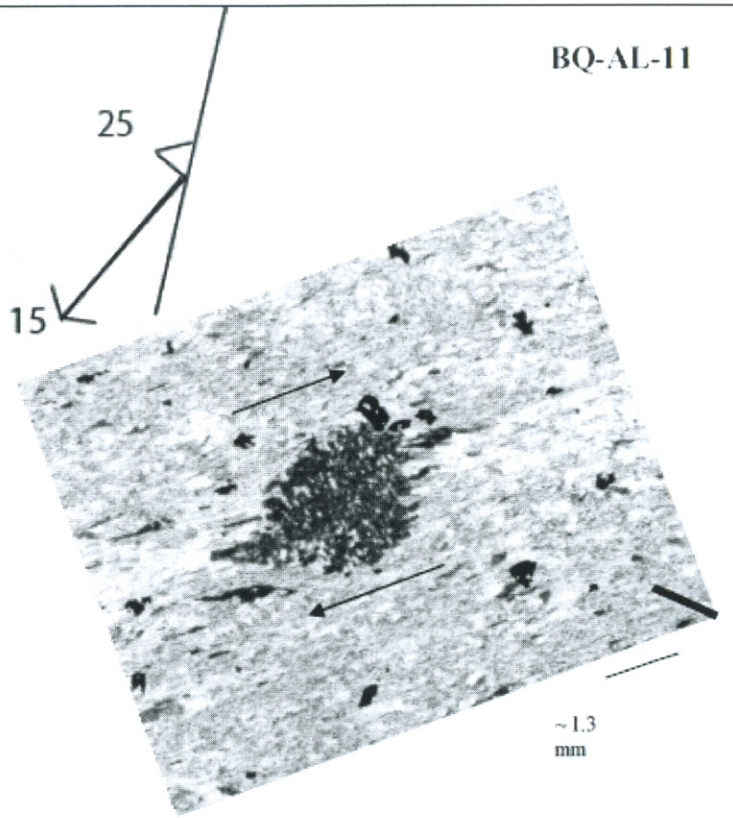

Biotite strain shadows showing top-to-the-east shear on S2.

BQ-AL-34

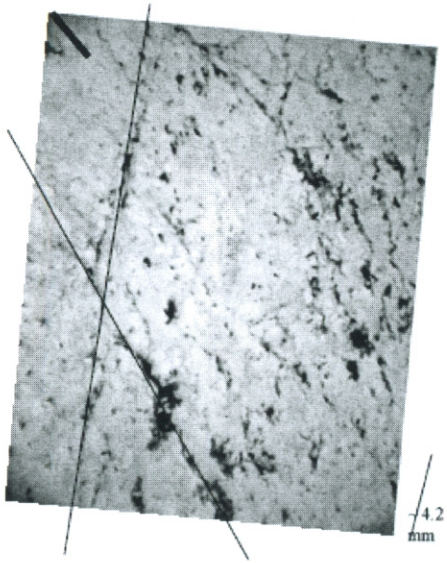

Two tectonic fabrics developed in the pluton sample.

BQ-AL-34

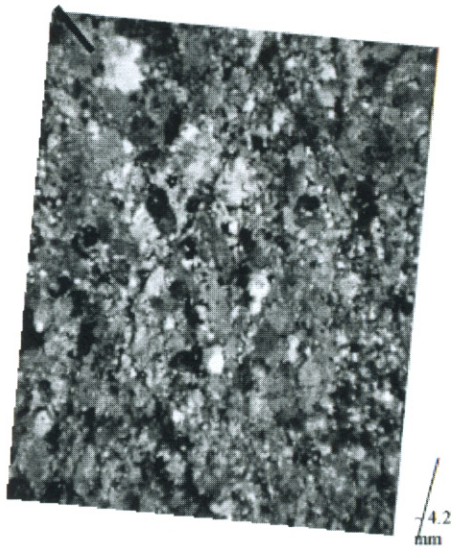

Same as on left but with crossed polars

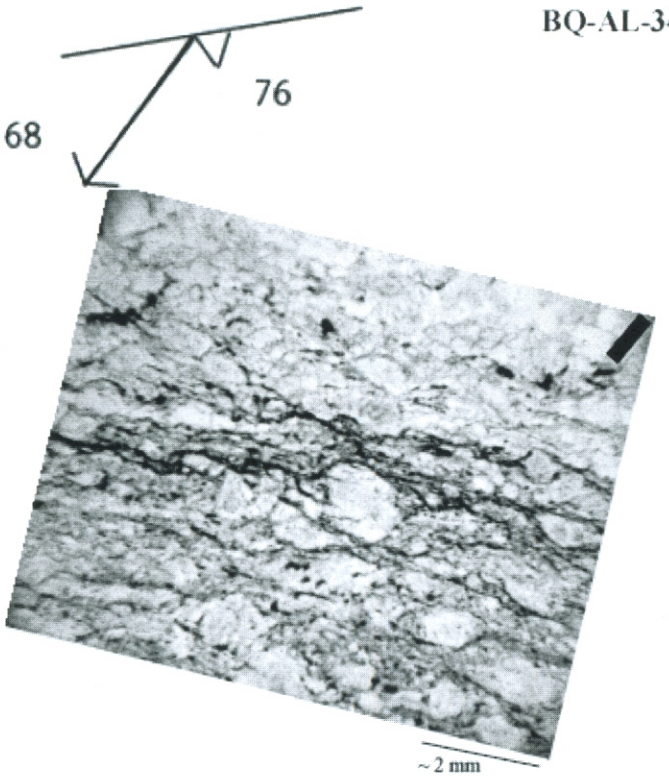

2 domains in slide, mylonite and relatively undeformed. Grain size reduction, no mymekitic texture. Alignment of undulatory quartz, plag and mica.

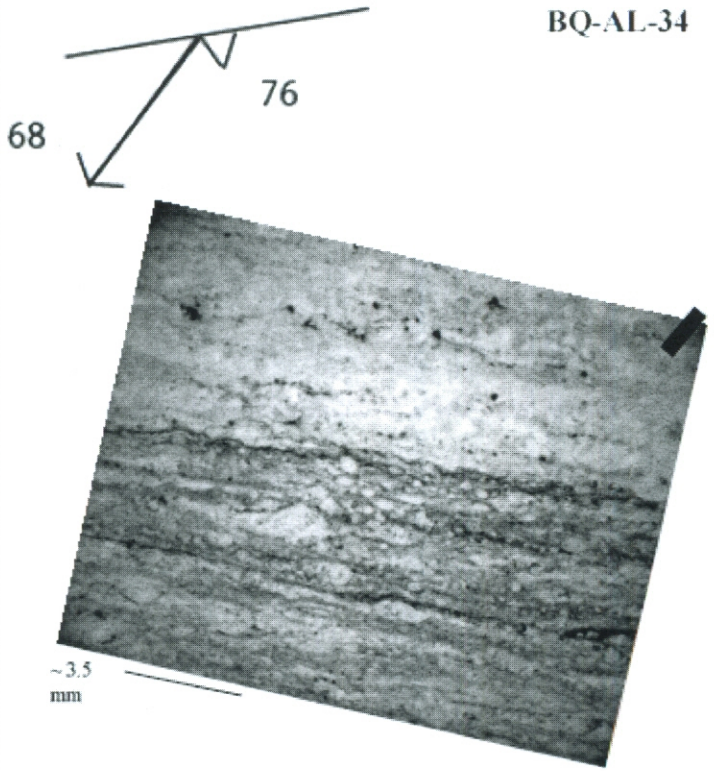

2 domains in slide, mylonite and relatively undeformed. Grain size reduction, no mymekitic texture. Alignment of undulatory quartz, plag and mica.

BQAL-3

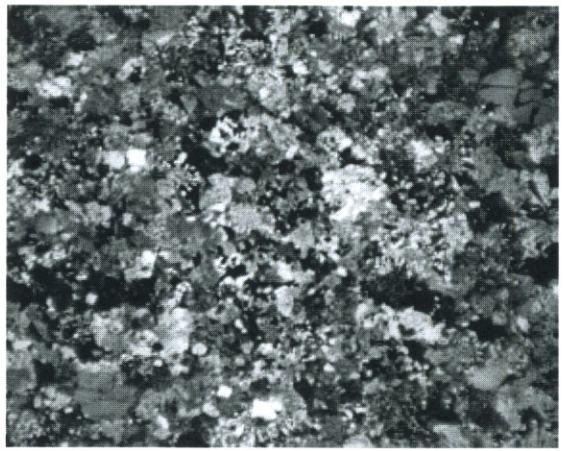

~4.2
mm

Myrmekite in unfoliated pluton sample.

Photo shows contact between foliated xenolith and granite, with the foliation deflected by the feldspar porph. This provides evidence that this fabric predates pluton emplacement.

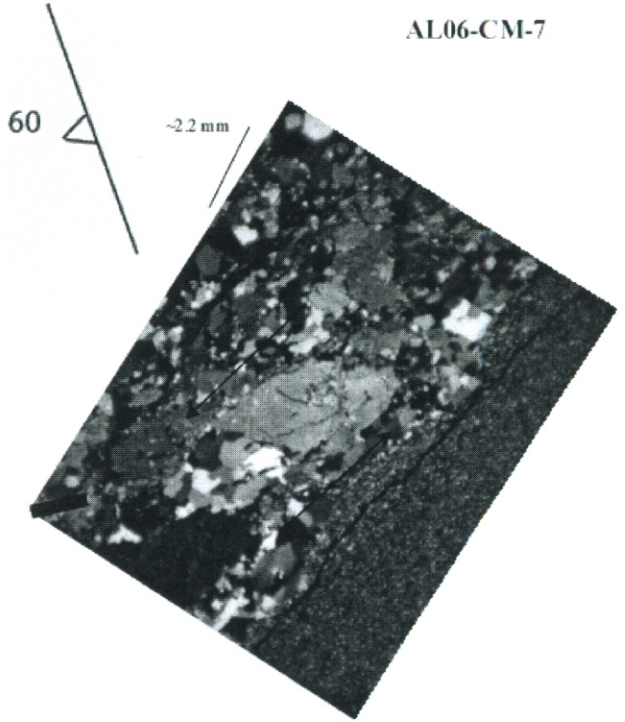

Sinistral west side up shearing shown by feldspar porph in granite.

AL06-CM-7

60

~.75 mm

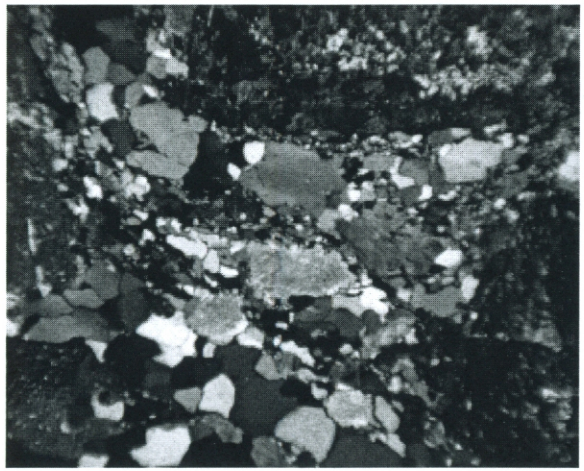

Dynamically recrystallized quartz

AL06-CM-7

60

~.75 mm

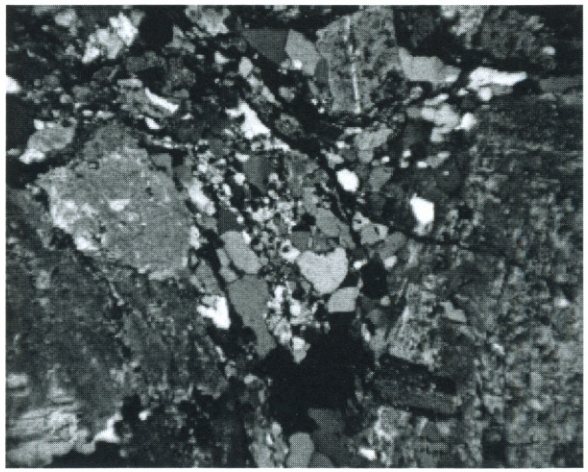

Dynamically recrystallized feldspar

AL06-CM-2

~.75 mm

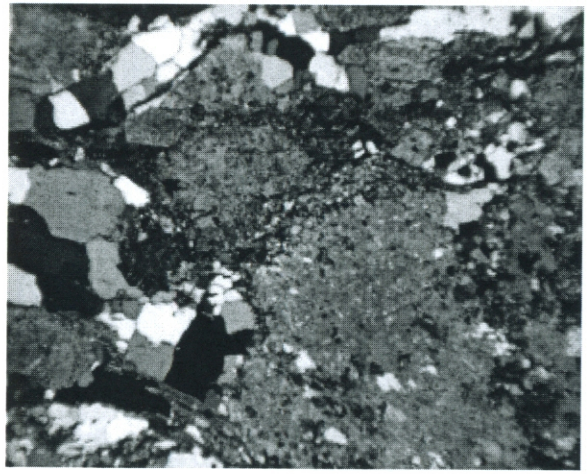

Subgrain development in feldspar.

AL06-CM-2

~.75 mm

Quartz fabric—looks undeformed almost, could be regime 3.

No undulatory extinction, LPO, SPO, or subgrains.

AL06-CM-6

~.75 mm

Recrystallized quartz

Brittle cracking in feldspar

AL06-CM-6

~.75 mm

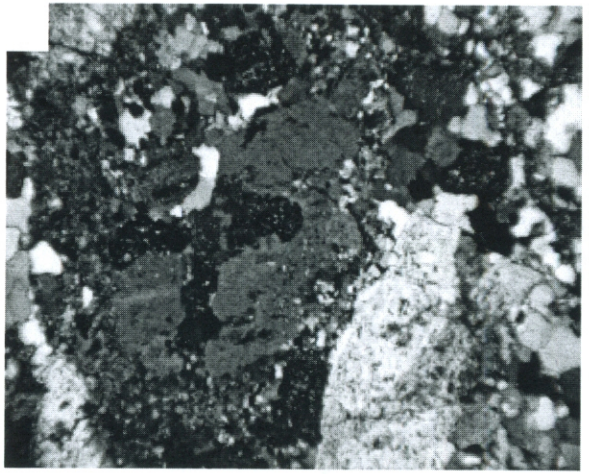

Subgrain development in feldspar.

AL06-CM-6

~.75 mm

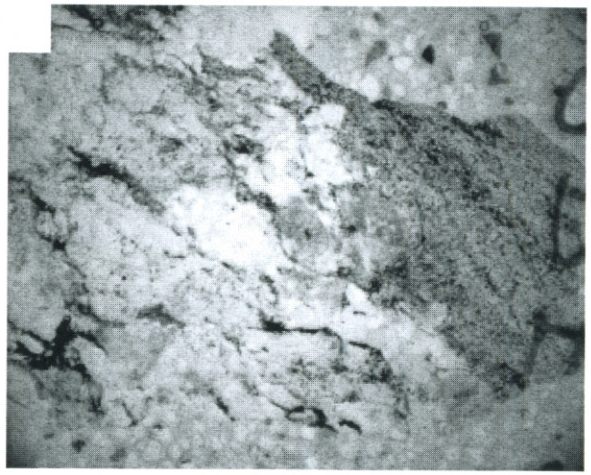

Parallel fabrics in granite and country rock (this photo shows that contact and that relationship)

Mineral assemblages

Unit	qtz	plag	bt	musc	grt	chl	mon /Z	carb	ep	k-spar	czo	spl	tour	ox	hem	hbl	act	sph
Xsru	x	x	±	±	x			x	x	±	±	±		x				
Xsrl	x	x	x	x	±	retr		x										
Xsrl	x	x	x					x	x					x				
Xlp	x	x	x	x			x			x		x						
Xla	x	x		x			x		x		x			x				
Xs	x	x	x	x	x	blue								x				
Xla-Xa	x	x				bm			x		x					x		
Xwq	x			x			x	x							x			
Xsq	x			x														
Xsq-Xs	x					blue												
Xbs	x	x		x	x	bm			x				x					
Xbr	x	x	x	x					x		x			x				x
Xbsu	x	x	x	x		blue			x		x	x		x				x

APPENDIX II. UNIT DESCRIPTIONS

Modified from the Becker 7.5 Minute Quadrangle Open File Report (Luther et al., 2005)

Santa Fe Group

QTsp: Sierra Ladrones Formation, deposits of ancestral Abo Arroyo (middle Pleistocene to Pliocene) — Reddish-brown (5YR 4/4) massive silty clay. Upper boundary with pebble gravel contains an eroded soil with light reddish-brown to pink (65YR 6/4-7/4) silty clay with Stage III+ pedogenic carbonate morphology. Gravels of unit Qpa may be part of this deposit, but these gravels have been included with the alluvium of Abo Arroyo pending further work on the adjacent Black Butte and Turn quadrangles. Interpretations of deep seismic reflection profiles and gravity data suggest that low-density basin-fill may be less than 1 km thick west of the front of the Los Pinos and southern Manzano Mountains (cf. Cape et al., 1983). These deposits may only occupy a small thickness of the Santa Fe Group stratigraphic succession exposed on the map area.

OLIGOCENE UNITS

To: Volcanics Undivided (Oligocene)
White to pinkish-gray, moderately to poorly sorted, moderately consolidated, fine- to very coarse-grained sandstone with scattered volcanic pebbles and cobbles. Also contains interbedded rhyolitic tuffs and basalt and basaltic andesite flows. Correlates to the Spears Formation and Oligocene volcanic rocks of the Mogollon-Datil volcanic field. Unit is at least 350 m thick.

MESOZOIC UNITS

Kth: Tres Hermanos Formation (Upper Cretaceous)
Uppermost beds are about 40 ft (12 m) pale-brown to dusky yellow shale that contains fish scales. Middle beds consist of shelly coquinoid conglomerate containing clams, snails, and shark teeth; grayish-orange and gray shale, siltstone, and fine-grained sandstone; at top of middle sequence of beds is a 5 ft (1.5 m) thick moderate brown coquina of *Crassostrea soleniscus*, identified by W. A. Cobban, USGS (written commun., 1981). Lower beds are very pale orange to moderate-brown, medium-to coarse-grained sandstone and conglomerate that locally contains fossil wood. Entire sequence includes probable equivalents of Dakota Sandstone and Mancos Shale. About 760 ft (230 m). (Description from Myers, Sharps, and McKay, 1986).

TRd: Dockum Formation (Upper Triassic)
Upper beds are poorly exposed red siltstone and shale; middle beds, fine-grained, moderate-red crossbedded sandstone that forms ledges and cliffs; lower beds are grayish-red to moderate-red siltstone and fine-grained sandstone. May be equivalent to Chinle Formation. About 180 ft (54 m) thick. (Description from Myers, Sharps, and McKay, 1986).

PALEOZOIC UNITS

Ps: San Andres Limestone (Lower Permian)
Upper beds, about 26 ft (8 m) of moderate reddish-brown siltstone and fine-grained sandstone; may be equivalent to Bernal Formation of Bachman (1953). Grayish- to very pale orange, light-gray to medium-light-gray, and brownish-gray fetid limestone comprises the bulk of the San Andres; may be gypsiferous near top; lower beds are sandy. Pinkish-gray to grayish-orange well-sorted, fine-to medium-grained quartz sandstone near middle. In vicinity of Gibbs Place, upper beds are mostly gypsum. About 164 ft (50 m) thick. (Description from Myers, Sharps, and McKay, 1986).

Pg: Glorieta Sandstone (Lower Permian)
Reddish-brown, grayish-orange, and yellowish-orange, fine-to medium-grained, well-sorted quartz sandstone. Typically forms cliffs or very steep slopes; beds as much as 10 ft (3 m) thick. Thickness ranges between 150-190 ft (46-58 m). (Description from Myers, Sharps, and McKay, 1986).

Py: Undivided Yeso Formation (Lower Permian)
Formation consists of orange sandstone and siltstone; white gypsum; and yellowish-gray gypsiferous limestone and sandstone. (Description from Myers, Sharps, and McKay, 1986).

Pyjc: Joyita Sandstone and Canas Gypson Members of the Yeso Formation (Lower Permian)
Joyita Sandstone Member is grayish-orange to moderate-reddish-brown siltstone and fine-grained sandstone; lower part is gypsiferous and is gradational from underlying Canas Member. About 120 ft (37 m) thick. Canas Gypsum Member is poorly exposed grayish-white gypsum with thin beds of gypsiferous siltsone near middle of member. Because of generally poor exposures and difficulty in locating contacts in most of the map area, the Canas Member and overlying Joyita Member were mapped as one unit. Joyita is about 240 ft (74 m) thick. (Description from Myers, Sharps, and McKay, 1986).

Pyt: Torres Member of the Yeso Formation (Lower Permian or Leonardian)
Poorly exposed gypsum with interbedded limestone lenses. Gypsum is bedded and weathers very light gray. Limestone lenses are up to 5 feet (1.5 m) thick and weathers light-olive gray. Base of member mapped at base of gypsum. Lower 100 feet (31 m) exposed in southeast part of quadrangle; upper beds not present in quadrangle.

Pym: **Mesa Blanca Sandstone Member of the Yeso Formation** (Lower Permian or Leonardian)
Thin-bedded, fine-grained sandstone and siltstone. Weathers pinkish-gray, pale-red, reddish brown to white. Trace fossils observed on bedding surfaces along with ripple marks and cross bedding. Associated soil is orange to pink. Unit forms gentle slopes and undulating terrain. About 250 feet (76 m) thick.

Pa: Abo Formation (Lower Permian or Leonardian and Wolfcampian)

Overall finer-grained than lower part of Abo Formation (Pal), and composed of thin – to thick-bedded micaceous siltstone and fine-grained sandstone. Upper portion contains sandstone and occasional granule conglomerate interbedded with siltstones and mudstones. Weathers light red and pale reddish brown, with local white and green oxidation/reduction spots. Cross laminae, ripple-marks, mudcracks and interbedded paleosols observed. Fossil plant debris and some bioturbation present. Uppermost 20-30 feet (6-9 m) interbedded with light orange-tan sandstones similar to those in the Yeso Formation. About 450 feet (137 m) exposed in southeastern portion of quadrangle. Thickness ranges from about 420 ft (125 m) to 775 ft (235 m).

Pal: Lower Abo Formation (Lower Permian or Leonardian and Wolfcampian)
Base of unit mapped at top of last laterally extensive marine limestone of underlying Bursum Formation; unit disconformably overlies Bursum Formation. Basal contact is poorly exposed and covered by Quaternary deposits. Unit is coarser grained and darker in color than the upper portion of the overlying Abo Formation, weathers dark purple to dark reddish brown and is coated by abundant desert varnish. Contains poorly sorted medium- to coarse-grained, cross-bedded, thick-bedded sandstones (arkosic wacke to wacke) to granule conglomerates. May contain calcite cement. Sandstone beds are more laterally continuous than those of underlying Bursum Formation. Basal sandstone may contain 10 cm limestone clasts. Rare thin lenses of thin (<20 cm thick) nodular bedded, poorly exposed, unfossiliferous (non-marine?) limestone beds at base. Unit is thin (<50 feet) and only present in the southeastern portion of the quadrangle, but is thicker and more pervasive in adjoining Scholle quadrangle. Unit is not regionally extensive, as it does not occur in the Lucero uplift region, ~80 km across the Rio Grande Rift (Lucas and Ziegler, 2004).

Pb: Bursum Formation of the Madera Group (Lower Permian)
Base of unit mapped as last appearance of well-exposed cherty limestone from uppermost IPm-5, which is typically overlain by <5 m of cover followed by 1-2 m thick coarse-grained reddish arkosic sandstone with irregular bottom contact. In northern quarter of quadrangle, basal sandstone thins and is eventually replaced by gray-white crinoid packstone. Limestone beds overlying this basal sandstone (skeletal wackestone-lime mudstones) are thin (< 2m) and contain fusulinids *Triticites creekensis* Thompson and *Leptrotriticites* sp. (Myers, 1977), finely abraded or large, intact gastropods, ramose bryozoa, crinoids, and bivalves, and rare small chert nodules (<2 cm). Middle portion of unit composed of interbedded fine-to coarse-grained cross-bedded sandstone (lithic to arkosic wacke and arkose) that may contain calcite cement, occasional granule-pebble conglomerate, red mud-shale, and micaceous siltstone; thickness of sandstone beds varies laterally. Top of unit composed of well- to poorly-exposed < 16 feet (5 m) thick light gray, thin bedded, nodular, fossiliferous limestone bed (skeletal wackestone) that contains small (1 mm thick) stringers of red sandstone, bivalves, crinoids, fenestrae, and fusulinids (*Scwagerina pinosensis* Thompson) sp. (Myers, 1977). Sandstone weathers reddish-brown to purplish-brown; limestone weathers olive-gray; shale and siltstone weather red. About 150 - 250 feet (46-76 m) thick.

IPM-5 through IPM-1: Informal map units within the Wild Cow Formation (Lower Permian, Upper and Middle Pennsylvanian) of the Madera Group
Informal map units within the Wild Cow Formation as previously mapped by Myers (1977) and Myers et al. (1981). Units broken out into three intervals that contain cliff-forming limestone (IPM-5, IPM-3, and IPM-1) interbedded with two slope-forming siliciclastic-dominated intervals (IPM-4 and IPM-2). Contains fusulinids of Virgilian, Missourian, and Desmoinesian ages (Myers, 1977).

PIPum: Upper Madera Group Formations
Includes IPm-5 through IPm-2, which are described below

IPm-5: (middle and upper part of La Casa Member of Myers et al., 1981) (Upper Pennsylvanian -Virgilian)
Base of unit mapped at base of first cliff-forming limestone overlying slope-forming IPm-4. Cliff- and slope-forming interval composed of three distinctive, mappable, thick (~3-8 m) limestone cliffs separated by ~10-25 m-thick slope-forming intervals. Lower limestone cliff (~4 m) composed of thick-bedded limestone (skeletal wackestone) with laterally continuous dark chert band at base (<10 cm thick) and capped by meter-scale cross-bedded limestone or cross-bedded, laterally discontinuous sandstone. Middle limestone (~3 m; skeletal wackestone) contains irregular –shaped dark chert nodules in upper 2 meters. Upper limestone (~8 m; skeletal wackestone) contains large irregular-shaped light gray chert nodules. Upper 10's of meters of unit composed of recessed, 1-m thick limestone beds containing abundant dark brown chert nodules that weather light tan. Limestones contain phylloid algae, bivalves, crinoids, brachiopods, and abundant bioturbation. Slope-forming intervals composed of interbedded green and purple micaceous siltstone, sandstone, and mudstone. *Triticites creekensis* Thompson? fusulinids present (Myers, 1977). Approximately 250 feet (76 m) thick.

IPm-4: (Pine Shadow Member and lower La Casa Member of Myers et al., 1981) (Upper Pennsylvanian – Virgilian)
Base of unit mapped at the top of the last limestone cliff in underlying IPm-3. Slope-former (poorly exposed) composed of interbedded sandstone, siltstone, and mudstone with occasional laterally discontinuous limestone beds. A thick sandstone interval (10's m thick) is present just north of gas pipeline road in middle of quadrangle and southern part of quadrangle. Mud-siltstones contain ripple laminations and soft sediment deformation. Plant debris and cross-bedding observed in some sandstone beds. Base of unit marked by distinctive thin (<1 m) orange dolomite bed overlain by white sandstone (quartz arenite). Approximately 560 ft (170 m) thick. Thickness varies laterally within map area by 9 m and is thinner to north (Myers, 1977).

IPm-3: (upper part of Sol se Mete Member of Myers et al., 1981) (Upper Pennsylvanian – Missourian)
Base of unit mapped at base of first limestone cliff overlying covered interval in lower portion of Sol se Mete Member (IPm-2). Thin- to thick-bedded cliff-forming limestone (wackestone through grainstone) containing three persistent, mappable cliffs: 1) lower limestone that contains dark chert bands (0.5 m long, <20 cm thick), 2) middle limestone

interbedded with orange-weathering silty limestone and sparse chert bands, and 3) thick-bedded upper limestone with distinctive orange-brown mottling in upper 2 meters. Fossils include gastropods, bryozoan, rugose corals, phylloid algae, brachiopods, and abundant bioturbation. Approximately 65 ft thick (20 m).

IPm2: (lower portion of Sol se Mete Member of Myers et al., 1981) (Upper Pennsylvanian – Missourian)
Base of unit mapped as top of last limestone bed in underlying Los Moyos Limestone. Slope-former (poorly exposed) interpreted to be fine-grained siliciclastic deposits (siltstone) interbedded with limestone beds (mudstone through grainstone) with marl interbeds, rip-up clasts, and plane laminations, and laterally discontinuous white and green sandstones with local granules (subarkose) (1-2 m thick). About 100 ft thick (30 m).

IPm1: (Los Moyos Limestone) (Middle Pennsylvanian – Desmoinesian)
Basal contact with underlying Sandia Formation placed at the base of the first limestone bed. Medium- to thick-bedded, cliff-forming limestones (lime mudstones through skeletal wackestones and grainstones). Individual limestone beds 1- 2 m thick. Contains dark chert in small pods (<5 cm) in lower 40 meters, middle 20 meters, and in uppermost limestone bed. Minor amounts of interbedded sandstone (quartz arenite through micaceous lithic wacke), quartz and feldspar granule conglomerate, and poorly exposed siltstones and mudshales. Fossils include bivalves, bryozoa, crinoids, fusulinids, chaetetids, and abundant bioturbation obscuring primary sedimentary structures. Weathers medium gray. About 560 ft thick (172 m).

IPs: Sandia Formation (Middle Pennsylvanian)
Interbedded sandy, fossiliferous limestones, shales, siltstones, sandstones, and conglomerates. Fossil types include marine fossils and plant debris. Limestone in upper part weathers light- to medium-gray with dark brown chert. Basal beds are orthoquartzitic quartz-pebble conglomerates with angular pink feldspar grains. Upper contact with Wild Cow Formation gradational and placed at last sandstone bed. Lower contact is fault contact with Precambrian rocks. About 600 feet (183 m) thick.

PROTEROZOIC UNITS

Xu: Proterozoic Undivided
Includes all units listed below

Xlp: Los Pinos Granite
Pink, weathers red, massive, medium- to coarse-grained, microcline + orthoclase + quartz + albite granite. Interspersed with hornblende dikes.

Xbsu: Blue Springs Upper Schist
Green to white, chlorite + muscovite schist. The apparent uppermost unit of the Manzano Peak (F_2) synclinorium, found east and northeast of the Los Pinos granite (Xlp) in the

eastern region of the quadrangle. Equivalent to the Metaclastics Series pCm of Myers and McKay (1974).

Xbr: Blue Springs Rhyolite
Black and brown to gray with lenticular quartz-feldspar pink colored stripes within darker layers. Interpreted as a metarhyolite due to the presence of potassium feldspar in the felsic lenses and a geochemical composition close to rhyolite. Equivalent to the part of pCa, the argillite of Myers and McKay (1972), named the Blue Springs Quartzite (bq1) by Bauer (1983).

Xbs: Blue Springs Schist Green to white, garnet + chlorite + quartz + muscovite schist. Crenulated with well preserved garnet. Equivalent to the part of pCa, the argillite of Myers and McKay (1972) and the Sais Quartzite (sq3) of Bauer (1983).

Xbq: Blue Springs Quartzite Member (of Blue Springs Schist)
Thinly-bedded, medium-grained quartzites, interbedded with chlorite-muscovite schist and quartz-muscovite schist. Partly equivalent to Sais Formation and lower part of the Pine Shadow Springs of Myers and McKay (1972); mapped as Blue Springs Formation (bs1) by Bauer (1983).

Xsq: Sais Quartzite
Thinly-bedded, reddish, schistose quartzite. Bedding planes commonly show mica concentrations. Grains size ranges from very fine to coarse sand. Primary structures include preserved cross bedding. Originally called the White Ridge and Sais quartzites of Myers and McKay (1972), called the White Ridge Quartzite 2 (wq2) of Bauer (1983).

Xes: Estadio Schist marker unit
Coarse-grained, staurolite + garnet + biotite schist. Shows multiple episodes of deformation and contains local crenulation cleavage and at least three generations of foliation. Probably originally deposited as a mudstone layer within the sandstone. Equivalent to the Lower part of the Pine Shadow Springs of Myers and McKay (1972); called the White Ridge schist (ws1) of Bauer (1983).

Xwq: White Ridge Quartzite
Coarse-grained, impure, orange to gray, thinly-bedded, aluminous quartzite. Fairly immature metasedimentary rock with well preserved cross bedding. Cross- bedding indicates overturned bedding. The upper part of the unit has a distinctive red, andalusite + muscovite, foliated, schistose layer. Part of the Lower part of the Pine Shadow Springs of Myers and McKay (1974); called the White Ridge Quartzite 2 (wq2) of Bauer (1983).

Xa: Abajo Schist
Schistose metasedimentary rocks intruded by or interlayered with mafic meaigneous dikes and flows. The metasedimentary rocks are rich in staurolite, garnet and amphibole porphyroblasts. Possible protoliths could be siltstones. Correlated with the Lower part of the Pine Shadow Springs of Myers and McKay (1974). Euivalent to units A,B,C of Parchman (1976) and Bosque metasediments of Edwards (1976).

Xla: Abajo Lithic Arenite
Composed of a variety of metasedimentary rocks including meta-pelites, meta-arkose and impure quartzite. The chlorite schist, and some quartzites interbedded with metarhyolite are thinly-bedded; more massive, quartzite domains are locally dominant. Locally, garnet staurolite schist and may be related to the intrusion of gabbroic dikes (now amphibolite). Compositional layering (S_0) is commonly preserved and is generally at low angle to dominant schistosity (S_1). Correlated with the lower metaclastic series of Reiche (1949) and the lower part of the Pine Shadow Springs and Flaggy Schist zones of Myers and McKay (1972, 1974). Equivalent to units A,B,C of Parchman (1976) and Bosque metasediments of Edwards (1976).

Xa: Amphibolite
Black to dark green, fine-to coarse-grained amphibolites with varying amounts of macroscopic white plagioclase that ranges in texture from salt and pepper to smeared-out shear banding. Coarse-grained metadiorites are present locally. Mafic units have apparent widths up to 150+m and may thicken, thin, fork, and pinch out along strike. Equivalent to the pCb "basic schist" of Myers and McKay (1972). May be confused with the intrusive gabbro described above, but some units may be part of the supracrustal sequence. These were mapped as Basic Schist and Mixed Flow units by Myers and McKay (1972) and as non-rhyolitic components of the Sevilleta Formation by Bauer, 1983.

Xsr: Sevilleta Metarhyolite
Felsic, meta-igneous rocks with quartz and feldspar phenocrysts. Generally pink to gray, blocky-fracturing, porphyritic aphanites with quartz and feldspar clasts ~1mm in diameter. Texture ranges from thin, well developed compositional banding to massive. Planar features, such as ~1mm-~5cm flow bands or shear bands, are common and range considerably in thickness. Quartz veins, pegmatite and massive schistose units are present locally and generally parallel foliation. Equivalent to the Sevietta metarhyolite of Reiche (1949) and Myers and McKay (1972). Subdivided as follows:

Xsru: Upper metarhyolite member
Brown to pink, finely-banded sericitic metarhyolite; 0.5-3.5mm feldspar and quartz crystals.

Xsrm: Middle metarhyolite member
Dark gray to black, finely-banded rhyolite; 0.5-2mm angular to rounded quartz clasts.

Xsrl: Lower metarhyolite member
Medium gray to black, dense, finely-banded metarhyolite; speckled with 1.0-2.5mm white feldspar crystals.

Xsrh: Hornblende schist member

Olive to dark-green, aphanitic, vesicular, flow-banded rock. Gneissic with feldspar augen in places. Interfingers with metarhyolite members (Xsru, Xsrm, Xsrl) and merges with overlying Abajo Lithic Arenite unit (Xla).

REFERENCES

Anderson, J.L., 1983, Proterozoic anorogenic granite plutonism of North America, *in* Medaris L G, J., Byers, C.W., M, M.D., and C, S.W., eds., Proterozoic Geology: Geological Society of America Memoir, Volume 161, p. 133-154.

Baer, S.H., 2004, Geologic and tectonic evolution of the Manzano Peak Quadrangle, central New Mexico [M.S. thesis]: Albuquerque, University of New Mexico.

Baer, S.H., Karlstrom, K.E., Bauer, P., and Connell, S.D., 2004, Geology of the Manzano Peak 7.5-min. quadrangle, Valencia and Torrance Counties, New Mexico, New Mexico Bureau of Mines and Mineral Resources, Open-file Geologic Map OF-GM 61.

Barnes, M.A., Anthony, E.Y., Williams, I., and Asquith, G.B., 2002, Architecture of a 1.38-1.34 Ga granite-rhyolite complex as revealed by geochronology and isotopic and elemental chemistry of subsurface samples from west Texas, USA: Precambrian Research, v. 119, p. 9-43.

Bauer, P., Karlstrom, K.E., Bowring, S.A., Smith, A.G., and Goodwin, L.B., 1993, Proterozoic plutonism and regional deformation--new constraints from the southern Manzano Mountains, central New Mexico: New Mexico Geology, v. 15, p. 49-55.

Bauer, P.W., 1983, Geology of the Precambrian rocks of the southern Manzano Mountains, New Mexico [M.S. thesis]: Albuquerque, University of New Mexico.

Beers, C.A., 1976, Geology of the Precambrian rocks of the southern Los Pinos Mountains, Socorro County, New Mexico: Socorro, New Mexico Inst. Min. Tech.

Bowring, S.A., 1990, Growth, stabilization, and reactivation of Proterozoic lithosphere in the southwestern United States: Geology, v. 18, p. 1203-1206.

Brookins, D.G., Bolton, W.R., and Condie, K.C., 1980, Rb-Sr isochron ages of four Precambrian igneous rock units from south-central New Mexico: Isochron/west, v. 29, p. 31-37.

Brown, C.L., Karlstrom, K.E., Heizler, M., and Unruh, D., 1999, Paleoproterozoic deformation, metamorphism, and 40Ar/39Ar thermal history of the 1.65-Ga Manzanita pluton, Manzanita Mountains, New Mexico: New Mexico Geological Society Guidebook, v. 50th Field Conference, p. 255-268.

Cather, S.M., Karlstrom, K.E., Timmons, J.M., and Heizler, M., *in review*, A palinspastic reconstruction of Proterozoic basement-related aeromagnetic features in north-central New Mexico: implications for Mesoproterozoic to late Cenozoic tectonism.

Chamberlain, R.M., Karlstrom, K.E., Connell, S.D., Brown, C.L., Nyman, M.W., Cavin, W.J., and Parchman, M.A., 1997, Geology of the Mount Washington 7.5-minute quadrangle: Bernalillo and Valencia Counties, New Mexico, New Mexico Bureau of Mines and Mineral Resources.

Chamberlin, R.M., Karlstrom, K.E., Connell, S.D., Brown, C.L., Nyman, M.W., Hitchcock, C., Kelson, K.I., Noller, J., Sawyer, T., Cavin, W.J., and Parchman, M.A., 1997, Geology of the Mt. Washington 7.5' quadrangle, Bernalillo and Valencia Counties, New Mexico, New Mexico Bureau of Mines and Mineral Resources, Open-file Geologic Map OF-GM 8.

Collins, W.J., 2002, Hot orogens, tectonic switching, and creation of continental crust: Geology, v. 30, p. 535-538.

Condie, K.C., and Budding, A.J., 1979, Geology and geochemistry of Precambrian rocks, central and south-central New Mexico: New Mexico Bureau of Mines and Mineral Resources, v. Memoir 35, p. 1-58.

Daniel, C.G., and Pyle, J.M., 2006, Monazite-xenotime thermochronometry and Al2SiO5 reaction textures in the Picuris Range, northern New Mexico, USA: New evidence for a 1450-1400 Ma orogenic event: Journal of Petrology, v. 47, p. 97-118.

Doran, L., 2002, Banded metasiltstones in Trigo Canyon: The story they tell about the Proterozoic deformational history of the Manzano Mountains [B.S. thesis]: Albuquerque, University of New Mexico.

Duebendorfer, E.M., Chamberlain, K.R., and Heizler, M.T., 2006, Filling the North American Proterozoic Tectonic Gap: 1.60--1.59-Ga Deformation and Orogenesis in Southern Wyoming, USA: Journal of Geology, v. 114.

Hansen, E., 1971, Strain facies: New York, Springer Verlag.

Harris, C.W., and Eriksson, K.A., 1989, Allogenic controls on the evolution of storm and tidal shelf sequences in the Early Proterozoic Uncompahgre Group, southwest Colorado, USA: Sedimentology, v. 30, p. 189-213.

Harris, C.W., Gibson, R.G., Simpson, C., and Eriksson, K.A., 1987, Proterozoic cuspate basement-cover structure, Needle Mountains, Colorado: Geology, v. 15, p. 950-953.

Hill, B.M., and Bickford, M.E., 2001, Paleoproterozoic rocks of central Colorado: Accreted arc or extended older crust?: Geology, v. 29, p. 1015-1018.

Hirth, G., and Tullis, J., 1992, Dislocation creep regimes in quartz aggregates: Journal of Structural Geology, v. 14, p. 145-159.

Jessup, M.J., Karlstrom, K.E., Connelly, J., Livaccari, R., Tyson, A., and Rogers, S.A., 2005, Complex Proterozoic crustal assembly of southwestern North America in an arcuate subduction system: The Black Canyon of the Gunnison, southwestern Colorado: AGU Monograph, v. The Rocky Mountain Region - An Evolving Lithosphere: Tectonics, Geochemistry, and Geophysics, p. 21-38.

Jolly, W.T., 1975, Subdivision of the Archean lavas of the Abitibi area, Canada, from Fe--Mg--Ni--Cr relations.: Earth and Planetary Science and Letters, v. 27, p. 200-210.

Jones, J.V., III, 2005, Proterozoic tectonic evolution of southern Laurentia: New constraints from field studies and geochronology in southern Colorado and northern New Mexico, U.S.A. [PhD thesis]: Austin, University of Texas.

Kalakay, T.J., John, B.E., and Lageson, D.R., 2001, Fault-controlled pluton emplacement in the Sevier fold-and-thrust belt of southwest Montana, USA: Journal of Structural Geology, v. 23, p. 1151-1165.

Karlstrom, K.E., Ahall, K.I., Harlan, S.S., Williams, M.L., McLelland, J., and Geissman, J.W., 2001a, Long-lived (1.8-1.0 Ga) convergent orogen in southern Laurentia, its extensions to Australia and Baltic, and implications for refining Rodinia: Precambrian Research, v. 111, p. 5-30.

Karlstrom, K.E., Amato, J., Williams, M.L., Heizler, M., Shaw, C., Read, A., and Bauer, P., 2004, Proterozoic tectonic evolution of the New Mexico Region: A synthesis, *in* Mack, G., and Giles, K., eds., The Geology of New Mexico: A Geologic History, Volume Special Publication II, p. 1-34.

Karlstrom, K.E., and Bowring, S.A., 1988, Early Proterozoic assembly of tectonostratigraphic terranes in southwestern North America: Journal of Geology, v. 96, p. 561-576.

Karlstrom, K.E., Bowring, S.A., Chamberlain, K.R., Dueker, K.G., Eshete, T., Erslev, E.A., Farmer, G.L., Heizler, M., Humpreys, E.D., Johnson, R.A., Keller, G.R., Kelley, S.A., Levander, A., Magnani, M.B., Matzel, J.P., McCoy, A.M., Miller, K.C., Morozova, E.A., Pazzaglia, F.J., Prodehl, C., Rumpel, H.M., Shaw, C., Sheehan, A.F., Shoshitaishvili, E., Smithson, S.B., Snelson, C.M., Stevens, L.M., Tyson, A., and Williams, M.L., 2002, Structure and Evolution of the Lithosphere Beneath the Rocky Mountains: Initial Results from the CD-ROM Experiment GSA Today, v. 12, p. 4-10.

Karlstrom, K.E., Brown, C.L., Armour, J., Lewis, J., and Connell, S.D., 1999, Geology of the Bosque Peak 7.5 minute quadrangle, Valencia and Torrance Counties, New Mexico, New Mexico Bureau of Mines and Mineral Resources, Open-file Geologic Map OF-GM 24.

Karlstrom, K.E., Connell, S.D., Ferguson, C.A., Read, A., Osburn, G.R., Kirby, E., Abbott, J.C., Hitchcock, C., Kelson, K.I., Noller, J., Sawyer, T., Ralser, S., Love,

D.W., Nyman, M.W., and Bauer, P., 1994 Geology of the Tijeras 7.5-min quadrangle, Bernalillo County, New Mexico: New Mexico Bureau of Mines and Mineral Resources, Open-file Geologic Map OF-GM 4.

Karlstrom, K.E., Connell, S.D., Rogers, S.A., and Crawford, E.B., 2001b, Geology of the Capilla Peak 7.5-min. quadrangle, Valencia and Torrance Counties, New Mexico, New Mexico Bureau of Geology and Mineral Resources, Open-file Geologic Map OF-GM 27.

Karlstrom, K.E., Dallmeyer, R.D., and Grambling, J.A., 1997, 40Ar/39Ar evidence for 1.4 Ga regional metamorphism in New Mexico: Implications for Thermal Evolution of Lithosphere in the Southwestern USA: Journal of Geology, v. 105, p. 205-233.

Karlstrom, K.E., and Humpreys, E.D., 1998, Persistent influence of Proterozoic accretionary boundaries in the tectonic evolution of southwestern North America: Interaction of cratonic grain and mantle modification events: Rocky Mountain Geology, v. 33, p. 161-180.

Karlstrom, K.E., and Williams, M.L., 1998, Heterogeneity of the middle crust: Implications for strength of continental lithosphere: Geology, v. 26, p. 815-818.

Kirby, E., Karlstrom, K.E., Andronicos, C.L., and Dallmeyer, R.D., 1995, Tectonic setting of the Sandia pluton: An orogenic 1.4 Ga granite in New Mexico: Tectonics, v. 14, p. 185-201.

Larson, T.E., and Sharp, Z.D., 2003, Stable isotope constraints on the Al2SiO5 'triple-point' rocks from the Proterozoic Priest pluton contact aureole, New Mexico, USA: Journal of Metamorphic Geology, v. 21, p. 785-798.

Le Bas, M.J., Le Maitre, R.W., Streckeisen, A., and Zanettin, B., 1986, A Chemical Classification of Volcanic Rocks Based on the Total Alkali-Silica Diagram: Journal of Petrology, v. 27, p. 745-750.

Luther, A.L., Karlstrom, K.E., Scott, L.A., Elrick, M., and Connell, S.D., 2005, Geology of the Becker 7.5 minute quadrangle, Valencia and Socorro Counties, New Mexico, New Mexico Bureau of Mines and Mineral Resources, Open File Geologic Map OF-GM 100.

Magnani, M.B., Miller, K.C., Levander, A., and Karlstrom, K.E., 2004, The Yavapai-Mazatzal boundary: A long-lived tectonic element in the lithosphere of southwestern North America: GSA Bulletin, v. 116, p. 1137-1142.

Myers, D.A., McKay, E.J., and Sharps, J.A., 1981, Geologic map of the Becker quadrangle, Valencia and Socorro Counties, New Mexico, U. S. Geological Survey Map, GQ-1556

Myers, D.A., Sharps, J.A., and McKay, E.J., 1986, Geologic map of the Becker SW and Cerro Montosa quadrangles, Socorro County, New Mexico, U.S. Geological Survey Geological Quadrangle Map I-1567.

Nyman, M.W., Karlstrom, K.E., Kirby, E., and Graubaud, C.M., 1994, Mesoproterozoic contractional orogeny in western North America: Evidence from ca. 1.4 Ga plutons: Geology, v. 22, p. 901-904.

Read, A., Karlstrom, K.E., Connell, S.D., Kirby, E., Ferguson, C.A., Ilg, B., Osburn, G.R., Van Hart, D., and Pazzaglia, F.J., 1995, Geology of the Sandia Crest 7.5-min quadrangle, Bernalillo and Sandoval Counties, New Mexico, New Mexico Bureau of Mines and Mineral Resources, Open-file Geologic Map OF-GM 6.

Read, A.S., Karlstrom, K.E., Grambling, J.A., Bowring, S.A., Heizler, M., and Daniel, C.G., 1999, A middle-crustal cross section from the Rincon Range, northern New Mexico: Evidence for 1.68-Ga, pluton-influenced tectonism and 1.4 Ga regional metamorphism: Rocky Mountain Geology, v. 34, p. 67-91.

Reiche, P., 1949, Geology of the Manzanita and North Manzano Mountains, New Mexico: Bulletin of the Geological Society of America, v. 60, p. 1183-1212.

Rogers, S.A., 2001, New structural interpretation, mircostructural analyses, and preliminary monazite geochronology of Proterozoic rocks in the central Manzano Mountains, New Mexico [Honors Thesis thesis]: Albuquerque, University of New Mexico.

Scott, L.A., Elrick, M., Connell, S.D., and Karlstrom, K.E., 2005, Preliminary Geologic Map of the Scholle 7.5-minute Quadrangle, Valencia, Torrance, and Socorro Counties, New Mexico Bureau of Geology and Mineral Resources, Open-file Geologic Map OF-GM 99.

Shastri, L.L., 1992, Proterozoic Geology of the Los Pinos Mountains, Central New Mexico: Timing of Plutonism, Deformation, and Metamorphism [M.S. thesis]: Albuquerque, University of New Mexico.

Soegaard, K., and Eriksson, K.A., 1985, Evidence of tide, storm, and wave interaction on a Precambrian siliciclastic shelf: the 1,700 m.y. Ortega Group, New Mexico: Journal of Sedimentary Petrology, v. 55, p. 672-684.

—, 1989, Origin of thick, first-cycle quartz arenite successions: evidence from the 1.7 Ga Ortega Group, northern New Mexico: Precambrian Research, v. 43, p. 129-141.

Spear, F.S., 1993, Metamorphic phase equilibria and pressure-temperature-time paths, Mineralogical Society of America 799 p.

Stark, J.T., and Dapples, E.C., 1946, Geology of the Los Pinos Mountains, New Mexico: Geological Society of America Bulletin, v. 57, p. 1121-1172.

Thompson, A.G., Grambling, J.A., and Dallmeyer, R.D., 1991, Proterozoic tectonic history of the Manzano Mountains, central New Mexico: New Mexico Bureau of Mines and Mineral Resources Bulletin, v. 137, p. 71-77.

Thompson, A.G., Grambling, J.A., Karlstrom, K.E., and Dallmeyer, R.D., 1996, Mesoproterozoic Metamorphism and 40Ar/39Ar Thermal History of the 1.4 Ga Priest Pluton, Manzano Mountains, New Mexico: The Journal of Geology, v. 104, p. 583-598.

Williams, M.L., Karlstrom, K.E., Lanzirotti, A., Read, A.S., Bishop, J.L., Lombardi, C.E., Pedrick, J.N., and Wingsted, M.B., 1999, New Mexico middle-crustal cross sections: 1.65-Ga macroscopic geometry, 1.4-Ga thermal structure, and continued problems in understanding crustal evolution: Rocky Mountain Geology, v. 34, p. 53-66.